Smoothed particle hydrodynamics modeling of brash ice

Ivan Montenegro Cabrera

Master Thesis

presented in partial fulfillment
of the requirements for the double degree:
"Advance Master in Naval Architeture"conferred by University of Liege
"Master of Sciences in Applied Mechanics, specialization in Hydrodynamics, Energetics and Propulsion"conferred by Ecole Centrale de Nantes

develop at University of Rostock
in the framework of the

"EMSHIP"
Erasmus Mundus Master Course
in "Integrated Advance Ship Design"

Ref. 159652-1-2009-1-BE-ERA MUNDUS-EMMC

Supervisor:	Prof. Nicolai Kornev, University of Rostock
Reviewer:	Prof. David Le Touzé, Ecole Centrale de Nantes

Rostock, January 2017

ABSTRACT

In the context of arctic navigation through man-made channels, brash ice is a very common type of ice through which ships navigate, that basically consists in several layers of rigid ice pieces floating in water, thus, affecting its resistance and behavior.

The high complexity of the prediction of these impacts in terms of the physical description makes it a non-tackled problem in the present time, although some simplified approaches have been proposed and its mechanical properties have been studied up to some extent.

The objective of this work is to study, propose and implement a suitable numerical model for brash ice simulations based on the available experimental data and previous work on ice dynamics.

Four options are briefly analyzed, a full SPH approach for single-phase granular flows and for two-phase mediums, a coupling method between SPH and DEM and a physical based method. The SPH approach for single-phase granular flows is then selected and a differential equation for brash ice is proposed with its respective SPH discretized form.

An SPH open-source code is selected after a detailed discussion of the different options to accomplish this task based on several variables that were highly important in terms of future possible developments and the scope this work.

For the implementation a detailed description of this tool and of the modifications is provided. This study focuses on two main modifications, a new rheological implementation and a new buoyancy condition.

A convergence study in time is performed, to assess reliability and to pick the appropriate parameters for the simulation, with these parameters a sensitivity analysis is performed checking the influences of the different rheological variables in the resistance force, velocity fields and pressure fields.

Finally the work will be compared with experimental data obtained from a cylinder resistance test conducted in the HSVA ice tank facilities, the comparison will focus mainly on the resistance measured on the experiment and also will provide a visual comparison of the velocity fields and the overall behavior of the medium.

The report ends with conclusions on the new approach here proposed and several suggestions for further development.

CONTENTS

List of Figures

List of Tables

DECLARATION OF AUTHORSHIP

I declare that this thesis and the work presented in it are my own and have been generated by me as the result of my own original research.

Where I have consulted the published work of others, this is always clearly attributed.

Where I have quoted from the work of others, the source is always given. With the exception of such quotations, this thesis is entirely my own work.

I have acknowledged all main sources of help.

Where the thesis is based on work done by myself jointly with others, I have made clear exactly what was done by others and what I have contributed myself.

This thesis contains no material that has been submitted previously, in whole or in part, for the award of any other academic degree or diploma.

Date: January 13, 2017 *Signature*

INTRODUCTION

In arctic operation routes it is very common for a ship to navigate through brash ice, while doing so, several characteristics are significantly affected such as the resistance and the behavior. Within the current scope of increasing arctic navigation, it becomes a problem of high importance to develop a numerical method able to predict such implications. Figure 1 illustrates brash ice.

Figure 1: Ship navigating through brash ice

At the moment the problem has not yet been addressed completely or successfully, but in general it is addressed by model-scale experiments and class rules calculations, that may or may not yet capture the full complexity of real brash ice.

Several approximated theories have been proposed in the past, that can estimate the resistance in a very rough way and for a very short range of velocities. Also only one simulation attempt is known, Prof. Konno, 2009 [11], as far as the people involved in this research are aware of, and it is only useful for short channels of navigation, although several breakthroughs are still on the way.

Master's Thesis

Within this context, the present Master's thesis focuses on developing a new approach to address this problem, specifically with the SPH method. The topic is the following:

Smoothed particle hydrodynamics modeling of brash ice

The main objective is to study, develop and implement a full SPH numerical simulation to model this type of ice, suitable for the challenges this industry faces and in

agreement to experimental observations and several theoretical remarks.

Implementation

The simulation is performed in the framework of an open source code called DualSPHysics [5]. The code is written in C++ language for CPU implementation and CUDA for GPU implementation, for this specific implementation the linux CPU code version was used.

Basically two main modifications were performed to some inside functions to achieve the goals of the project.

Contents description

The following work is divided in three main parts, the first as an introduction and compilation of relevant information available, and the last two as the core of this research, from the development of the new equations to the implementation and results obtained.

The first one is focused in describing brash ice, exploring some theoretical work done during the 80's and also summarizing some experimental key results and observations of brash ice mechanical properties and on ship resistance experiments performed.

Based on these insights the second part is focused on a methodology evaluation and selection. After the methodology selection, the development of brash ice differential equations in a continuum medium is provided with its numerical counterpart in the SPH framework. At the end of this part a suitability analysis to select the ideal open source for such methodology is performed and a selection is made to move forward to the implementation stage of the project.

The third part is focused on the description of the most important parts of the new implementation starting from the tool selected until the necessary modifications. Then a convergence analysis is performed to select the right parameters for the new medium simulations, with these parameters a sensitivity analysis is performed. Then the results of the simulations are compared with experimental data focusing mainly in the resistance force but also visual comparisons on the velocity fields and general behavior of the medium.

Finally this work is concluded with some conclusions on the new proposal and a description of the possible future tracks to follow for further development.

Part I
THEORETICAL AND EXPERIMENTAL ASPECTS

1 BRASH ICE SHIP RESISTANCE INTRODUCTION

1.1 Brash ice description

In arctic routes of navigation, when a channel is first broken by an ice-breaker it leaves a trail of big ice pieces that are re broken once and again by the passing of other ships in operation. Figure 2 show a vessel in brash ice from an inside perspective.

Figure 2: Vessel in brash ice side view

This repetitive process has two main consequences, the first is that the ice pieces reach a stable state of size and shape and are no longer subject to major modifications such as breaking or melting, and the second is that the formation of these ice pieces is enhanced and the amount of pieces increases during this process thus thickening the brash ice layer.

Figure 3 shows a common brash ice look after its formation.

Figure 3: Brash ice layer above water

The accumulation of these particles alongside with the buoyant effects would make the whole brash ice layer to spread and would stop the thickness from increase, but as observations have proven the formation of submerged lateral piles of ice in the edges of the channel produce the necessary lateral pressure to allow the brash ice thickness to continue increasing. This piling up on the edges is explained by the frictional interaction between these ice pieces and buoyant forces acting all over the brash ice Figure 4 [2] show this effect.

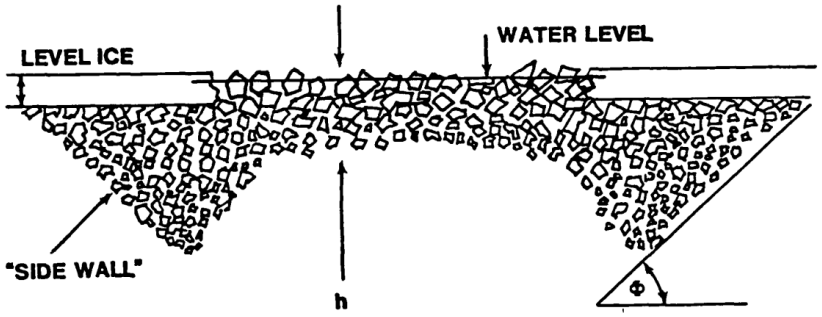

Figure 4: Transversal view of lateral piles at the edge of the channel

As a medium brash ice is regarded experimentally as rigid pieces of ice in water, although in real scenarios several types of ice will be part of the brash ice layer, such as small ridges, mush ice and more. This particularity makes the testing or modeling more complicated due to the amount of different interactions involved.

With that being said it is worth to mention that the majority of the works done in the subject ignores this fact and assumed the rigidity of the ice pieces to be a basic principle for the calculation, this work also will take this assumption but generally speaking there is no need for that restriction in our formulation if the appropriate considerations are taken.

1.2 Comments on Mellor's theoretical approach

Due to the complexity of the physics involved in brash ice, there is basically no study attempts from the theoretical point of view except for the work of Mellor [1] which will be shortly discussed here due to the important links, key ideas and their possible applications into the proposed simulation.

In his work brash ice is described as a granular medium that behaves as a yielded Mohr-Coulomb solid at low ship speeds, in this way the lateral stresses are easily obtained once the value of the vertical component of pressure is known from a simple hydrostatic relation taking into account whether the brash ice layer is above or below the waterline.

Once these remarks have been made the side pressure is calculated by the Rankine theory of soils where brash ice is taken as having an active pressure, the rest of the necessary parameters are taken from experimental data [1], but it is worth to mention that the values are very scatter and that makes this first approximation highly dependent on future experimental results.

Finally using this approach a formula is given to calculate the maximum brash ice thickness that a ship can navigate through. This formula is based on the ship breadth, and actually refers to the brash ice thickness needed to stop the ship forward movement for a given propulsive power.

Although the results are quite good as a first approach, the real fact to highlight in this work is the behavior described and the physics used to address the problem as a granular medium.

2 BRASH ICE EXPERIMENTAL BEHAVIOR

2.1 Mechanical properties

Brash ice mechanical behavior has been scarcely studied up to some extent, the main difficulty being, testing this mixture as a single medium, that means, coming up with an experiment that can actually shed light on the shear strength, cohesion and more properties. The medium consideration for brash ice will be further discussed in Section 2.2.

The first experiment reviewed for this work was carried out in HSVA facilities by Hellmann [3], here a shear box was designed specifically to test the mechanical properties of brash ice, the results of the test showed a specific shear behavior consisting on three shear modes as shown in Figure 5, the first two following a normal Mohr-Coulomb frictional pattern and the third one almost following a plastic one.

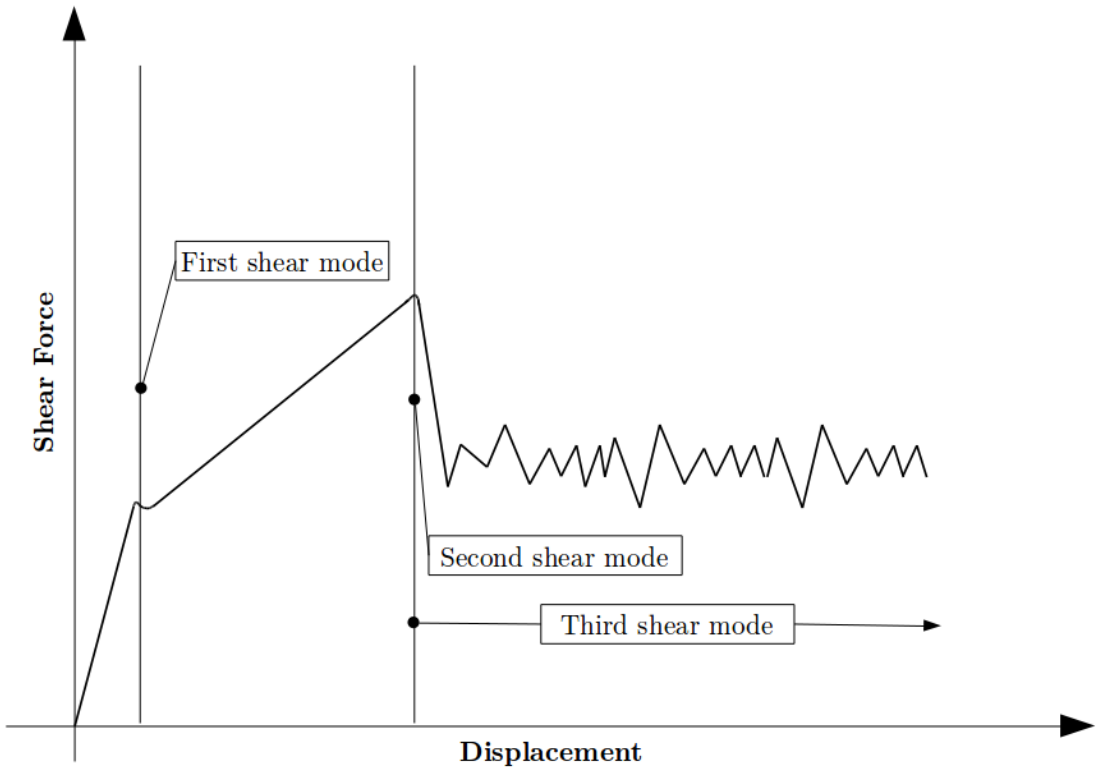

Figure 5: Brash ice shear modes

Several remarks have to be made about this behavior, first, the test has been conducted at several speeds but all below 100 mm/s, second, the reduction of the area used for the shear stress calculation was not taken into account, and finally a certain amount of normal stress had to be produced inside the box so this is not exactly a pure shear stress value.

Although some improvements were made based on this work by Sandkvist [4], these were mainly in the way of applying the normal pressure, so the former remarks still hold.

The results obtained in these experiments reflect clearly that the shear mode theory holds, but also that the values of the friction angles and shear strength of the brash ice need further experimentation to be evaluated safely.

The dispersion of the results and the lack of information about the exact contents of each mix medium, this is, percentages of mush, brash and so on, have to be taken into account to properly assess their influences on the parameters of this formulation.

Still these experiments show in general that the kind of behavior that can be assigned to a granular medium such as brash ice is that of a Mohr-Coulomb solid in the first two modes and then a plastic behavior once it is yielded in the third mode. The values of parameters will be discussed later in this work but the behavior here shown will set the basis of our first steps towards a simulation.

2.2 Brash ice as a medium

Following the same line of the work reviewed before, several tests were conducted by the US-Navy during the 80's, in his document about brash ice behavior [2], several concepts are clarified and one hypothesis is put forward that will in fact be of major importance in this simulation attempt.

It is important to remark that regarding brash ice as a medium adds several simplifications that can have major impacts on the results, first the size distribution of ice pieces is completely regarded as independent of the characteristics, the same goes for the irregular geometries which in general are considered as pseudo-spheres, also it is important to point out that since the medium is a mixture of water and ice specific considerations will have be taken into account in the formulation as it i shown in section 4.1.

The first idea important to discuss is the concept of brash ice as a medium with specific characteristics and specific behavior, both working together to completely define the so-called rheology[1] of the medium, this will define the behavior of brash ice in all the conditions that the experiments allow us to predict.

To propose a specific rheology for this medium first three experimental observations are given as key for the behavior of this medium:

1. When it is not refrozen brash ice has no tensile strength. It is regarded as a collection of rigid ice pieces floating in water.

2. A brash ice channel generally closes again after a ship has passed through it.

3. Roughly speaking, brash ice pieces maintain their relative positions after a vessel passage.

From these important remarks several conclusions can be made, first brash ice rheological model can be neither elastic (as for level ice) nor viscous turbulent (as open water), this concluded from experimental observations 1 and 3 respectively, meanwhile the lack of tensile strength discards an elastic model, the lack of mixing of ice pieces points to a non turbulent behavior of the medium as a whole, and so brash ice will not behave like level ice or water.

Several experiments were made with different type of ice-going ships to test the resistance in this medium, and a specific trend was found, at low Froude numbers the new medium behaves as a Mohr-Coulomb soil such as the one described in Mellor's work, and after a certain threshold, where the medium is fluidized, the behavior resembles to a laminar one as shown in Figure 6.

[1]This term is used in fluid mechanics to name the relation that exists between the strain-rate tensor and the extra stress tensor, and it will be fairly discussed later in this work, one example would be a viscous rheology which is the common standard model for fluids.

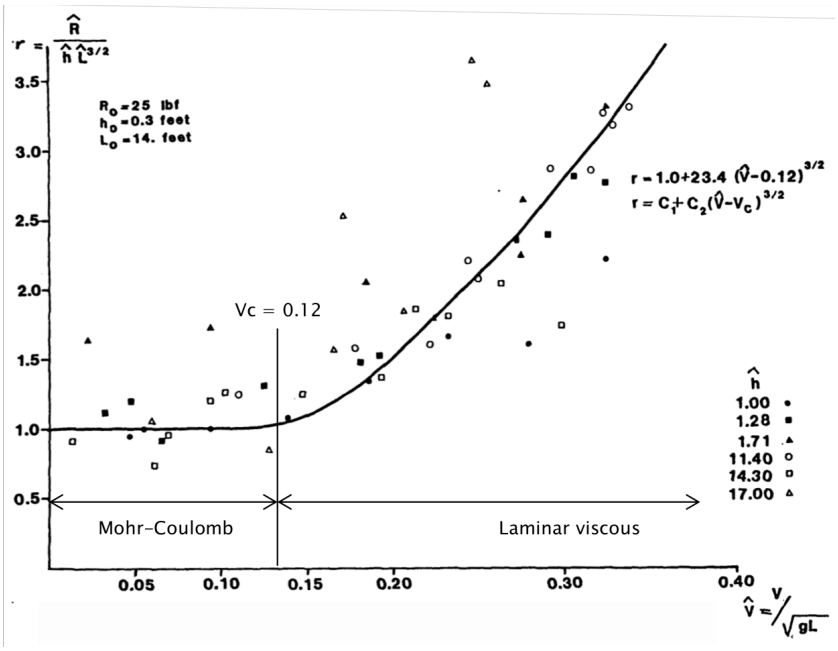

Figure 6: Brash ice rheological model proposal [2]

The importance of this proposal lays in the fact that here all the behaviors of brash ice can actually be captured in a single model with as much simplicity as is needed for the first steps in a simulation process. This simplicity can be implemented in a granular medium once all the parameters are known, it is then important to have in mind that although the parameters for the mohr-coulomb region have been studied, as explained in previous sections, the parameters for the laminar viscous region have not yet been found experimentally.

The only value known for the laminar viscous region is the Froude number of the vessels shown in Figure 6 as $V_c = Fn = 0.12$, this can be used as a velocity threshold to the laminar viscous zone, but for a medium model a strain-rate value is needed and this value has not yet been investigated.

Thus the model can be used to idealize brash ice as a single medium with different rheological behaviors depending on the speed of the body tested or the strain-rate of the medium. With this key idea in mind and several others exposed before an analysis of some methods to address the problem in a simulation can be done.

Part II
EVALUATION AND SELECTION OF METHODS

In order to do a numerical implementation of brash ice, it is necessary first to review briefly which are the options that could be used in terms of physical formulation and numerical discretization, and determine which is the most suitable for this project. Second, after selecting one, a more profound explanation is needed to cover the full basis of the idea. Finally to select an open source method suited for the application. It is then the intention of this section to cover all these details.

3 EVALUATION OF METHODS

3.1 SPH single-phase method

The first method discussed for a simulation attempt is based on the observations mentioned before about the granular behavior of brash ice and the rheological relation of a viscous-plastic medium proposed. It is necessary then to properly defined the idea of a granular medium[2] modeled as a continuum medium and write down the necessary equations to represent it.

From the known equations of fluid mechanics in the Lagrangian form expressed in the tensorial notation[3] we have:

$$\frac{d\rho}{dt} + \rho\frac{\partial v^k}{\partial x^k} = 0 \text{ ... Continuity equation}$$

$$\rho\frac{dv^\alpha}{dt} = \frac{\partial \sigma^{\alpha\beta}}{\partial x^\beta} + \rho g^\alpha \text{ ... Momentum equation}$$

The stress term ($\sigma^{\alpha\beta}$) in the momentum equation can then be decomposed in an isotropic pressure term and an extra stress term as follows:

$$\sigma^{\alpha\beta} = -p\delta^{\alpha\beta} + \tau^{\alpha\beta}$$

And a common formulation for the extra stress tensor[4] is:

$$\tau^{\alpha\beta} = \eta\dot{D}^{\alpha\beta}$$

Where $\dot{D}^{\alpha\beta}$, the deviatoric strain-rate tensor can also be decomposed as follows:

$$\dot{D}^{\alpha\beta} = D^{\alpha\beta} - \frac{1}{3}D^{kk}\delta^{\alpha\beta}$$

$$D^{\alpha\beta} = \frac{1}{2}\left(\frac{\partial v^\alpha}{\partial x^\beta} + \frac{\partial v^\beta}{\partial x^\alpha}\right) \text{... strain-rate tensor}$$

[2]For further details see section 4.1.
[3]Full expansion of this notation leads to the common partial differential equations of fluid mechanics.
[4]Also called viscous or deviatoric stress tensor.

The decomposition shown above is typical in fluid mechanics, but now for a granular flow the term η has to account for different kinds of frictional relations instead of just the viscosity. These relations are called the rheology of the medium, and in general are set up in such a way that they are functions of an invariant of the system, usually the second invariant of the deviatoric strain-rate tensor ($II_{\dot{D}}$) is selected and the expressions are left as follows:

$$\eta = f(II_{\dot{D}}) \ ... \text{ where}$$

$$II_{\dot{D}} = \tfrac{1}{2}\left[\dot{D}^{\alpha\beta}\dot{D}^{\alpha\beta} - (\dot{D}^{kk})^2\right]$$

And since $\dot{D}^{\alpha\beta}$ is a deviatoric tensor in 3D the second invariant is reduced to the following expression:

$$II_{\dot{D}} = \frac{1}{2}\left[\dot{D}^{\alpha\beta}\dot{D}^{\alpha\beta}\right]$$

In this way several functions can be selected to account for the rheology such as viscoplastic models [8], fully plastic models [6], or frictional models such as Mohr-Coulomb types [7].

Each one with its own unique characteristics that are useful to model specific processes, for example the Mohr-Coulomb models has been used in 2D or 3D[5] to model dynamical systems where several solid particles exhibit friction interaction, the fully plastic and viscoplastic are proposed for different mediums that can change its behavior according to specific parameters.

This formulation alongside with the equations of a continuous medium completely models a granular flow in a rather easy way. From the point of view of a computational model, these equations in the Lagrangian form can be solved by several numerical methods, the smoothed particle hydrodynamics (SPH) method[6] is proposed in this work to take full advantage of this kind of formulation.

An example of this methodology is provided in Figure 7, here a Mohr-Coulomb type rheology simulation [7] is performed for ice floes floating in water moving under the action of wind, left hand of the figure shows a SPH simulation with the granular flow equations shown above and the right hand side shows same simulation following a particle approach. The comparison is given to evaluate the effectiveness of the SPH method against more conventional particle methods.

[5]The 3D extension its called Levy-Mises rheology.
[6]For further information see section 4.2.

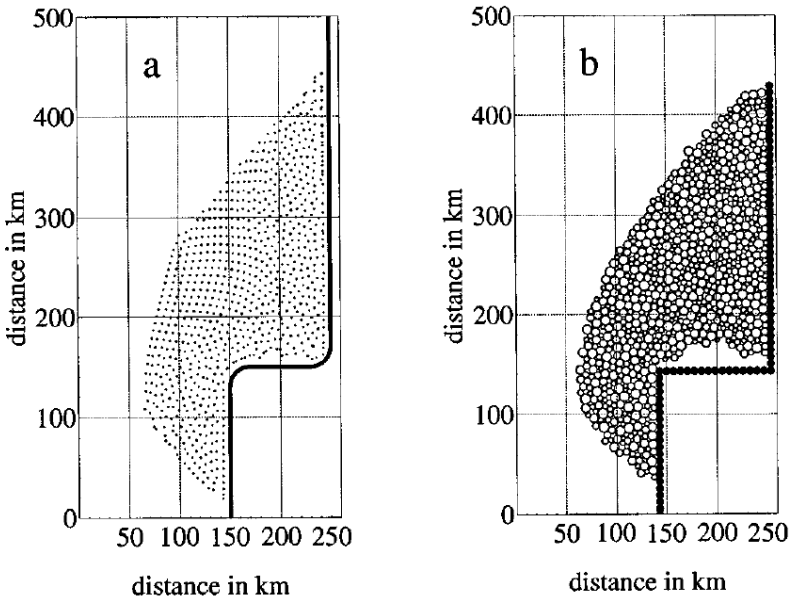

Figure 7: Example of Frictional Mohr-Coulomb type Rheology [7]

Also it is worth to keep in mind that this formulation is ideal to replicate the brash ice behavior described experimentally taking into account the plastic and viscous response at the same time, avoiding more non-linearities coming from the convective terms and keeping track of the free surface in a natural way.

On the downside several effects are completely disregarded giving rise to the possibility of lack of physical consistency, mainly because only one medium can be expressed and in reality the brash ice lower layer will be in contact directly with water and these effects cannot be replicated with only one phase, although a reasonable boundary condition can be implemented to account for this interaction. Also the particles size is completely missing in the formulation, although a correction in the thermodynamic pressure can be added to account for this.

In general this mathematical formulation and numerical method together, have proven to be an effective way of modeling granular flows and are currently the trend when a simulation of this kind of mediums is performed.

3.2 SPH two-phase method

The second methodology studied is an extension to the previous one, basically it has the same features but in this case the water can be added as an independent phase into the formulation to account for the interaction of the lower layer of brash ice with water.

To add the second phase on the formulation a couple of changes have to be performed into the mathematical formulation of the problem, and also some adjustments have to be made in the numerical SPH discretization. Below a brief discussion of two different methods to accomplish this goal.

The first methodology is based on the concept of volume fractions with this idea all the phases can be represented and solved in the same equation thus avoiding the need to decouple the equations for each phase and thus just handling one [10]. The volume fraction basically describes the ratio between the two mediums and affects the velocity calculation in the continuity equation and adds a specific term in the extra stress tensor calculation inside the momentum equation.

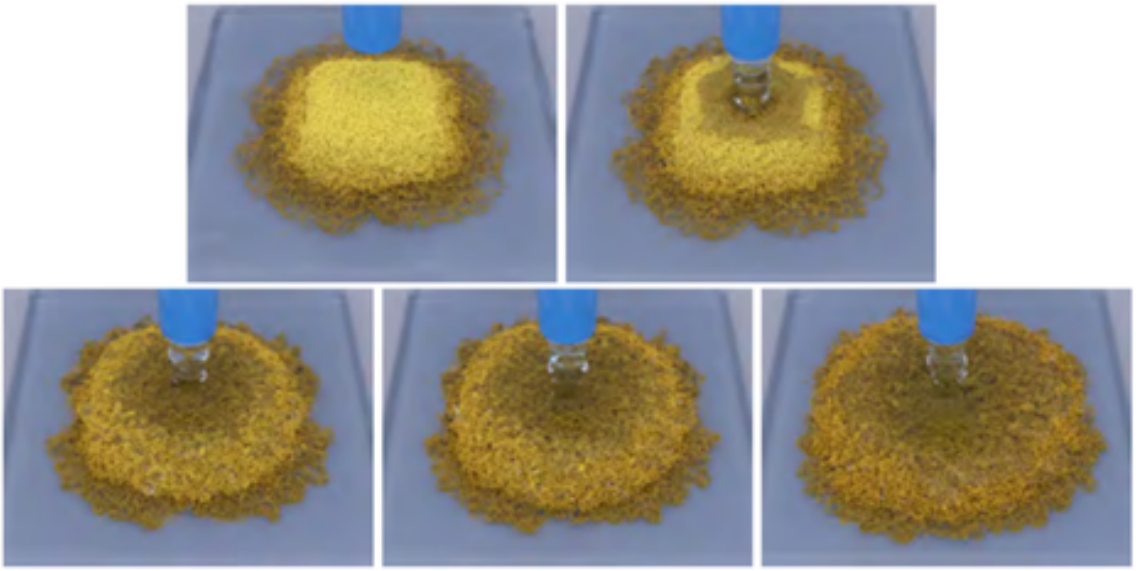

Figure 8: Example of two phases simulations with first methodology [10]

Several features such as mixture, porosity and changes of phases can be taken into account in this models, making them very attractive for simulations of granular soils and fluids dynamical interaction as shown in Figure 8, here an example of sand mixing with water is provided. Sand is modeled as a porous medium and thus it can get wet by water, at the end the pile of sand collapses due to a decrease in its deviatoric stress tensor.

The second methodology takes into account both phases separately linking them by adding some forces[7] at the interface and by allowing the granular phase to have a complex rheology so that it behaves differently depending on the conditions to better represent the interaction between both phases[9]. See Figure 9.

[7]Seepage forces.

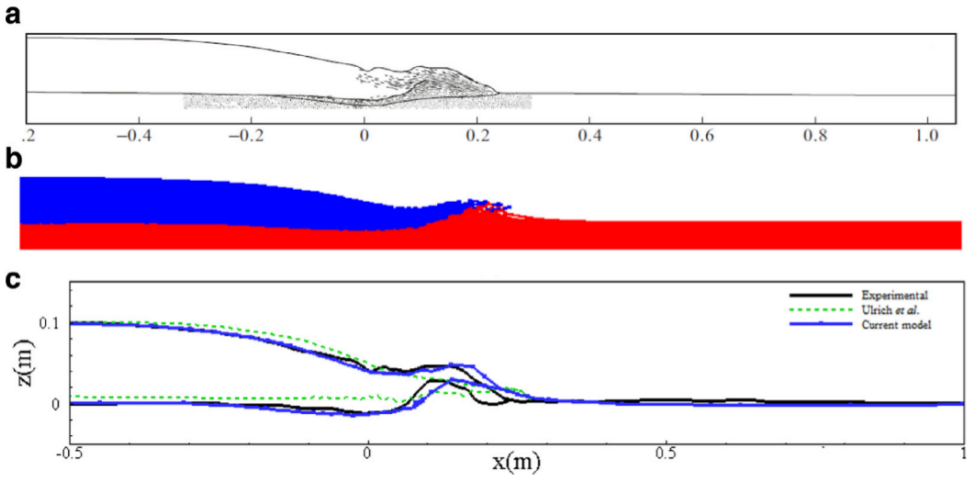

Figure 9: Example of 2 phases simulations with second methodology [9]

Both methodologies are quite interesting and certainly will model the physical characteristics of brash ice better than the previous one, taking into account not only the interface with water but also mixing effect in the stern flow where the concentration of the granular phase can decrease and thus water will take its place.

On the downside the methodology is quite new and is still under research, also the complexity added in the numerical discretization is quite high. Although the formulation is quite similar, is expected to have a big negative impact in the implementation and simulation time.

3.3 Coupling methods

The third methodology is completely different than the first two and it is based on the experimental observation that brash ice can be regarded as rigid pieces of ice floating in water, so a methodology to describe solid-solid interaction and fluid-solid interaction is needed [19].

Since both interactions are not the same in terms of the physical formulation, two mathematical discretizations are needed together with a way to couple them to account for the full interaction, in this case and according to the research made the Discrete Element Method (DEM) and SPH will be studied to represent the solid-solid and the fluid-solid interaction respectively. See Figure 10.

The reason why these methods are selected is simple, for solid-solid interactions DEM is one of the most recommended methods and it has been highly used in the industry and for the fluid-fluid/solid interaction SPH can have some advantages because of the particle formulation and also because of its availability in the open sources explored for this project[8].

[8]See 5.2 for further information.

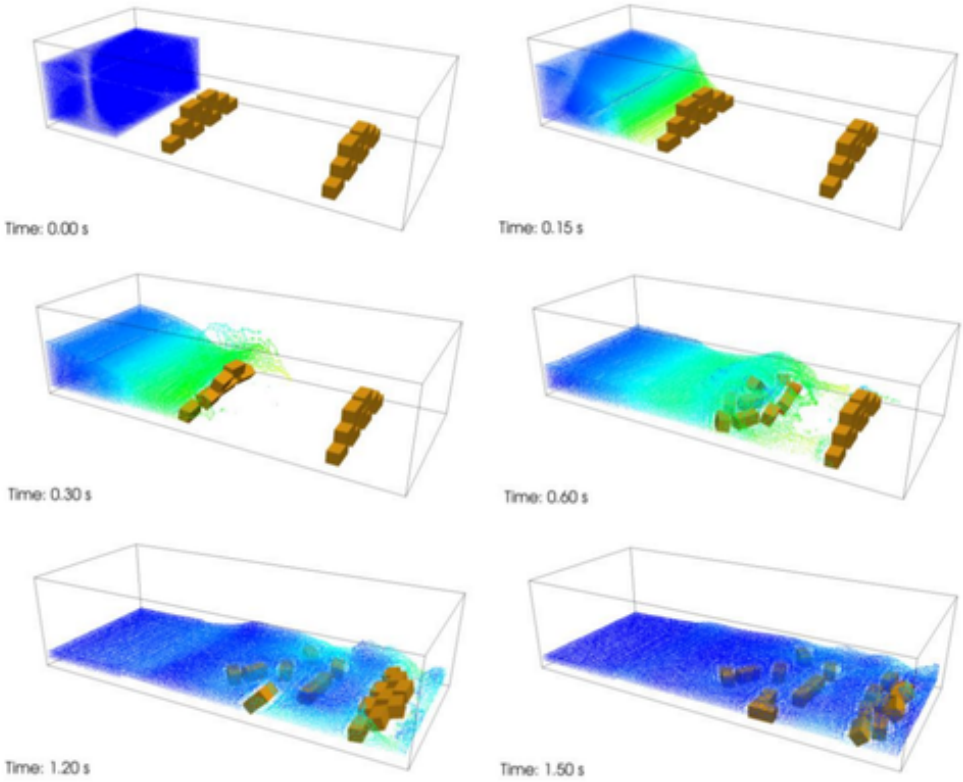

Figure 10: Example of coupling method [19]

It is clear that this methodology will correctly represent the movement of the ice chunks in the water flow, also it will capture in a much better way the idea of rigid bodies moving in water and interacting between themselves, taking into account different shapes and sizes, and finally it will provide high visualization features for each ice piece that will be able to contrast with images or videos of experiments.

On the downside the computational time will increase dramatically, at least 10 times more, and the model will most likely fail at high speeds due to the rigid formulation of the ice pieces that will not properly represent the experimental observations of laminar behavior after the medium is fluidized.

3.4 Physically based methods

The fourth and last methodology is the only one based on a previous simulation attempt of brash ice performed by Prof. Konno in Japan [11], the general idea of this simulation lies in a concept known as physically based modeling which is a method used to simulate numerous, independent solid bodies interactions with features such as collisions, friction and more.

The forces coming from the fluid-solid interaction are modeled as virtual forces that affect each piece individually as follows:

$$\vec{F} = -\frac{1}{2} C_D A \rho |\vec{v}| \vec{v}$$

This formulation is then implemented within the framework of the Open Dynamics Engine (ODE), which is a library capable of calculating collisions, interaction forces and the momentum equations of rigid bodies. The idea is calculate the resistance of a ship passing through a short brash ice channel, although several improvements to increase the amount of ice particles and the complexity of their shapes in the model are currently under progress. See Figure 11.

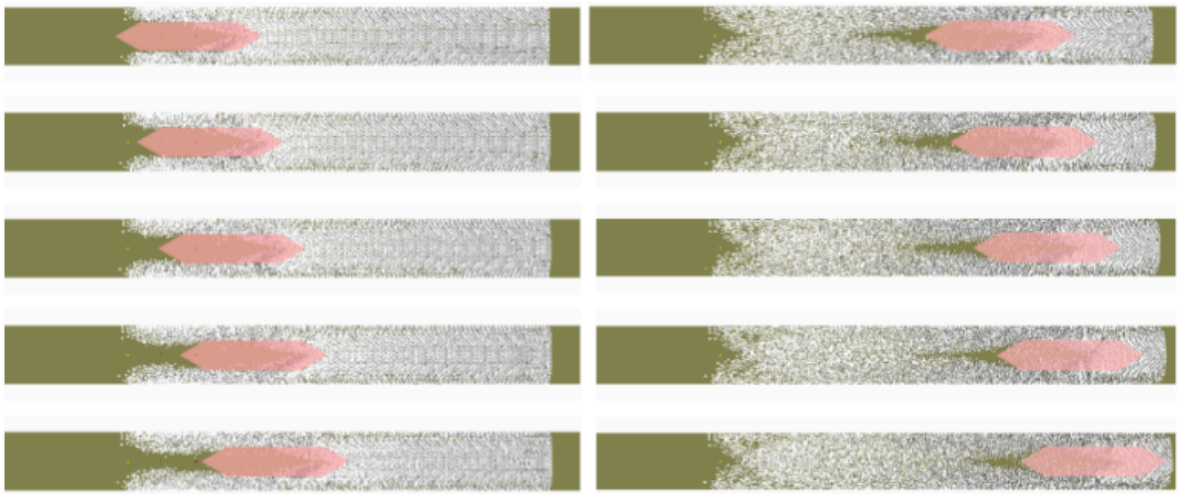

Figure 11: Example of physically based method [11]

This methodology has the advantage of being very good at describing the physics of the complex system and also simplifying in a nice way the interaction of water without the need of modeling the water domain, also it uses the ODE which is an open source suitable for this kind of simulation.

On the downside for the moment only short channels of brash ice can be modeled and several computational techniques have to be applied to be able to simulate larger channels, making the problem a high computational task, also as before the model may not be able to capture the right behavior at high speeds when brash ice is fluidized according to experiments.

3.5 Comparison and selection

After having briefly described four methodologies for attempting a simulation of brash ice and also having exposed in a somewhat rough manner the mathematical formulation of the physics involved and the numerical approaches, with their respective advantages and disadvantages, it is now important to select the ideal one for performing this task.

Below the 6 criteria used to assess the selection of the methodology are briefly listed and explained:

1. **Theoretical complexity:** This item refers to the amount of time needed to research and gather all the information needed and state of the art on the subjects.

2. **Physical representation:** This item refers mainly to the amount of simplifications made from the real phenomena, such as the ones described before.

3. **Equation development:** This item addresses the time needed to actually set up the system of equations to be solved for brash ice, since there is no such thing as a constitutive equation for modeling brash ice, it is clear that depending on the theory some methodologies will be more straight forward than others, and some extra knowledge has to be gained.

4. **Numerical method:** This item reflects the amount of time needed to pass from the equations to a discretized system that will be implemented.

5. **Program implementation:** This item reflects the amount of time estimated for implementation and it is highly dependent on the approach taken for the implementation, which could be full implementation or modification of a preexisting code[9].

6. **Cases testing:** This item reflects the estimated amount of time that the necessary trials of the new implementation will need to check several important features such as convergence, sensitivity and the overall runs for further development.

Basically all these factors were evaluated in terms of the expected time they cold take, being this the limiting factor in the work performed, so each one was evaluated with a score from 0 to 5 (worst to best) so the most suitable methodology is the one having the highest score.

METHOD	Single phase SPH	Two phases SPH	Coupling SPH+DEM	Physically based
Theoretical complexity	5	4	3	5
Physical representation	3	4	5	4
Equation development	4	3	2	3
Numerical method	5	2	2	3
Program implementation	4	4	2	3
Cases testing	5	2	1	3
TOTAL	26	19	15	21

Table 1: Selection of methods

As it is clear from the table the most suitable project taking into account all the constrains the first methodology is the most suitable for this work, although every single one remains as an alternative and are useful ideas for future developments.

[9]See section 5.1.

In the next section an extended discussion on all the theoretical concepts needed to set up the necessary equations and the numerical discretization will be provided, also the open source software selection for the single phase SPH approach will be studied and all the required topics for the implementation will be presented.

4 BRASH ICE MODEL

4.1 Granular flow definition

To start building the whole idea of brash ice ice as a granular flow first an accurate definition of granular flow is needed. For the purpose of this work a granular flow will be defined as a flow of grains (called the dispersed phase) in a fluid medium (called the carrier phase)[10], this means that more than two phases can be taken into account in the same medium.

In fact, a granular flow behaves neither as a solid nor as a fluid, having a behavior regarded as granular which means that have features of both [12], for example just as the experiments of brash ice have shown, first as a mohr-coulomb solid behavior and then a laminar viscous behavior just as a normal fluid. So although it is still a quite new topic under development this branch of physics can be regarded as a very useful way and actually one of the most used way for modeling dynamical processes of different mixtures of solid grains in fluid mediums.

Granular flows can be modeled as continuum mediums as briefly explained in section 3.1, by using the classical continuum equations of fluid mechanics, just by modifying the viscosity term, this powerful representation is very useful but some details have to be taken into account.

Two main problems have to be carefully explained here, first how to treat the multi-phases interaction within the same medium[11] and second how to make sense of the concept of pressure [13]:

> **Multiphases interaction:** The problem can be tackled with the rheology of the medium, the extra stress tensor[12] can be split in two components one for the fluid phase and one for the solid phase can be taken into account, thus accounting for both effects in a single stress term. Complex rules can then be proposed to account for special features of each phase, such as turbulent dissipation for the fluid phases or frictional laws for the solid grains phases. For the grain phases the relations usually are based on the plastic potential theory[13] and cannot be created disregarding these theoretical considerations, although some empirical formulations have been proposed [15].

[10] Actually its definition is quite broad and it can vary from a single phase grain phase dominant to more complicated two phase fluid-solid, depending on the characteristics of the mixture e.g. concentration.

[11] Not to be confuse with a the two phases approach but rather a method to take into account both solid and fluid mediums inside the same medium which is still a one phase.

[12] As defined in section 3.1.

[13] Theory used to predict velocity distributions of granular medium at yield that makes the connection between the stresses and deformation.

The pressure: The second problem is quite more complex, the first thing to bare in mind is that the common notion of hydrostatic pressure of a fluid medium cannot be directly apply in a granular flow due to the fact that granular flows can sustain friction interactions thus the pressure in a pile of grains will never exceed an specific value, this points out a big difference in the nature of the interaction between particles. This interaction is always of short time duration for fluid particles but has the possibility of being of long duration for grain particles. The second thing to have in mind is that the nature of the collisions of the particles for the thermodynamical balance is completely inelastic for the granular medium meanwhile for the fluid is regarded as completely elastic. The way around this problem is calculating different thermodynamical pressures for each phase and adding them in the pressure term.

When these two main problems are solved or are assumed in a specific way then a complete granular flow formulation can be provided inside the already known formulation of the continuum mechanics equations shown in section 3.1, below some examples of stress terms formulations for granular flows in 2D and 3D, showing some of the features that have been discussed before:

MOHR-COULOMB RHEOLOGY 2D [7]. See Figure 7.

$\sigma^{\alpha\beta} = P\delta^{\alpha\beta} - \tau^{\alpha\beta}$ Classic stress tensor decomposition.

$\tau^{\alpha\beta} = 2\eta\left(D^{\alpha\beta} - \frac{1}{2}D^{kk}\delta^{\alpha\beta}\right)$ Extra stress tensor formulation in 2D.

$\eta = min\left\{\frac{P\sin\phi}{D^1 - D^2}, \eta_{max}\right\}$ Mohr-Coulomb rheological formulation in 2D.

P : Thermodynamical pressure

$D^{\alpha\beta}$: Strain-rate tensor

ϕ : Friction angle

VON MISES AND LEVY MISES RHEOLOGY 3D [6][13]. Mohr-Coulomb rheology extension in 3D.

$\sigma^{\alpha\beta} = P\delta^{\alpha\beta} - \tau^{\alpha\beta}$ Classic stress tensor decomposition.

$\tau^{\alpha\beta} = \frac{2P\sin\phi}{\sqrt{II_{\dot{D}}}}\dot{D}^{\alpha\beta}$ Extra stress tensor formulation in 3D.

$\dot{D}^{\alpha\beta} = D^{\alpha\beta} - \frac{1}{3}D^{kk}\delta^{\alpha\beta}$ Deviatoric strain-rate tensor in 3D.

$II_{\dot{D}} = \frac{1}{2}\dot{D}^{\alpha\beta}\dot{D}^{\alpha\beta}$ Second invariant of the strain-rate tensor.

POULIQUEN–JOP–FORTERRE (JPF) EMPIRICAL RHEOLOGY 3D [15]. See Figure 12.

$$\begin{cases} D^{\alpha\beta} = 0, & \text{if } \mid \tau^{\alpha\beta} \mid < \mu_s P \\ \tau^{\alpha\beta} = \dfrac{\mu(I)P}{\mid D^{\alpha\beta} \mid} D^{\alpha\beta}, & \text{if } \mid \tau^{\alpha\beta} \mid \geq \mu_s P \end{cases}$$

$\sigma^{\alpha\beta} = P\delta^{\alpha\beta} - \tau^{\alpha\beta}$ Classic stress tensor decomposition.

$\mid D^{\alpha\beta} \mid = \sqrt{\frac{1}{2} D^{\alpha\beta} D^{\alpha\beta}}$ Second invariant of the strain-rate tensor.

$\mid \tau^{\alpha\beta} \mid = \sqrt{\frac{1}{2} \tau^{\alpha\beta} \tau^{\alpha\beta}}$ Second invariant of the shear stress tensor.

$\mu(I) = \mu_s + \frac{\mu_l + \mu_s}{\frac{I_o}{I} + 1}$ Empirical viscosity.

P : Isotropic pressure

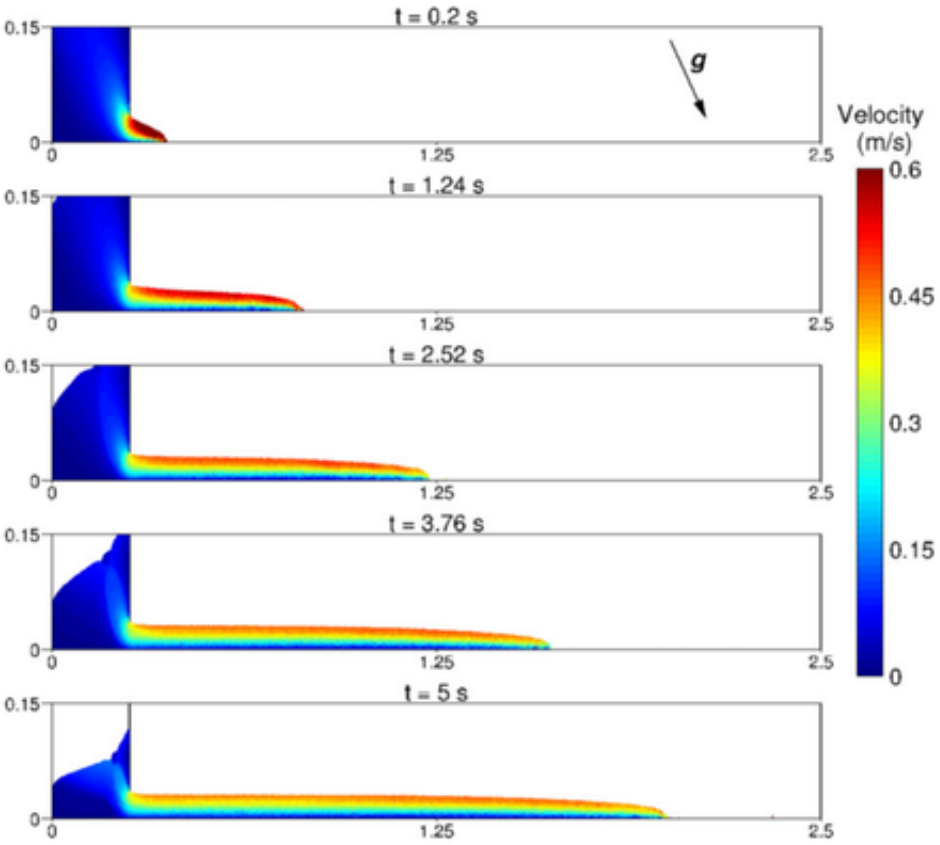

Figure 12: JPF Rheology example. Simulation using an empirical rheology in a dense granular medium under gravity. This rheology involves 5 parameters two grain-scale and three macroscopic constants.

VISCOUS-PLASTIC RHEOLOGY 2D [16]. See Figure 13.

$\sigma^{\alpha\beta} = -P\delta^{\alpha\beta} + 2\upsilon D^{\alpha\beta} + (\zeta - \upsilon)D^{kk}\delta^{\alpha\beta}$ Stress tensor decomposition.

$\zeta = \dfrac{P}{2\Delta}$ Non-linear bulk viscosity.

$\upsilon = \dfrac{\zeta}{e^2}$ Non-linear shear viscosity.

$P = \tan^2\left(\dfrac{\pi}{4} + \dfrac{\phi}{2}\right)\left(1 - \dfrac{\rho_i}{\rho}\right)\dfrac{\rho_i g t_i}{2}\left(\dfrac{N}{N_{max}}\right)^j$ Pressure equation extension for river ice.

$\Delta^2 = I_D^2 + \dfrac{II_D}{e^2}$ Delta function of the invariants.

I_D : First invariant of the strain-rate tensor

II_D : Second invariant of the strain-rate tensor

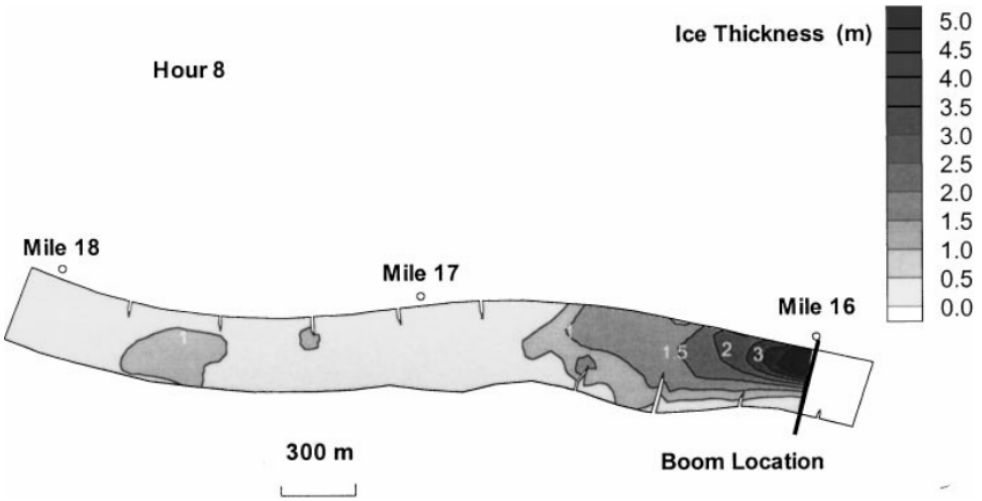

Figure 13: Viscous-plastic rheology. Simulation of river ice dynamics using a complex relation dependent on both first and second strain-rate tensor invariants and also with a pressure modification considering concentration features.

HERSCHEL-BULKLEY-PAPANASTASIOU (HBP) RHEOLOGY 3D [9]. See Figure 9. Rheological behavior that accounts for both plastic and viscous behavior in the same function with the regulation of the parameters m and n.

$\sigma^{\alpha\beta} = P\delta^{\alpha\beta} - \tau^{\alpha\beta}$ Classic stress tensor decomposition.

$\tau^{\alpha\beta} = f_1\dot{D}^{\alpha\beta}$ Extra stress tensor formulation.

$f_1 = \dfrac{\tau_c}{\sqrt{II_{\dot{D}}}}\left[1 - e^{-m\sqrt{II_{\dot{D}}}}\right] + 2\mu|4II_{\dot{D}}|^{\frac{n-1}{2}}$ HBP rheological formulation.

m : Constant to control the Newtonian region
n : Constant to control the Plastic region
$II_{\dot{D}}$: Second invariant of the deviatoric strain-rate tensor
μ : Apparent dynamic viscosity
τ_c : Limit shear strength

PITMAN–SHAEFFER–GRAY–STILES YIELD FUNCTION 3D [12]. Complex rheological behavior, extension of the levy-mises rheology that can handle dilatation and consolidation, making it a more complete description of granular flows.

$$\sigma^{\alpha\beta} = (P - ({}^{f}\mu^{bulk} D^{kk}))\delta^{\alpha\beta} + 2{}^{f}\mu^{shear}\dot{D}^{\alpha\beta} \qquad \text{Stress tensor decomposition.}$$

$${}^{f}\mu^{bulk} = \frac{P}{\sqrt{4\sin^2\phi II_{\dot{D}} + D_{kk}^2}} \qquad \text{Bulk viscosity.}$$

$${}^{f}\mu^{shear} = \frac{P\sin^2\phi}{\sqrt{4\sin^2\phi II_{\dot{D}} + D_{kk}^2}} \qquad \text{Shear viscosity.}$$

The intention of these examples is to show some of the features previously mentioned and clarify the idea of the characteristics of granular flows model as continuum mediums which will be crucial to proceed in this attempt.

4.2 SPH basic formulation for continuum mechanics

The smoothed particle hydrodynamics method was first invented in the 70's to study dynamical fission instabilities in rapidly rotating stars[14] in astrophysics and since then several new applications have been developed. In the 80's a full application to a fluid dynamics was devised, the main differences with the original method are the boundaries and the finite domain, both of which were successfully added into this numerical method.

The SPH method has gained popularity due to its completely mesh-free approach, a specific feature that allows to fully take advantage of the Lagrangian form of the continuum mechanics equations[15]. Nowadays this numerical method is widely used in fluid mechanics when a simulation with high deformations and(or) free surface under gravity is performed.

The method is based in kernel approximations of any given field function. The kernel approximation uses a kernel function W to approximate the function to estimate the value of a given field function in one point, this kernel function is an extrapolation of the Delta

[14]The method was preferable due to its full Lagrangian formulation which could capture fluids moving freely in 3D under the influence of self-gravity and pressure forces.
[15]See section 3.1.

Dirac function and thus guarantee the correct approximation in that point [14].

The benefits of this type of approximation appears when the gradients[16] of the field function are calculated, this operation is passed directly to the kernel thus simplifying the calculation[17]. The equations below show this approximation.

$$\langle f(x)\rangle = \int_\Omega f(x')W(x-x',h)dx' \qquad \text{Kernel approcimation of } f(x).$$

$$\langle \nabla f(x)\rangle = -\int_\Omega f(x')\nabla W(x-x',h)dx' \qquad \text{Kernel approximation of the gradient of } f(x).$$

$h:$ Smoothing length

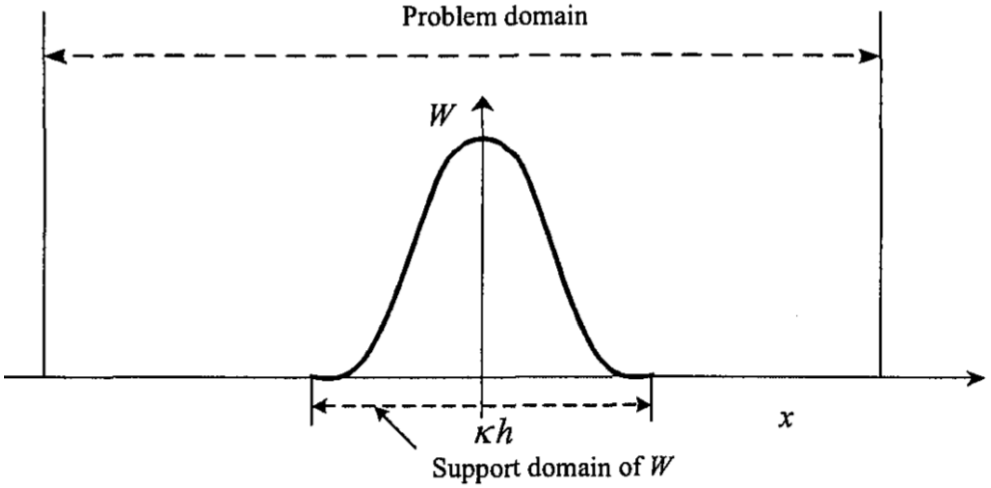

Figure 14: Kernel function approximation [14]

The kernel function has to comply with three main characteristics [14]:

1. **Normalization condition:** The value of the integral of the kernel function inside the support domain is the unity.

2. **The Delta Dirac property:** When the support domain approaches to zero, the kernel must approach the delta Dirac function.

3. **Compact condition:** Outside the support domain the value of the integral must vanish.

There exists a variety of kernel functions that have been studied, in this work the Quintinc Wendland formulation will be used, below the general formulation:

[16] In general any nabla operator.
[17] For basic proofs refer to [14].

$$W(r,h) = \alpha_D \left(1 - \frac{q}{2}\right)^4 (2q+1) \qquad \text{for } 0 \leqslant q \leqslant 2.$$

q : $\dfrac{r}{h}$

α_D : $\dfrac{21}{16\pi h^3}$ in 3D

r : Distance between particles

h : Smoothing length

After this approximation a second approximation known as the particle approximation where basically the domain surrounding the point, where the field function is being taken, is approximated by particles and thus the integral of the previous formulation changes into a summation applied to all this new surrounding particles, this particles have constant mass and can be regarded as Lagrangian packages of fluid that will move according to the equations of motion for a fluid.

It is important to mention that these "particles" are not real fluid particles and should not be confused with them, thus here they will be referred as SPH particles. The equations below show this approximation.

$m_j = \Delta V_j \rho_j$ Surrounding particle j mass.

$$\langle f(x) \rangle = \sum_{j=1}^{N} \frac{m_j}{\rho_j} f(x_j) W(x - x_j, h)$$ $f(x)$ particle approximation.

$$\langle f(x_i) \rangle = \sum_{j=1}^{N} \frac{m_j}{\rho_j} f(x_j) W_{ij}$$ $f(x_i)$ approximation for particle i.

$$\langle \nabla f(x_i) \rangle = \sum_{j=1}^{N} \frac{m_j}{\rho_j} f(x_j) \nabla_i W_{ij}$$ Gradient of $f(x)$ particle approximation.

$$\nabla_i W_{ij} = \frac{x_i - x_j}{r_{ij}} \frac{\partial W_{ij}}{\partial r_{ij}} = \frac{x_{ij}}{r_{ij}} \frac{\partial W_{ij}}{\partial r_{ij}}$$ Gradient of the kernel function W.

m_j : Mass of particle j

ΔV_j : Volume of particle j

ρ_j : Density of particle j

$f(x_j)$: Field function of particle j

W_{ij} : Kernel calculation between particles i and j

h : Smoothing length

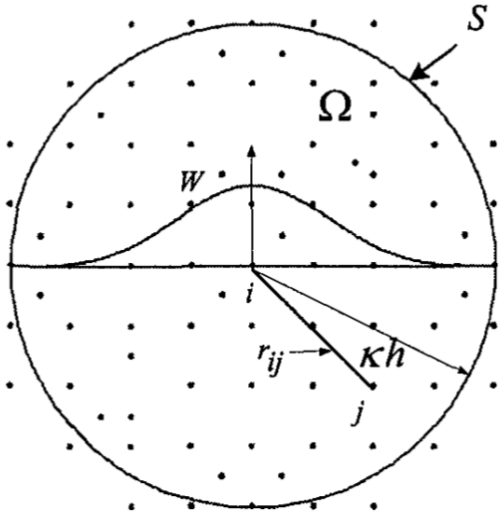

Figure 15: Particle aproximation [14]

With this discretization method basically the continuum equations can be discretized and both (the continuity equation and the momentum equation) can take several forms, below some of the most frequent use forms.

PARTICLE APPROXIMATION OF DENSITY

$$\rho_i = \sum_{j=1}^{N} m_j W_{ij} \qquad \text{SPH Density approximation example 1.}$$

$$\rho_i = \frac{\sum_{j=1}^{N} m_j W_{ij}}{\sum_{j=1}^{N} \frac{m_j}{\rho_j} W_{ij}} \qquad \text{SPH Density approximation example 2.}$$

$$\frac{d\rho_i}{dt} = \rho_i \sum_{j}^{N} \frac{m_j}{\rho_j} (u_{ij}^{\alpha}) \frac{\partial W_{ij}}{\partial x_i^{\alpha}} \qquad \text{SPH Density derivative example.}$$

PARTICLE APPROXIMATION OF MOMENTUM

$$\frac{du_i^{\alpha}}{dt} = \sum_{j}^{N} m_j \left(\frac{\sigma_i^{\alpha\beta} + \sigma_j^{\alpha\beta}}{\rho_i \rho_j} \right) \frac{\partial W_{ij}}{\partial x_i^{\beta}} \qquad \text{SPH Momentum equation example 1.}$$

$$\frac{du_i^{\alpha}}{dt} = \sum_{j}^{N} m_j \left(\frac{\sigma_i^{\alpha\beta}}{\rho_i^2} + \frac{\sigma_j^{\alpha\beta}}{\rho_j^2} \right) \frac{\partial W_{ij}}{\partial x_i^{\beta}} \qquad \text{SPH Momentum equation example 2.}$$

Given all the terms of the equation a small remark to calculate the pressure term has to be made. In the scope of the SPH method a specific branch known as WCSPH[18] is used

[18]Weakly compressible smoothed particle hydrodynamics.

to calculate this term with an equation of state, under the assumption that there is none or just a small degree of compressibility in the fluid, if a complete compressible medium is to be modeled the equation of energy conservation in its differential form would have to be solved along with the other two, thus making the system much more complex, so one more assumption is needed weak compressibility has to be supposed in the fluid to allow a given equation of state to evaluate the pressure term. Below a common example of this kind of equation:

TAIT'S EQUATION OF STATE [9]

$$P = b\left[\left(\frac{\rho}{\rho_0}\right)^{\gamma} - 1\right]$$

Where the parameters taken for this work have been set as $\gamma = 7$, $b = \frac{c_0^2\rho}{\gamma}$, where c_0 is the speed of sound in the medium, ρ the reference density and ρ_0 the particle density.

With this equation the SPH method is ready to be implemented and solved, the pressures can be computed, the continuity equation can be solved to calculate the density derivatives and the momentum equation to calculate the acceleration of the SPH particles. Now a numerical time scheme has to be used to go from one time step to the next one.

For this work an explicit scheme called Simplectic scheme with a predictor and corrector stage will be used, the method roughly consists in a half time step calculation of all the time derivatives and then a final correction for the full time step[19].

This summarizes the SPH complete scheme that is commonly used and will be the core of the implemented equations for this work.

4.3 Brash ice physical and numerical model

The rheological model selected in this work to model brash ice is a common viscoplastic model [6], which has a plastic perfect behavior to account for the strain independent resistance region that will be reached following a simple mohr-coulomb type frictional relation, and also has a laminar viscous region controlled by a strain-rate threshold based on the value of the root square of the second invariant of the deviatoric strain-rate tensor.

The key idea in this formulation is to try to capture all the experimental regions exposed in section 2.2. The differential equations then in tensorial notation are:

[19]For further information refer to [19].

$$\frac{d\rho}{dt} + \rho\frac{\partial v^k}{\partial x^k} = 0 \qquad \text{Continuity equation.}$$

$$\frac{dv^\alpha}{dt} = \frac{1}{\rho}\frac{\partial \sigma^{\alpha\beta}}{\partial x^\beta} + g^\alpha \qquad \text{Momentum equation.}$$

$$\sigma^{\alpha\beta} = -P\delta^{\alpha\beta} + \tau^{\alpha\beta} \qquad \text{Stress tensor classical decomposition.}$$

$$\tau^{\alpha\beta} = \eta\dot{D}^{\alpha\beta} \qquad \text{Extra stress tensor formulation.}$$

$$\eta = \begin{cases} 0, & \text{if } P < 0, \text{ Tension region} \\ \dfrac{2P\sin\phi}{\sqrt{II_{\dot{D}}}}, & \text{if } 0 < P \wedge 2Psin\phi < \tau_c \wedge II_{\dot{D}} < II^f_{\dot{D}}, \text{ Frictional region} \\ \dfrac{\tau_c}{\sqrt{II_{\dot{D}}}}, & \text{if } 2Psin\phi > \tau_c \wedge II_{\dot{D}} < II^f_{\dot{D}}, \text{ Plastic region} \\ \dfrac{2P\sin\phi}{\sqrt{II_{\dot{D}}}} + \mu, & \text{if } 0 < P \wedge 2Psin\phi < \tau_c \wedge II_{\dot{D}} > II^f_{\dot{D}}, \text{ Frictional plus viscous region} \\ \dfrac{\tau_c}{\sqrt{II_{\dot{D}}}} + \mu, & \text{if } 2Psin\phi > \tau_c \wedge II_{\dot{D}} > II^f_{\dot{D}}, \text{ Viscoplastic region} \end{cases}$$

Five regions are defined here for the rheological relation of the granular behavior, below a brief explanation, also a smaal diagram shown in Figure 16:

1. **Tension region:** No friction is applied to grains that are not under compression.

2. **Frictional region:** Strain independent friction region controlled by pressure that takes the medium to the plastic region, viscous influence is not accounted for if the viscous threshold $II^f_{\dot{D}}$ is not reached.

3. **Plastic region:** Strain independent plastic region with a maximum shear strength value τ_c, viscous influence is not accounted for if the viscous threshold $II^f_{\dot{D}}$ is not reached.

4. **Frictional plus laminar viscous region:** If $II_{\dot{D}}$ exceeds a certain threshold value $II^f_{\dot{D}}$ but the maximum shear strength τ_c has not been attain, the viscous value μ is added to avoid discontinuities in the field.

5. **Viscoplastic region:** If $II_{\dot{D}}$ exceeds a certain threshold value $II^f_{\dot{D}}$ and the maximum shear strength τ_C has been reached, the viscosity value μ is added to account for the complete viscoplastic behavior.

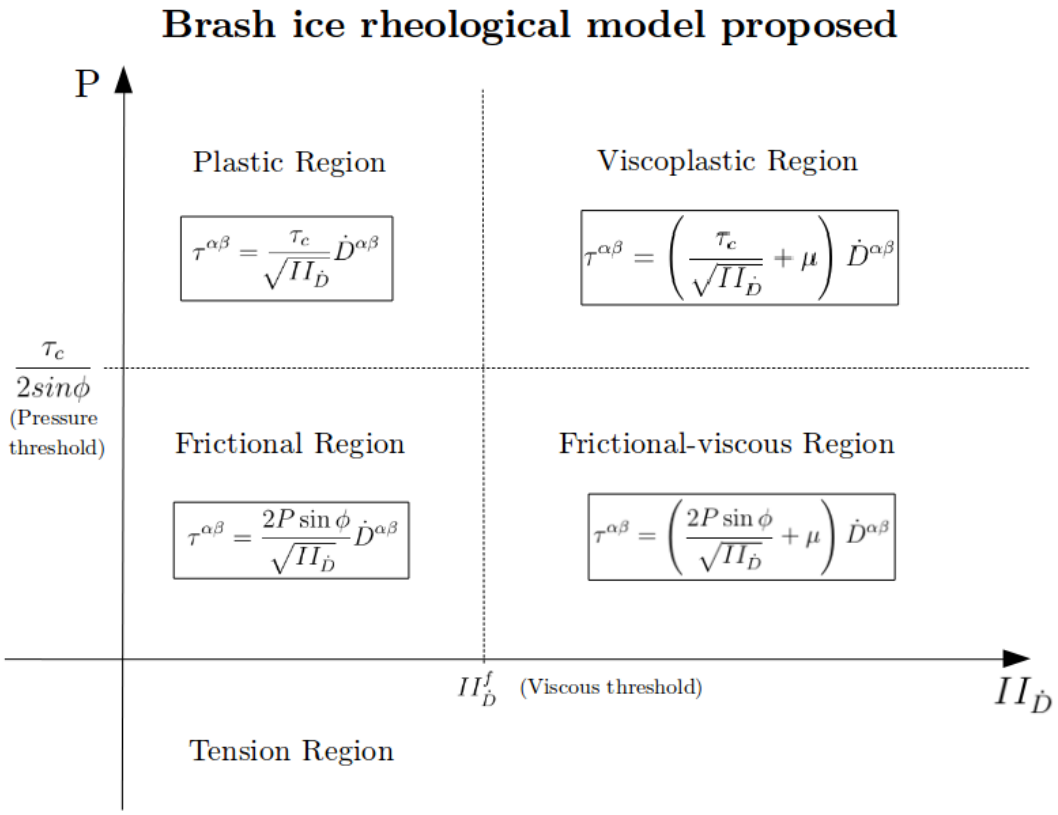

Figure 16: Brash ice rheological diagram

Four parameters are then needed to completely implement the model, from which only two are known up to some extent from experimental data, the shear strength τ_c and the friction angle ϕ. For the other two unknowns parameters more experiments are needed. In any case as part of this work some values are suggested taking into account different values of granular soils for the viscosity μ and assuming values for the viscous threshold $II^f_{\dot{D}}$.

According to the section 4.2 the corresponding equations for brash ice with the rheological model selected are:

$$\frac{d\rho_i}{dt} = \rho_i \sum_j^N \frac{m_j}{\rho_j}(u_i^\alpha - u_j^\alpha)\frac{\partial W_{ij}}{\partial x_i^\alpha} \qquad \text{Continuity equation.}$$

$$\frac{du_i^\alpha}{dt} = -\sum_j^N m_j \left(\frac{P_i + P_j}{\rho_i \rho_j}\right)\frac{\partial W_{ij}}{\partial x_i^\alpha} + \sum_j^N m_j \left(\frac{\tau_i^{\alpha\beta}}{\rho_i^2} + \frac{\tau_j^{\alpha\beta}}{\rho_j^2}\right)\frac{\partial W_{ij}}{\partial x_i^\beta} + g^\alpha \qquad \text{Momentum equation.}$$

$$\tau_i^{\alpha\beta} = \eta \dot{D}_i^{\alpha\beta} \qquad \text{Extra stress tensor.}$$

$$\dot{D}_i^{\alpha\beta} = D_i^{\alpha\beta} - \frac{1}{3}D_i^{kk}\delta^{\alpha\beta} : \text{ Deviatoric strain-rate tensor}$$

$$D_i^{\alpha\beta} = \frac{1}{2}\left(\sum_j^N \frac{m_j}{\rho_j}\left(u_j^\alpha - u_i^\alpha\right)\frac{\partial W_{ij}}{\partial x_i^\beta} + \sum_j^N \frac{m_j}{\rho_j}\left(u_j^\beta - u_i^\beta\right)\frac{\partial W_{ij}}{\partial x_i^\alpha}\right) \qquad \text{Strain-rate tensor.}$$

And thus the discretized versions of the equations selected to model brash ice are obtained in its most basic from. Now an open source software with the capacity of implementing this equations is needed, so the next section will be dedicated to the evaluation and selection of this software.

5 OPEN-SOURCE SOFTWARE EVALUATION

5.1 SPHysics serial, Parallel SPHysics and DualSPHysics

One of the first requirements in this project was the evaluation of an open-source software or a full implementation, the second option was discarded because of time constrains, so a suitable open-source code selection had to be made, the code was picked based on the specific methodology picked, taking into account that the code needed to solve the major tasks of SPH such as the searching algorithm, the continuum mechanics equations for fluids, the computation of the strain-rate tensor terms, and also the best usage of the available computer capabilities.

From the different open sources evaluated[20], a preliminary selection was done basically by taking into account the amount of information provided for future modifications and not only for users, and basically the search was reduced to three main options, all of them develop by Manchester University and University of Vigo [5], this mainly because of an specific turbulence model [17][18][19] known as SPS that is perfect as basis for the implementation of the selected rheological behavior. Following, a detailed description of these options mainly focusing on the characteristics that affect or help to implement the methodology selected.

First option SPHysics serial version [17]: This code was developed with the intention to serve as a tool for engineering applications, it is based on the SPH standard formulation. One of the best features of this code is the amount of information provided by the developers for users and for possible modifications, also the code is written in a very straight forward manner. As an extra feature it also allows the possibility of modeling cubic shapes as floating bodies and assign them initial rectilinear speeds.

To test running times the software was installed and several runs in 2D and 3D were made for different amount of SPH particles (See Figure 17), two details are worth to mention, first, since it is a serial code it does not take advantage of the total number of processors available, a considerable amount of time[21] is required for small 3D simulations of less than 60k SPH particles and second it has a limit of 100k SPH particles in the domain.

[20] Research based in several web pages dedicated to the subject such as www.sphere.org and also several forums between developers and users.

[21] Around 12 hours for models of 56k SPH particles, depending on the time step defined.

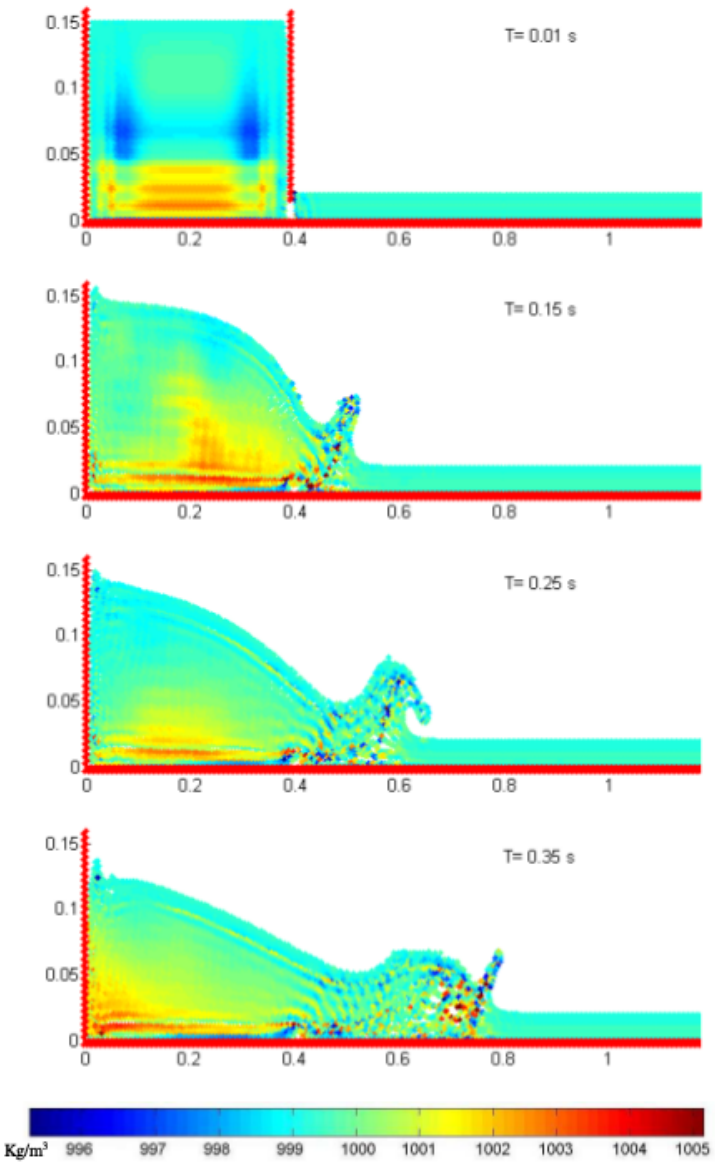

Figure 17: Dam break 2D simulation [17]

Second option SPHysics parallel version [18]: This code was developed as an extension of the previous version to allow much more complex computations and the possibility of taking advantage of the MPI[22] protocol and thus synchronize several computers or clusters, its worth to mention that out of the three main options this was the only one that was not tested.

Although it is clear that the time computations are very much reduced, and as per the guide simulations up to 7M SPH particles have been performed, the testing prove to be harder than expected due to the requirements for the computers, also the amount of code lines and its complexity increased which makes it difficult to modify. Basically aside from the MPI implementation details, the same extra features are shared between the serial version.

[22]Message passing interface, standard that defines the syntax and semantics developed to work in parallel computation for a wide variety of computer architectures.

Third option DuaSPHysics [19]: This code was developed as an extension of the serial version to allow MP[23] and GPU[24] implementation and also to enhance and improve its memory usage, for this purpose the language was changed from FORTRAN to C++ and CUDA, for the CPU and GPU implementations respectively.

The documentation of the code is not that complete and its complexity depends on the users C++ skills, it is worth to mention that only the CPU code was tested and used for this work, although the GPU capability is left as a speed boost in case needed. Also the improvement in memory management do not put limits on the number of SPH particles making it completely dependent upon the architecture and capabilities of the computer.

The computation times were tested for several 3D cases up to 1M SPH particles and the results proved to be several times faster than the serial version. Also, as extra features, the software includes the possibility of creating several geometries even import external geometries properly prepared (See Figure 18), coupling possibility between SPH and DEM method, predefined movements for different bodies and various types of boundaries bodies such as fixed or moving.

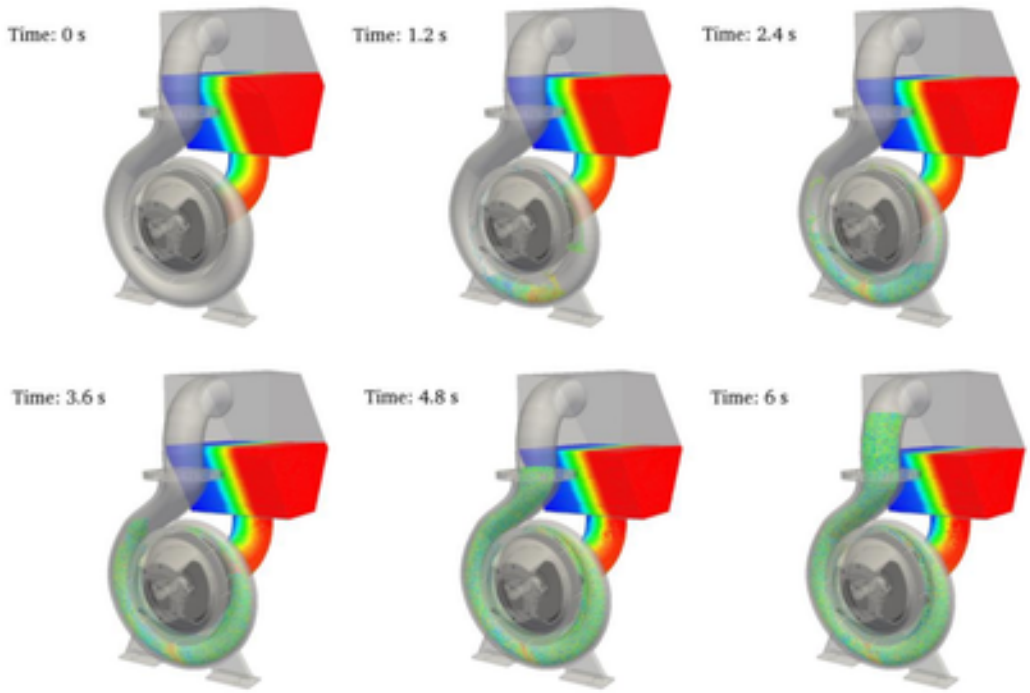

Figure 18: Pump simulation example [19]

5.2 Comparison and selection

After having described the details of the open source software evaluated for this work, some criteria will be described in order to select the most suitable for this development,

[23]Multiple processor implementation performed with Open MP, this allows to take advantage of all the processors available in a computer or cluster.

[24]Graphical processor unit implementation, only functional for NVIDIA graphic cards as a restriction of the CUDA controller.

the criteria will be assigned specific weights from 1 to 3 (less to most important respectively) and will be evaluated with scores going from 0 to 5 (worst to best respectively).

Below the 8 criteria used to asses the selection of the open source software with their respective weights in the parenthesis, are briefly listed and described:

1. **User friendliness (1):** This item measures how difficult it is to get used to the software just as a user, since it is required an understanding of its functioning to proceed with any modification.

2. **Documentation (1):** Amount of information provided by the developers in order become an average user and also in order to better understand the logics of the code to perform a modification.

3. **Computer architecture (1):** Refers to the computer requirements of each open source code, such as specific softwares or packages installation. And also refers to the capabilities for using multiprocessors (MP or MPI) or GPU's.

4. **Physical formulations (1):** What are the physical characteristics of a continuum medium already implemented in the open source that can be taken as an advantage for the implementation.

5. **Modifications needed (3):** How many modifications will be needed in terms of amount and complexity of the new code.

6. **Memory usage (3):** This item refers to the amount of memory used by the algorithm and the way it is allocated and stored, this is directly related to the amount of SPH particles that can be simulated.

7. **Computation speed (3):** This item refers to the amount of time it takes for a single simulation, for a given amount of SPH particles and time step selected.

8. **Future capabilities (2):** This item refers to the possibility of continuing this work, e.g. the capability of handling the geometry of a ship, or going into more complex rheologies or even more phases.

OPEN SOURCE	Serial SPHysics	Parallel SPHysics	DualSPHysics
User friendliness (1)	4	3	3
Documentation (1)	4	4	4
Computer architecture (1)	5	3	4
Physical formulations (1)	4	4	4
Modifications needed (3)	4	2	4
Memory usage (3)	2	4	4
Computation speed (3)	2	5	4
Future capabilities (2)	2	3	5
TOTAL	45	53	61

Table 2: Selection of Open source code

From table[25] 2 above it is easy to see that the software more suited for this task is DualSPHysics, mainly due to three factors: a very good memory usage that allows computations of millions of particles, the computational speed is fair and it can be accelerated and basically the amount of modifications needed is the same or less that for the other versions.

With the methodology selected, the equations completely formulated in the differential and in the numerical form and with an open source software picked for this specific kind of application, the next section of this work will focus mainly in the complete implementation of this idea.

[25]Results taking into account the weighing factors in the parenthesis.

Part III
IMPLEMENTATION AND COMPARISON

This part is dedicated to explain in a brief way the logic of the open source code selected to then explain the modifications proposed to implement the new rheological model. With this modifications a convergence and sensitivity analysis are presented. The new model is then compared with an experiment to check its capabilities and limits.

6 DUALSPHYSICS LOGICS

6.1 Main loop description

This section in intended to explain how the software logic works from both the user point of view and the developer point of view, with this purpose a brief description of the user interface is given and also the main features of the functions that are important for the simulation attempted in this work are introduced and detailed.

From the user point of view, first, the external parameters of the general geometrical and physical information are filled in a XML format sheet, this file contains all the entry data necessary to perform the simulations (see Figure 19) and it is the entry file for the preprocessing phase performed by an executable file called *GenCase4_linux64* [19] which generates all the information needed to start the main loop and thus the main executable file where all the computations are carried out (see Figure 20).

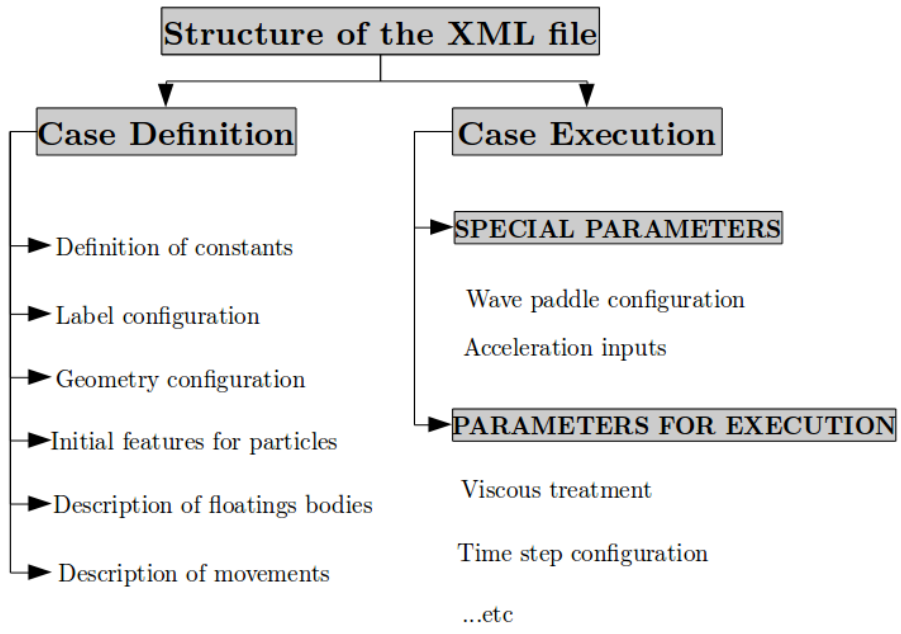

Figure 19: XML Input file description

From the developer point of view, the code can be explained starting from its main loop routine and then going inside to the specific inner functions. Thus the way these

inner functions can be altered to implement the relations discussed in part II can be described, giving a clear road map of the way the implementation was done.

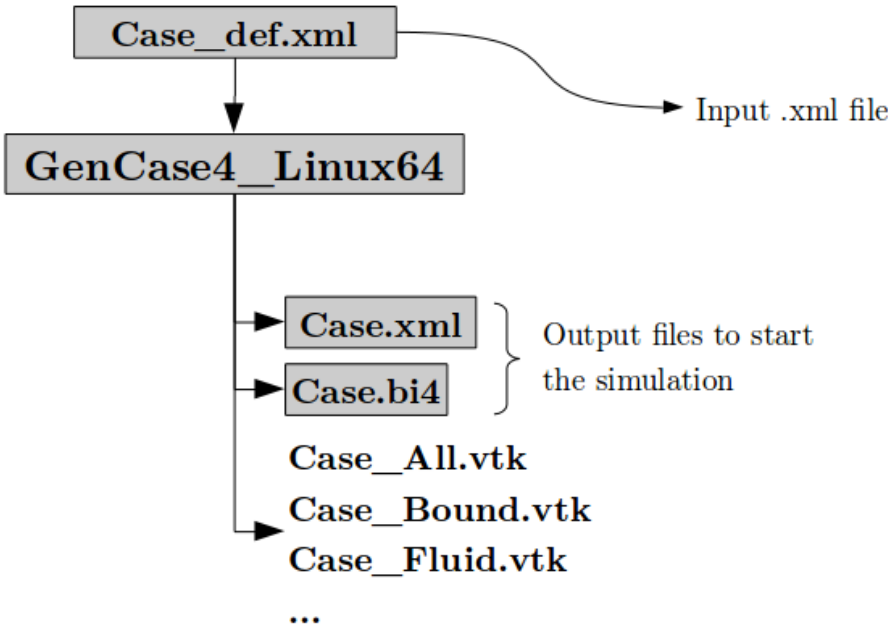

Figure 20: *GenCase4_linux64*, inputs and outputs

Once inside the main loop of the software, the decomposition of the operations executed can be described step by step. Following a brief explanation of the main structures needed to reach these main operations and their respective functions is given.

Basically the main loop starts by selecting between two explicit time schemes possibilities, either Verlet or Symplectic method.

The first one performs only one calculation per time step giving a computational time advantage, however every given number of time steps an extra step is included for stability reasons.

The second is a two staged method that has a predictor and corrector stages performing two calculations per time step, in the predictor phase the velocities are calculated in the middle of the time step and in the corrector stage all the characteristics are calculated for the full time step, this method has the advantage of being more stable and is preferable although it increases the computational time.

For this work only the Symplectic time scheme will be used[26]. The importance about first step is that inside this function called *ComputeStep()* (See Figure 21), all the computations of the continuity equation and of the momentum equation are performed.

[26]For further information on the mathematical formulation of both schemes refer to [19].

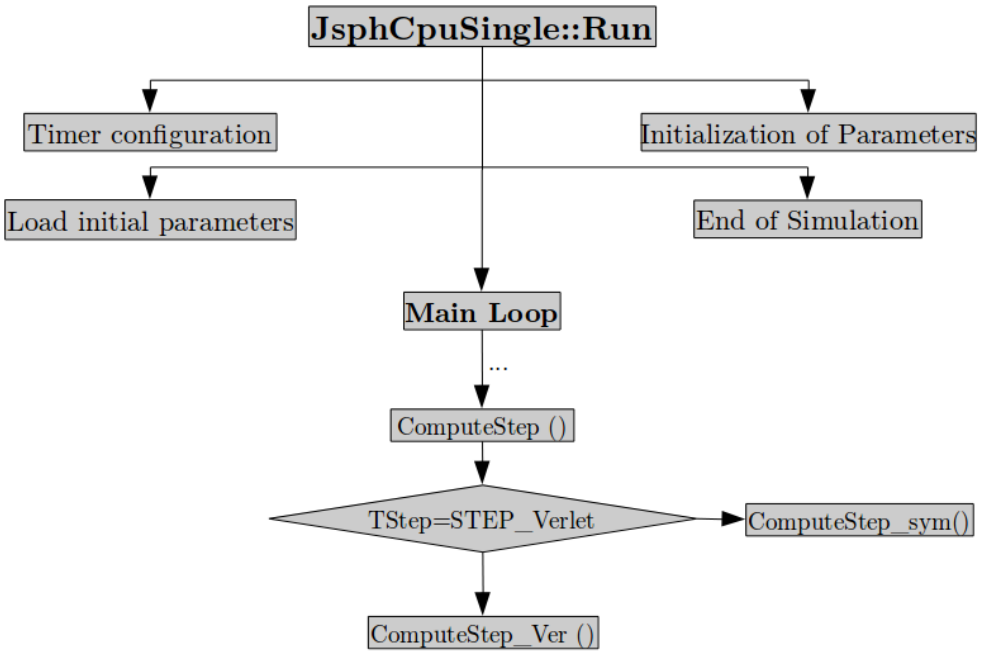

Figure 21: Main Loop Description

The symplectic method is then called by the function *ComputeStep_sym()*, and it is divided in two parts, predictor and corrector, both performing the same operations as it is shown in Figure 22.

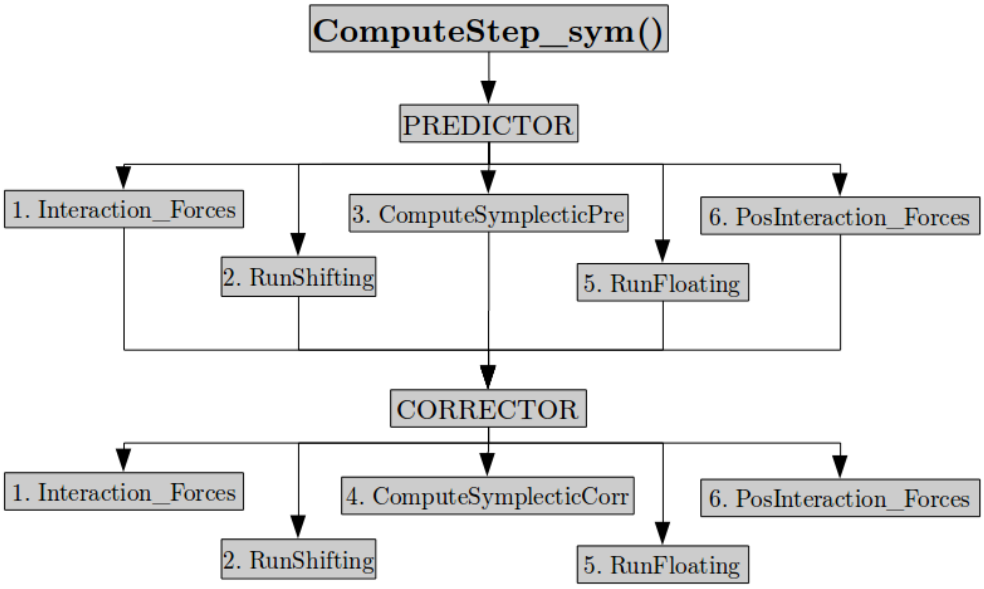

Figure 22: *ComputeStep_sym()* Description

The main tasks executed inside this function are briefly explained below:

1. ***Interaction_Forces*:** Calculates the density and velocity times derivatives for each particle[27], considering all contributions.

[27]For simplicity the word particle in this chapter stands for SPH particles unless otherwise specified.

2. ***RunShifting***[28]**:** Corrects the position of each particle with a Fick's concentration law, similar to a "re-meshing" algorithm, this, to avoid the formation of gaps between particles in the fluid domain.

3. ***ComputeSimplectic_Pre***[29]**:** Updates positions and velocities for half time step, this is for the predictor part, which means that it is calculated at half the time step.

4. ***ComputeSimplectic_Corr*:** Updates positions and velocities for the full time step, this is for the corrector part, which means that the variables are calculated at the full time step and the next time step computation will start with these values.

5. ***RunFloating*:** Computes forces exerted in a floating body, also computes its subsequent movement with the equations of motion for a rigid body.

6. ***PosInteraction_Forces*:** Erases and reallocates memory of the variables used in the continuity and momentum equations.

Basically the main loop executes all the computations needed, for each particle, the numerical estimation of the derivatives of density and velocity are calculated and the positions and velocities are all updated accordingly.

6.2 Interaction Forces method

Starting from the description made in the previous section here it is presented a brief look inside the *Interaction_Forces* method, due to its length, it will be breakdown to get to the crucial part that will be modified.

The *Interaction_Forces* method division is shown in Figure 23.

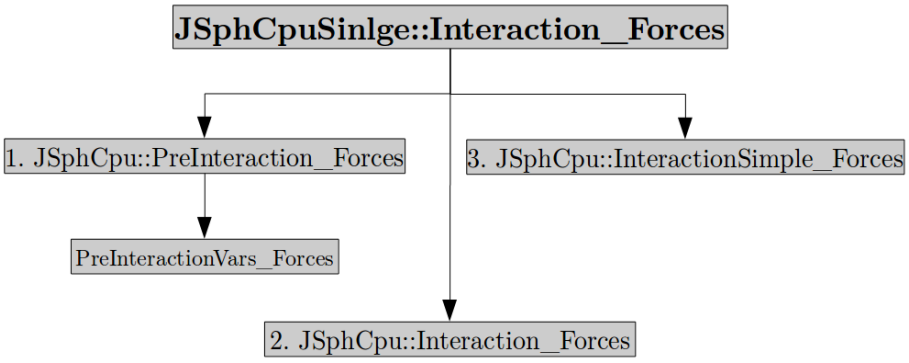

Figure 23: *JSphCpuSingle::Interaction_Forces* Description

Where the main tasks executed inside this function are briefly explained below:

1. ***PreInteraction_Forces*:** Initializes all the needed arrays to store the variables for each time update, such as density and velocity derivatives, also computes and

[28]For further information refer to [19].
[29]For further information refer to [19].

store the values of the pressure for each particle according to the Tait's Equation of State[30].

2. ***Interaction_Forces***[31]**:** Method that calculates all particles interaction, fluid-fluid, bound-fluid, moving-fluid, etc., according to the SPH formulation. All the calculations are made taking a double[32] variable type for the particle properties.

3. ***InteractionSimple_Forces*:** Same as the method described above but calculating all the variables in a simple floating format during the computation, which means less computer memory usage.

Since both methods *Interaction_Forces* and *InteractionSimple_Forces* are the same, only the first one is described here.

The method *JSphCpu::Interaction_Forces* relevant part can be divided in four more methods as shown in the Figure 24.

Below a brief explanation of each part:

1. ***InteractionForcesFluid*:** Inside this method the velocity and density time derivatives contribution is calculated for each particle, when the interaction is between two fluid particles or when the interaction is between a fluid particle onto a boundary particle.

2. ***InteractionForcesDEM***[33]**:** Calculates the interaction between boundary particles declared as DEM particles. Before making the calculation a conditional verifies if the interaction between boundary particles is going to be calculated with the DEM method, meanwhile the interaction between fluid and boundary particles will be calculated with the DBC methodology [21].

3. ***ComputeSpsTau***[34]**:** Adds a turbulence contribution computed by calculating extra stress tensor components with the Favre-averaged rate of strain tensor components using a methodology called Sub-particle scaling (SPS)[20].

4. ***InteractionForcesBound*:** Calculates the interaction of a boundary particle onto the fluid particles with the DBC methodology [21].

[30] See Section 4.2.

[31] Although the name is equal to the parent method, the difference is that both are defined in different classes so each one is called with the class name to which it belongs explicitly stated before the method is implemented.

[32] 8 bits variable.

[33] Discrete element method, used to calculate the motion of several solid particles with complex geometries and several degrees of freedom that are interacting.

[34] For further explanations see Section 6.4.

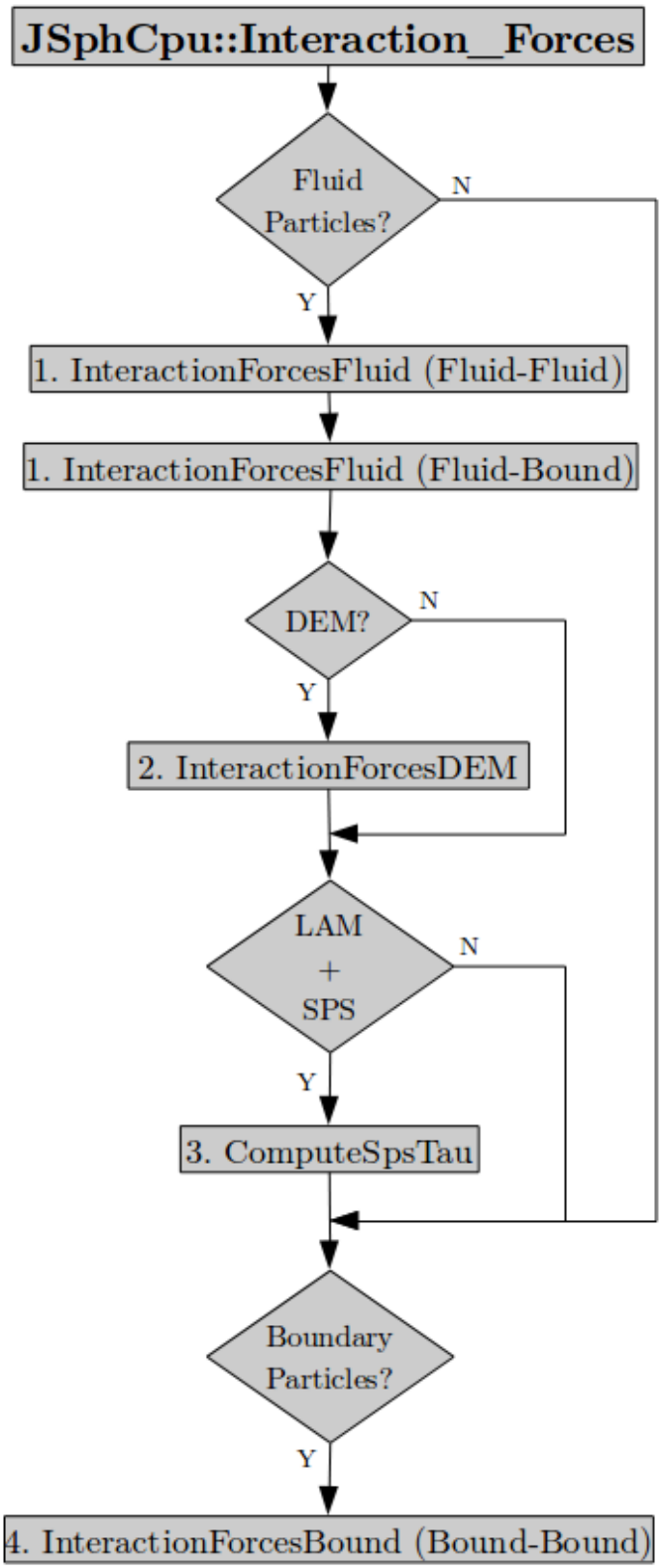

Figure 24: *JSphCpu::Interaction_Forces* Description

6.3 Interaction Forces Fluid method

In the method *InteractionForcesFluid* all the particles interaction contributions are calculated following the equations described in Section 4.3.

The main parts of the diagram are briefly explained and summarized below, Figure 25 shows a simplified diagram of the method.:

1. **Particle search and neighbour list:** Search for the neighbour particles and creates a cell-linked list from which to compute all the contributions.

2. **Acceleration pressure contribution:** Computes the acceleration contributions due to the pressure field with the formulation described in Section 3.1.

3. **Density time derivative:** Computes the density time derivatives with the formulation of the continuity equation described in Section 3.1.

4. **Acceleration viscous contribution:** Computes the acceleration contributions due to the artificial or laminar viscosity depending on the viscosity formulation selected.

5. **Acceleration turbulent contribution**[35]**:** Computes the acceleration contributions due to the SPS turbulent formulation.

6. **Delta SPH formulation**[36]**:** Correction applied in the continuity equation, that introduces a diffusive term to reduce the density fluctuations in the solution.

7. **Shifting algorithm**[37]**:** Correction applied to the position of particles, based on a Fick's concentration law, that avoids the formation of gaps between particles in the solution.

8. **Time derivatives summation:** Adds all the contributions for each particle and stores them to later update the positions and velocities in the predictor and corrector stages.

9. **Velocity gradient calculation:** At the end the velocity gradient components is calculated, to be used in the *ComputeSpsTau* method.

[35]For further explanations see Section 6.4.
[36]For further information refer to [19].
[37]For further information refer to [19].

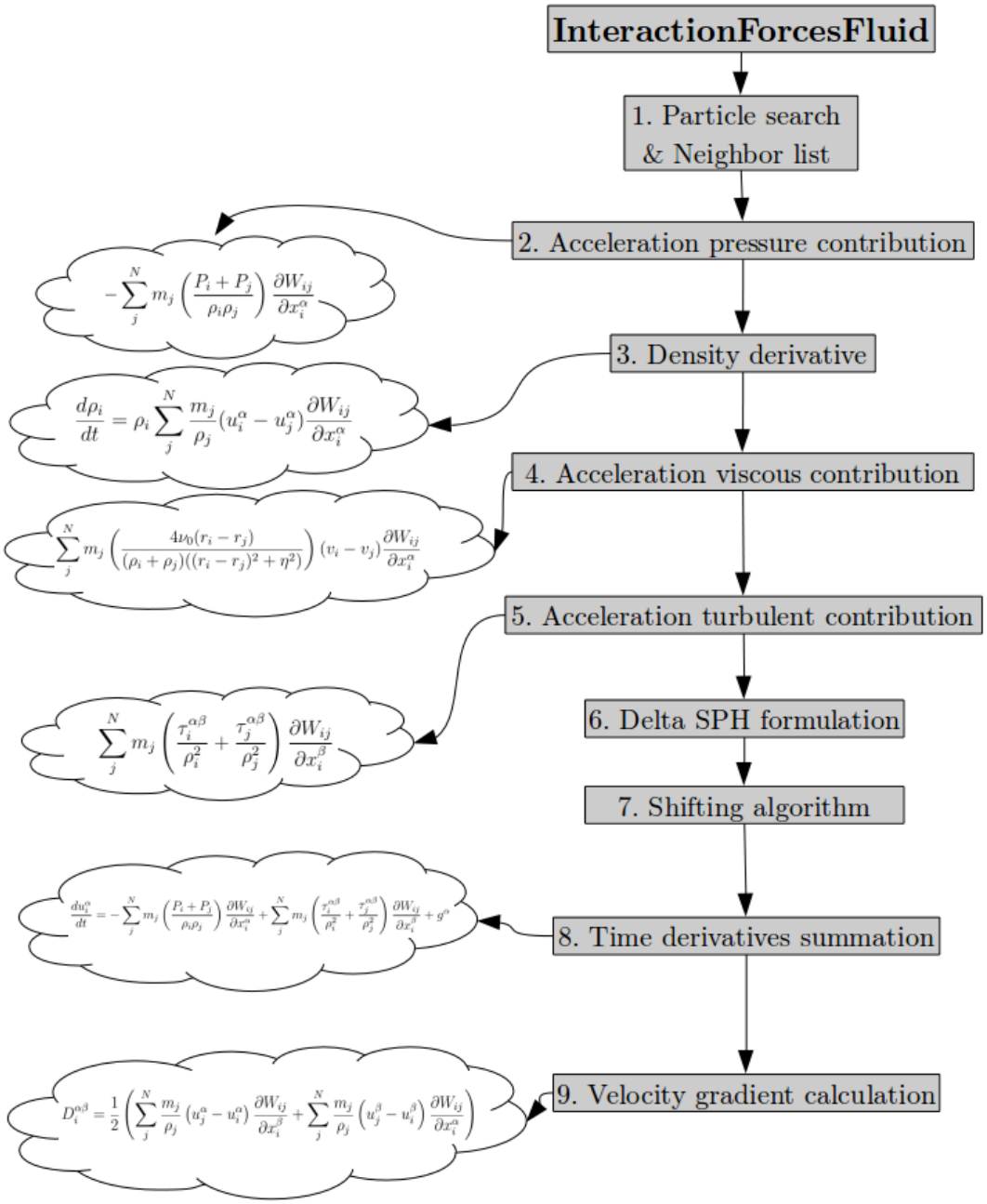

Figure 25: *InteractionForcesFluid* Description

The viscosity formulations available in the program are two:

1. **Artificial viscosity:** Numerical viscosity introduced to dissipate the oscillations of the density fields obtained in the solution, numerically it has the same formulation as the laminar viscosity up to the point that if the appropriate parameters are selected the same effects can be obtained.

2. **Laminar+SPS viscosity:** Numerical laminar viscosity formulation that allows the possibility to consider the SPS turbulent approach to compute the components of a new extra stress tensor that is taken into account inside the momentum equation as explained in Section 6.4.

The second is the most important for this work because it directly accounts for the extra stress tensor components in the momentum equation as formulated in Section 3.1, this means that any kind of rheological relation can be formulated mimicking the SPS method and the contributions of their components will be accounted inside the momentum equation.

The next section explains the inner workings of the *ComputeSpsTau* method, to understand the relation between the tensor components proposed.

6.4 Compute Sps Tau method

The method called *ComputeSpsTau ()*, calculates the SPS turbulence stress tensor components for each particle by a formulation using the velocity gradient components calculated in the method *Interaction_Forces()*, the formulation is given by the following relation [20] (See Figure 26).

$$\tilde{\tau}^{\alpha\beta} = \bar{\rho}\left(2\nu_t\tilde{S}^{\alpha\beta} - \frac{2}{3}\tilde{S}^{kk}\delta^{\alpha\beta}\right) - \frac{2}{3}\bar{\rho}C_I\Delta^2\delta^{\alpha\beta}$$

$$\tilde{S}^{\alpha\beta} = -\frac{1}{2}\left(\frac{\partial\tilde{u}^{\alpha}}{\partial x^{\beta}} + \frac{\partial\tilde{u}^{\beta}}{\partial x^{\alpha}}\right)$$

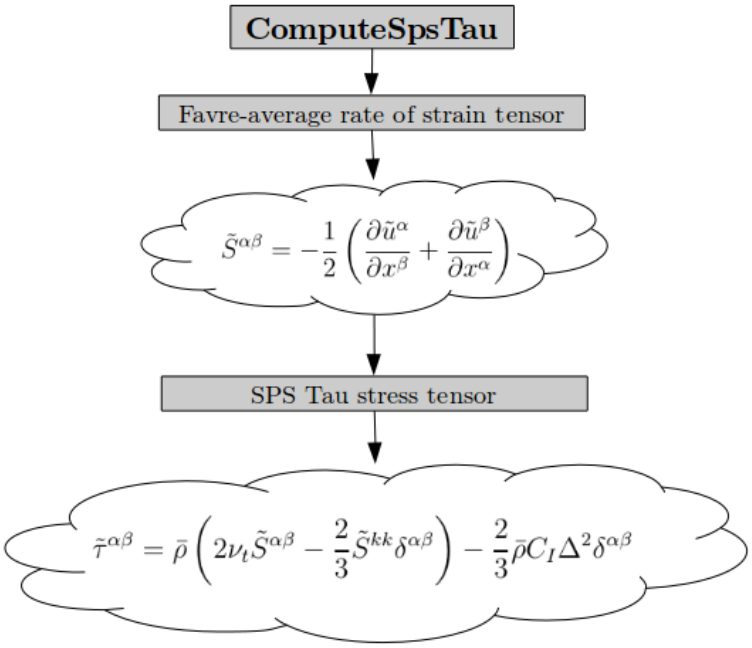

Figure 26: *ComputeSpsTau* Description

Where:

$\tilde{\tau}^{\alpha\beta}$: SPS stress tensor components.

$\tilde{S}^{\alpha\beta}$: Favre-filtered rate of strain tensor components.

$\bar{\rho}$: Favre-averaged rate of strain tensor components.

$\nu_t = (C_s\Delta)^2|S^{\alpha\beta}|$: Smagorinsky model to determine the eddy viscosity.

C_s: Smagorinsky constant 0.12.

$|\tilde{S}^{\alpha\beta}| = \sqrt{2(\tilde{S}^{\alpha\beta}\tilde{S}^{\alpha\beta})}$: Local strain rate.

C_I: Blin constant 0.00066.

Δ: Initial distance between particles.

$\tilde{S}^{kk}$: Rate of strain tensor trace.

After assigning a value to the tau stress tensor components the values are stored for each particle and are used in the method *Interaction_Forces()*, in the contribution of the acceleration due to turbulence, since each acceleration contribution is calculated independently the following SPH formulation is used:

$$\frac{du_i^\alpha}{dt} = ... + \sum_j^N m_j \left(\frac{\tau_i^{\alpha\beta}}{\rho_i^2} + \frac{\tau_j^{\alpha\beta}}{\rho_j^2} \right) \frac{\partial W_{ij}}{\partial x_i^\beta}$$

Where the dots stand for the rest of the acceleration contributions due to pressure and viscous terms.

As it is seen, the model links components coming from the rate of strain tensor to the components of the SPS tau stress tensor, thus the importance of this method lies in providing a direct way to set any kind of relation between these two tensors, hence any kind of rheology can be implemented here, having direct access to both tensors and allowing for different behaviors and different regions to be easily taken into account.

Next section discusses the modification implemented linking both formulation from Section 3.1 and the method here described.

7 MODIFICATION LOGIC AND ANALYSIS

7.1 Rheological implementation

As it was mentioned in Part II, the rheology selected to simulate the brash ice behavior is the viscoplastic model, as previous experiments suggest, this rheology can be directly implemented in the method *ComputeSpsTau ()*, Figure 27 shows a scheme of such implementation.

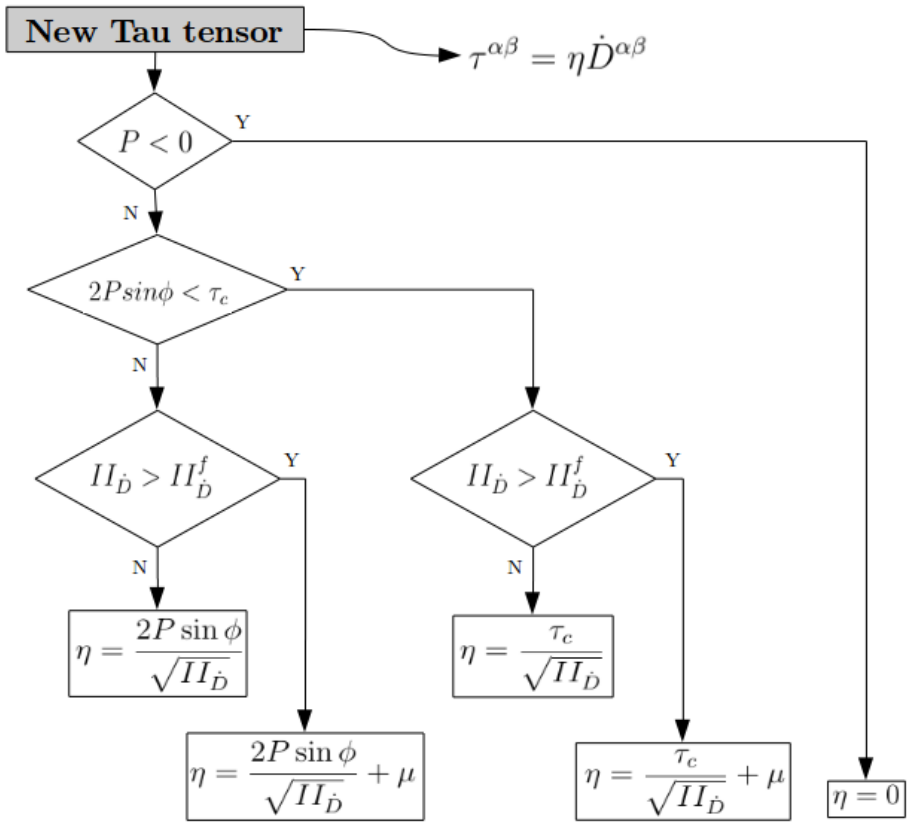

Figure 27: Viscoplastic rheology logic

The diagram shows the implementation performed, basically setting up the frictional and plastic region dependent on the pressure, and the viscous region dependent on the second invariant of the deviatoric strain-rate tensor. Also as explained before a transition region is implemented due to the fact that the thresholds for each region are dependent on different properties.

Some important considerations made on this model are described below:

1. **On the second invariant calculation ($II_{\dot{D}}$):** Originally the frictional and plastic formulation depend upon the fact that the second invariant of the strain rate tensor is positive, this is a condition satisfied if the fluid is incompressible [6], but for weakly compressible [9] and granular flows [12] another kind of formulation has to be used, this formulation is a slight modification linking the deviatoric strain-rate tensor and also its second invariant instead of using the simple tensor, thus ensuring a positive value all the time.

2. **On the thresholds:** Usually a common parameter dependent on the strain-rate tensor is used as a threshold for both transitions between the different regions. But in this case since the threshold for the viscous part is unknown, two different thresholds are proposed. The first will be controlled by the pressure of each particle and will be used to set a limit to the friction contribution this limit is the plastic region. The second controlled by the second invariant of the deviatoric strain-rate tensor that will control the emergence of the laminar viscous behavior region.

3. **On the continuity of the functions:** Due to the previous fact there is a possibility of a discontinuity on the extra stress components, and to avoid this some

extra regions were defined that add viscosity effects to regions where the strain rate threshold has been exceeded but not the pressure threshold.

4. **On the SPH formulation of the contribution:** As it is clear from section 4.3, the same discretization is not used for the pressure contributions and the rheological contributions, this was left this way for simplicity since the formulation was already implemented like this in the code, furthermore since the total stress tensor was split in the differential equations each part can be discretized independently and can thus different formulations can be used.

5. **On the rheological parameters to be selected:** The parameters selected when computing the comparisons have to be carefully checked due to the lack of accuracy in the experimental data and the lack of knowledge of some of them. In this way three out of the five parameters can be more or less used, but the remaining two will be proposed here to test the model under simple considerations, but should not be taken as validated values.

This implementation was successful and several runs were made to test the new model before making more modifications, these runs will not be subject to analysis in this work since it was not the only modification performed and tested.

The only thing missing is a way to provide an estimate of the interaction between the brash ice bottom layer and the water, this is, a way to mimic this interfase condition inside this simplistic model, otherwise no kind of comparison with experimental data can be performed.

The next section will discuss how this modification was executed and what implications it entails.

7.2 Pressure boundary implementation

One of the aspects that the methodology selected does not capture is the interaction between the brash ice lower layer with the water, as an attempt to recreate this effect a simple formulation was used, this simple formulation renders a buoyant pressure effect just as the one imposed by the water.

To accomplish this, a simple idea was developed, an acceleration in the z direction was added at the end of every acceleration summation of each particle, the value of this acceleration was calculated based on a simple hydrostatic pressure formulation, although several different approaches can be implemented. A z position threshold was defined arbitrarily at $Z_{th} = 1$, below this value the contribution of this pressure in the z direction acceleration is added. A simplified sketch of this formulation is shown in Figure 28.

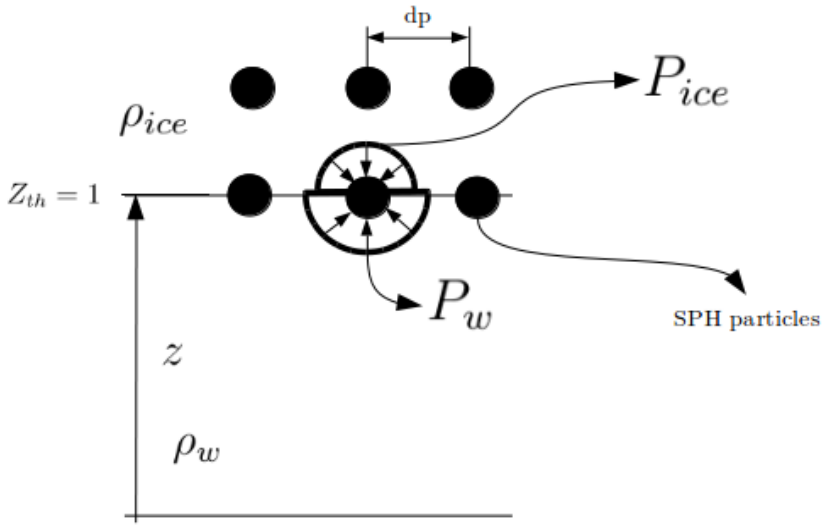

$$-P_{ice}kdp^2 + P_w kdp^2 = \rho_{ice}kdp^3(-a_z + a_z^*)$$

Using the following relations:

$$P_{ice}kdp^2 = a_z\rho_{ice}kdp^3 \qquad P_w = \rho_w gh$$

Pressure contribution, directly from the momentum equation

Hydrostatic pressure of the water layer below the ice

And thus the following relations are obtained:

$$a_z^* = \frac{\rho_w gh}{\rho_{ice}dp} \qquad a_z^* = \frac{\rho_w g\,[h + (1-z)]}{\rho_{ice}dp}$$

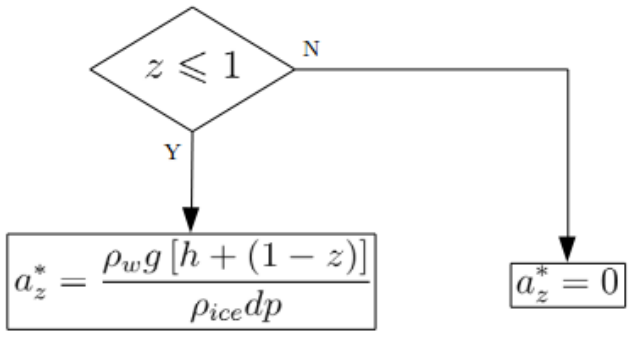

Figure 28: Pressure boundary scheme

Where:

Z_{th}: Defines the z coordinate below of which the new acceleration term due to hydrostatic pressure is applied at the end of the particle acceleration summation to counteract the pressure of the brash ice medium.

P_w: Hydrostatic pressure of the water below the brash ice medium.

P_i: Hydrostatic pressure of the brash ice medium on the the lower particles.

ρ_w: Water density.

ρ_i: Brash ice density.

a_z: Pressure acceleration contribution in the z direction from the brash ice layer above.

a_z^*: Hydrostatic pressure acceleration contribution in the z direction from the water under the ice brash layer.

g: Acceleration of gravity.

h: Brash ice thickness, also defined by the selection of the initial distance between particles and the amount of particles modeled as brash ice.

dp: Initial distance between particles.

k: Constant taken as one for a cube.

It is worth to mention that in the methodology here presented the pressure can also be computed with an equation of state with the water density instead of the hydrostatic formulation. Also it is important to mention that as trials have shown with this new boundary the medium is not stable at the beginning of any simulation.

The medium bounces up and down for a brief period of time until its own friction dissipates this oscillation, as far as it was tested[38] it took around 1 second for the medium to stop oscillating. As a consequence all the simulations presented in the following sections start with a one second period for dissipation before any body inside the medium starts moving, this period is called stabilization time.

7.3 Convergence analysis

Having explained both modifications made in the code the next objective then is to check the time convergence of any given model, with both modifications working. For this purpose an specific test scenario was set up[39], as it can be seen in the Figure 29.

[38] This is for the expected values of the rheological parameters with which it was tested.
[39] This reason for the creation of this specific scenario is explained in section 8.3.

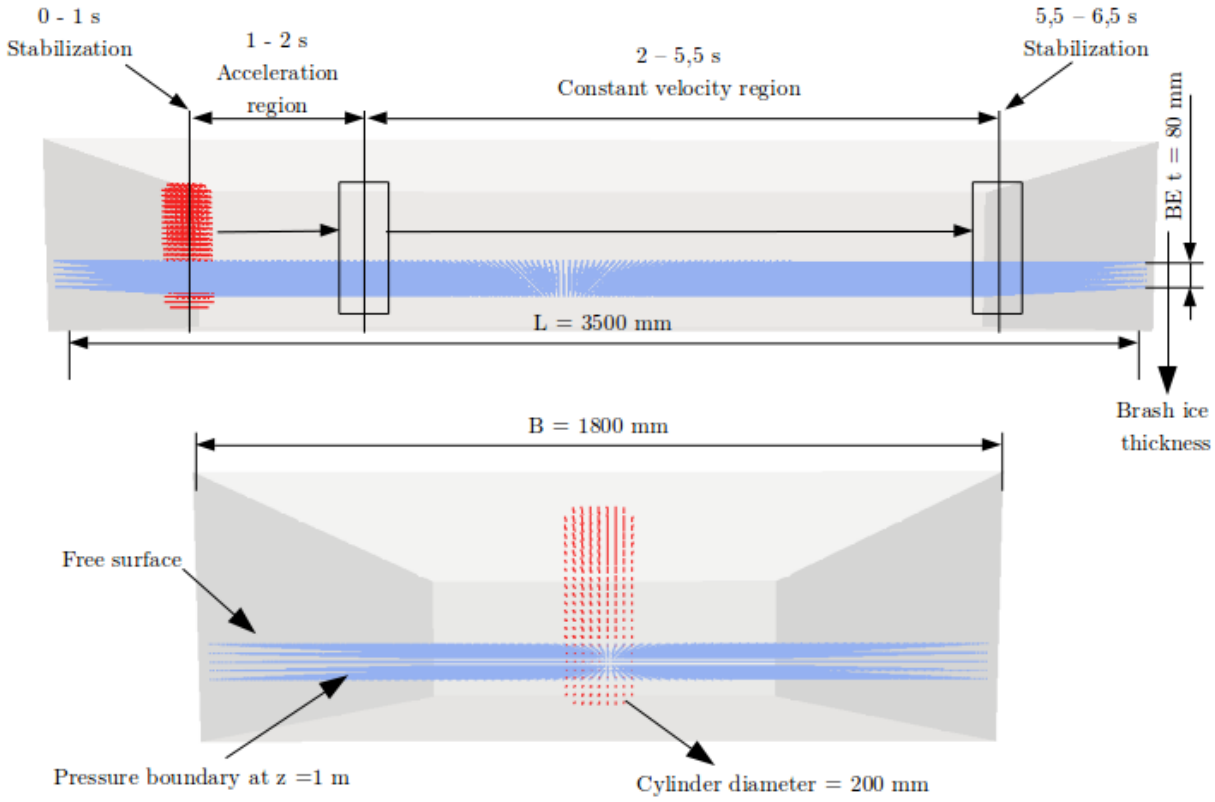

Figure 29: Model for convergence analysis longitudinal and front view

Basically the model selected consists in a boundary box containing one moving cylinder and a medium layer of a specific thickness placed above the Z_{th} explained in the previous section. The general dimensions are shown in Figure 29, and the details of the cylinder motion are given below.

It starts with 1 second standing still to let the medium stabilize due to the new boundary condition, then is subject to a 1 second period of constant acceleration until it reaches a velocity of 0,74 m/s, then a period of constant velocity is set for 3,5 s and finally it stops before arriving to the frontal boundary wall and is left to rest 1 more second at the end. This whole movement summarizes a simulation of 6,5 s.

Only time convergence analysis will be shown here, due to the fact that it is the intention of this SPH particles to represent the possible particles of the granular medium, that is why a distance between particles (Dp) of $0,02$ m was selected although almost same results were obtained with $0,025$ m and $0,015$ m, with the latter rending almost exact same results as for $0,02$ m, which suggests space convergence.

The following characteristics for the viscoplastic medium tested, have been selected to perform a convergence analysis:

$P_{th} = 0$	Pressure threshold to define the tension region.
$\tau_c = 3,5kPa$	Shear strength.
$P\phi = 50^\circ$	Friction angle.
$II_{\dot{D}} = 0.1s^{-2}$	Viscosity threshold.
$\mu = 10Pa \cdot s$	Viscosity.
$\rho_0 = 920kg/m^3$	Reference density, ice property.

This set of parameters is selected as reference for the time convergence study, although another set of values could be used, this specific set is expected to be inside the possible range of values. Now it is important to mention how the time step can be controlled and reduced to perform this analysis.

The open source code has a variable time step (Δt_f) calculator that is based on two different criteria, the first one based on the maximum force per unit mass measure inside the system, and the second based on the viscous diffusion term. Both formulations can be seeing below:

$$\Delta t_f = CFL \cdot min\left\{\Delta t_f, \Delta t_{c\nu}\right\}$$

$$\Delta t_f = min_i\left(\sqrt{\frac{h}{f_i}}\right)$$

$$\Delta t_{c\nu} = min_i\left(\frac{h}{c_s + max_i\left|\frac{h\vec{v}_{ij}\cdot\vec{r}_{ij}}{r_{ij}^2+\eta^2}\right|}\right)$$

Δt_f : Time step based on maximum force.

$\Delta t_{c\nu}$: Time step based on the viscous diffusion term.

CFL : Courant-Friedrich-Lewy number, dimensionless number used to defined the time step upper limit for the simulation.

h : Smoothing length.

f_i : Maximum force in the calculation domain.

The first equation just selects the minimum between both criteria and multiplies it with the CFL number which is manually set in the initial configuration parameters, thus out of all the parameters is the only one that can be externally controlled to reduce the time steps, although of course a novel criteria can also be implemented. It is also important to mention that the viscosity formulated in the software was set to zero since it its effects are not considered in the current model.

For this analysis then the CFL number has been selected to account for the decrements in the time step, starting from a value of 0.2 as recommended for water models

decreasing continuously by half its value in each run until the field values selected for evaluation reach convergence.

The field values selected for the convergence study are velocity and density. The values are measured as the history of this quantities in certain fixed points with a specific location shown in the Figure 30.

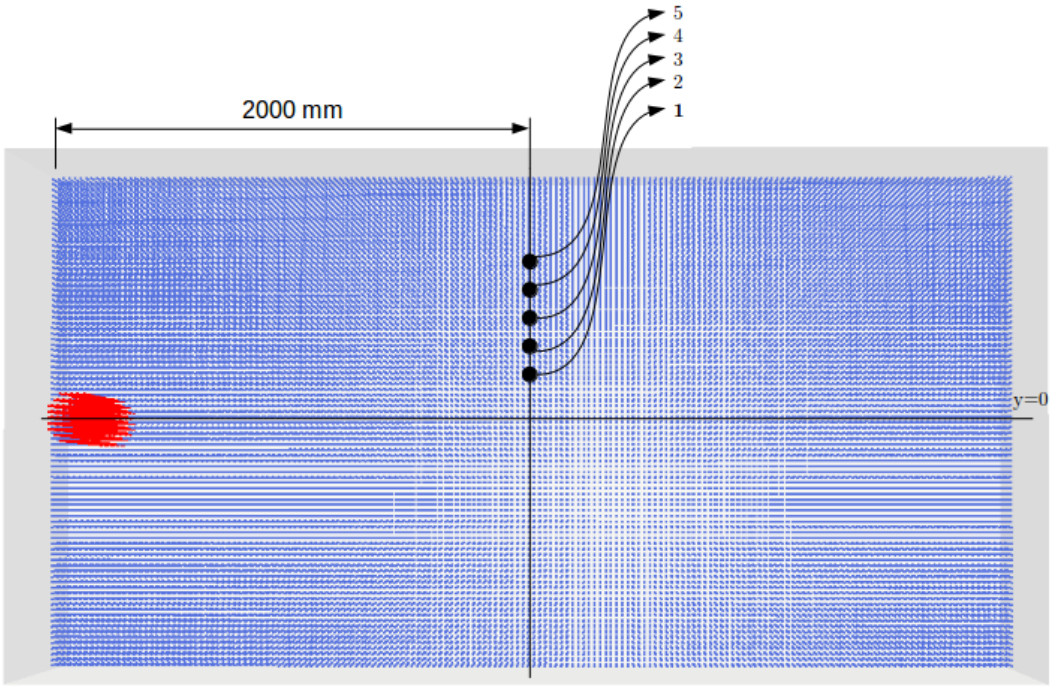

Figure 30: Points for convergence in time calculation

For further information the points coordinates in the y and z direction are indicated below, remembering the brash ice layer goes from $z = 1$ m to $z = 1.08$ m:

Point 1: $y_1 = 0.15$ m, $z_1 = 1.04$ m (the middle of the brash ice layer)

Point 2: $y_2 = 0.20$ m, $z_2 = 1.04$ m

Point 3: $y_3 = 0.25$ m, $z_3 = 1.04$ m

Point 4: $y_4 = 0.30$ m, $z_4 = 1.04$ m

Point 5: $y_5 = 0.35$ m, $z_5 = 1.04$ m

Below the result of the attempts of convergence for the velocity in the x direction and the density field.

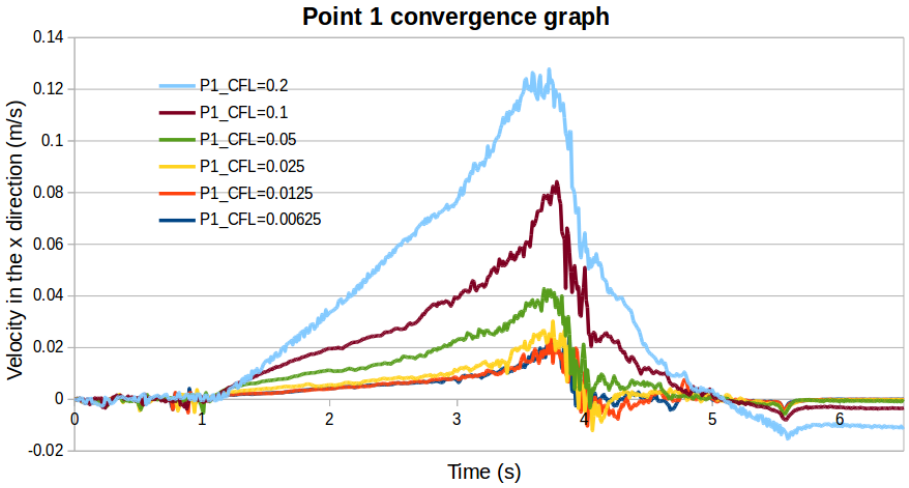

Figure 31: Point 1 velocity convergence graph

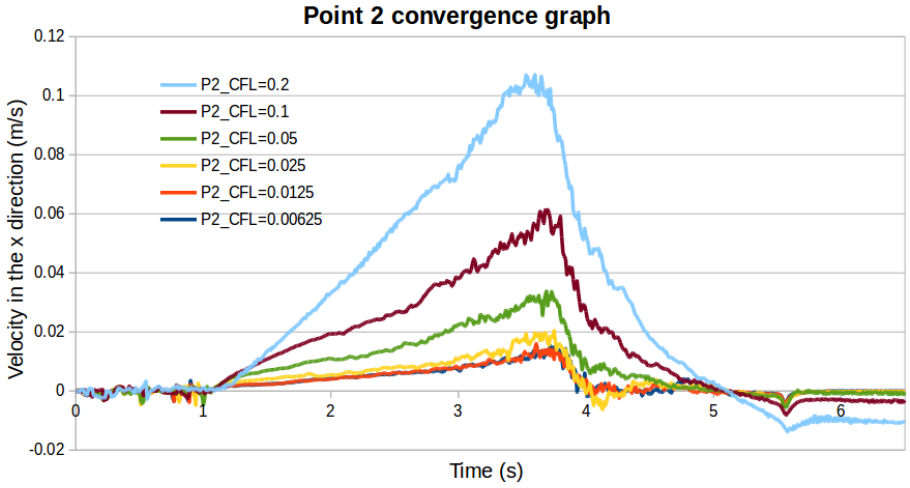

Figure 32: Point 2 velocity convergence graph

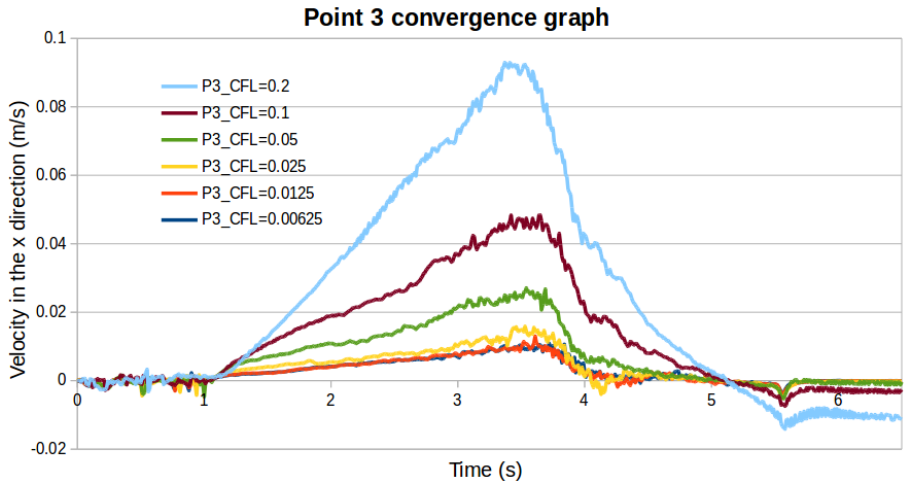

Figure 33: Point 3 velocity convergence graph

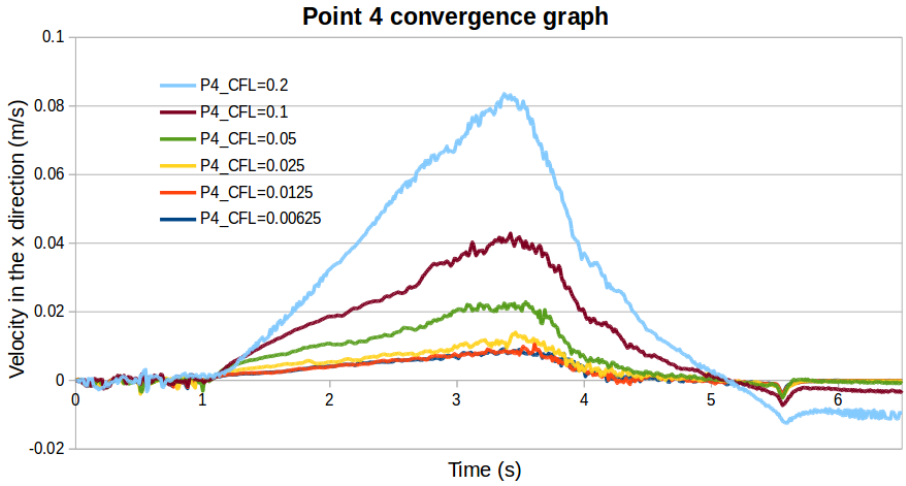

Figure 34: Point 4 velocity convergence graph

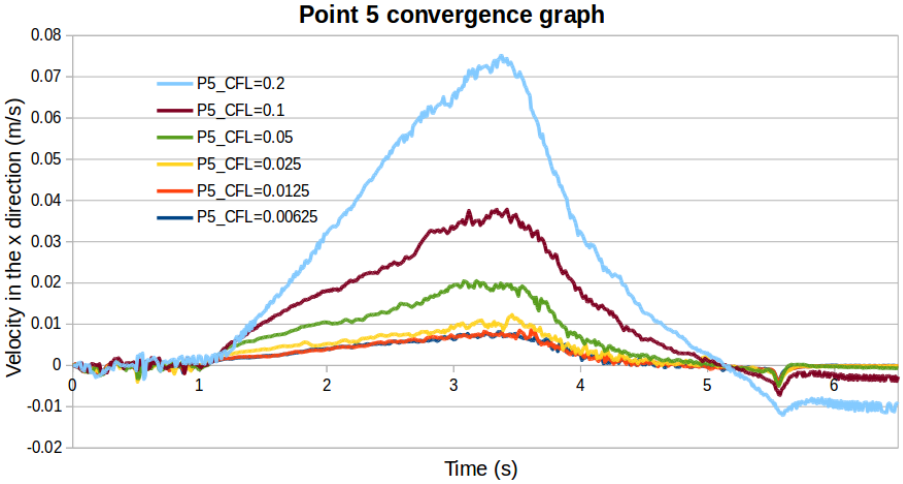

Figure 35: Point 5 velocity convergence graph

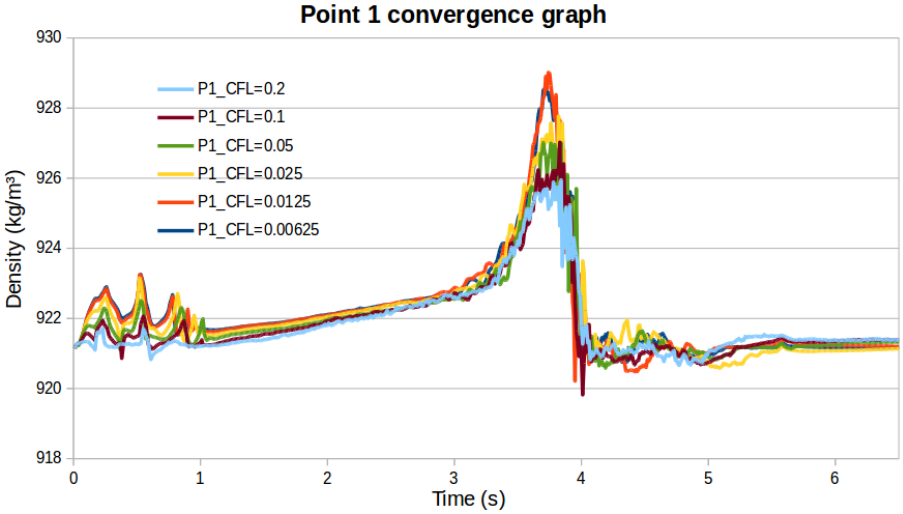

Figure 36: Point 1 density convergence graph

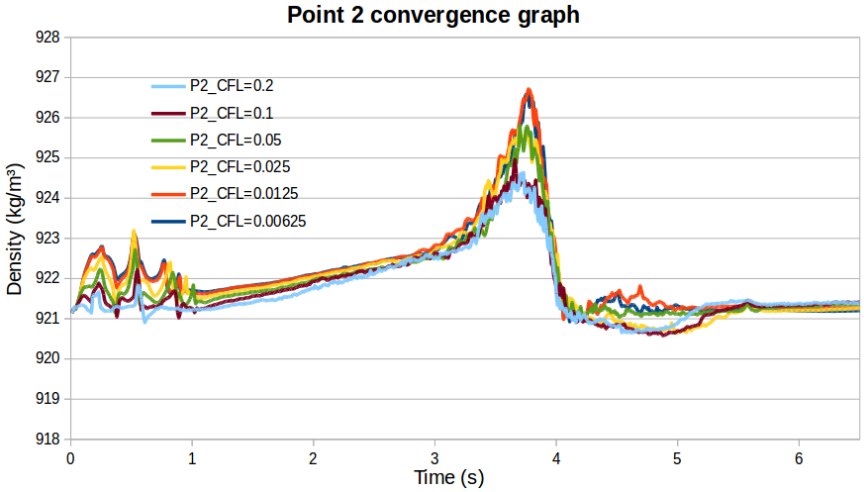

Figure 37: Point 2 density convergence graph

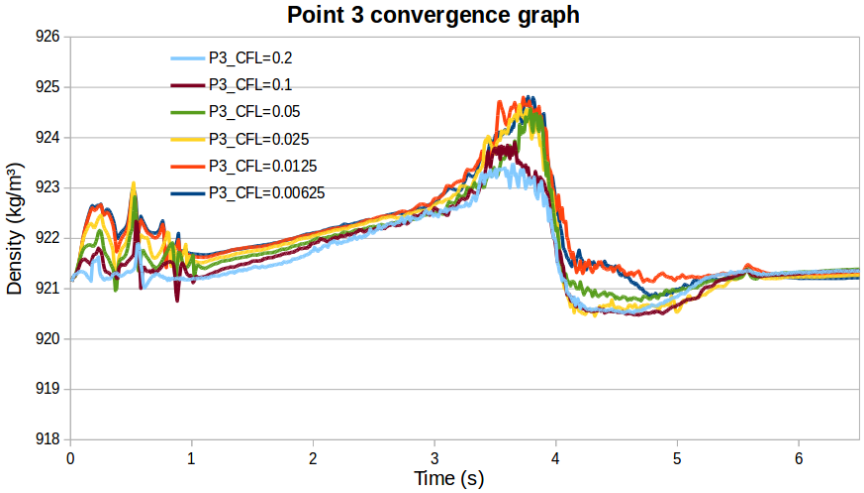

Figure 38: Point 3 density convergence graph

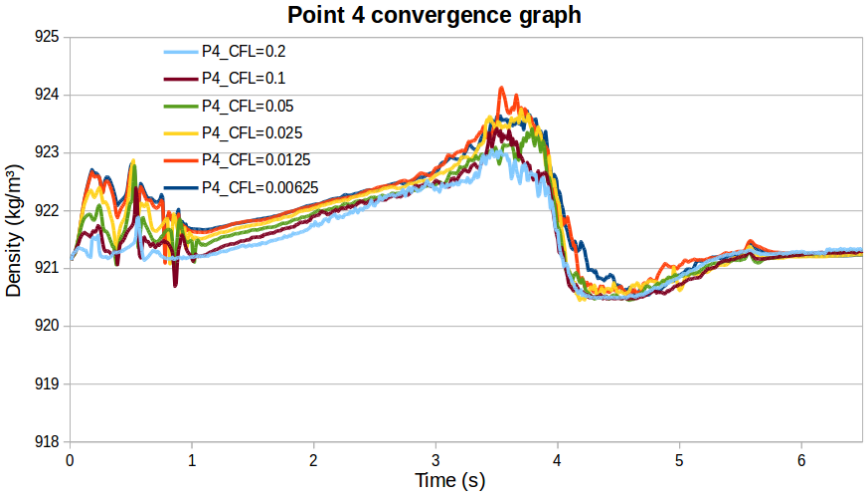

Figure 39: Point 4 density convergence graph

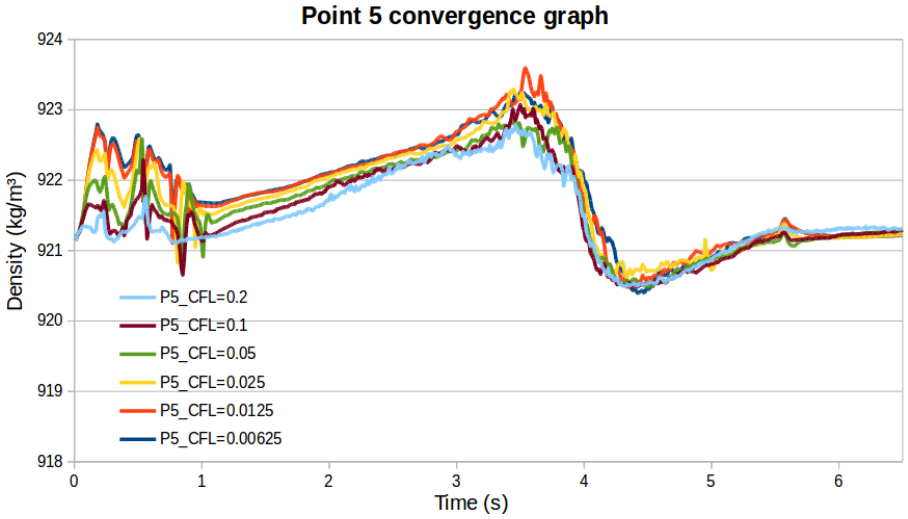

Figure 40: Point 5 density convergence graph

As it can be seen in the curves presented the convergence in the new rheological model is achieved with a very small time step in comparison with what it is used and recommended for the water alone, for a CFL number of 0.2 a time step of the order of $4.00 \cdot 10^{-4}$ and for a CFL number of 0.00625 a time step of the order of 10^{-5} are obtained, this was expected due to the non-linearities introduced in the viscoplastic rheology.

It also can be observed that convergence on both fields is more notorious more or less in the first 3.5 seconds of the simulation, this is before the cylinder passes next to the points selected, after this region a less clear convergence pattern is obtained. This characteristic is diminished for the velocity fields in points farther away from the cylinder, but it is not diminished in the density field of any given point.

The pattern just described clearly shows the difficulty of the method to correctly describe the stern flow, which can also be checked by visual inspection, the granularity of the flow added in the friction and plastic regions does not let the flow behave as desired after the cylinder perturbation has passed.

Although the velocity field shows a more clear convergence pattern, the density field can be seen moving between a range of values without approximating a specific one, but it still shows a specific behavior for different CFL numbers, and these values and patterns can be considered to be inside a certain range.

Taking into account the facts explained above it is clear that a CFL number equal to 0.0125 basically grants convergence, but the computational times are severely increased for a little gain in the accuracy of the field values. For this reason a CFL number equal to 0.025 is selected for the rest of the calculations made in the modified medium, this value clearly combines the velocity fields close to the converged values and also a good approximation of the density field taking into account all the details explained above, in addition it also provides a reasonable amount of time to run each simulation and check the model.

7.4 Sensitivity analysis

Having selected a time step and a particle distance values to ensure convergence, several results of the same model with different rheological parameters are calculated to evaluate the influence of each of them on the velocity field.

The same configuration of Section 7.3 is used but the parameters that regulate the new viscoplastic model will be analyzed. The analysis was divided in two parts. First, measuring the influence of the frictional and plastic regions changing only the shear strength τ_c and the friction angle ϕ, and second, measuring the influence of the viscous region changing only the viscous threshold $II_{\dot{D}}^{f}$ and the viscosity μ, below a brief summary of the cases compared:

Trial	τ_c (kPa)	ϕ (°)	$II_{\dot{D}}^{f}$ (s^{-2})	μ $(Pa.s)$	Observation
1	3,5	50°	0,1	10	Benchmark run for comparison
2	3,5	30°	0,1	10	Frictional angle influence
3	3,5	15°	0,1	10	Frictional angle influence
4	7	50°	0,1	10	Shear strength influence
5	1,5	50°	0,1	10	Shear strength influence
6	3,5	50°	10^6	10	No viscous influence
7	3,5	50°	0,1	100	Viscosity influence
8	3,5	50°	5	100	Viscosity threshold influence

Table 3: Parameters for Sensitivity Analysis

From the values shown on the table, only the τ_c and the ϕ have been experimentally studied before and some values have been obtain although a big uncertainty is given in the results. In general the τ_c value is proposed to be in the range of 1 kPa and 6,6 kPa [3][4], also the ϕ value is proposed in the range of 10° and 50° [1][4].

The other two values were just tested in a wide range of possibilities just to measure their influence. The value of the dynamical viscosity μ can vary but for granular flows and it can be considered to be in the range of 0 Pa·s to 150 Pa·s. The values of the viscosity threshold were selected to be able to see its incidence in the model, but no prior knowledge of a possible value was known so the values here presented do not represent experimental known values.

Following some relevant results of the simulations run are presented to describe their influences and possible explanations.

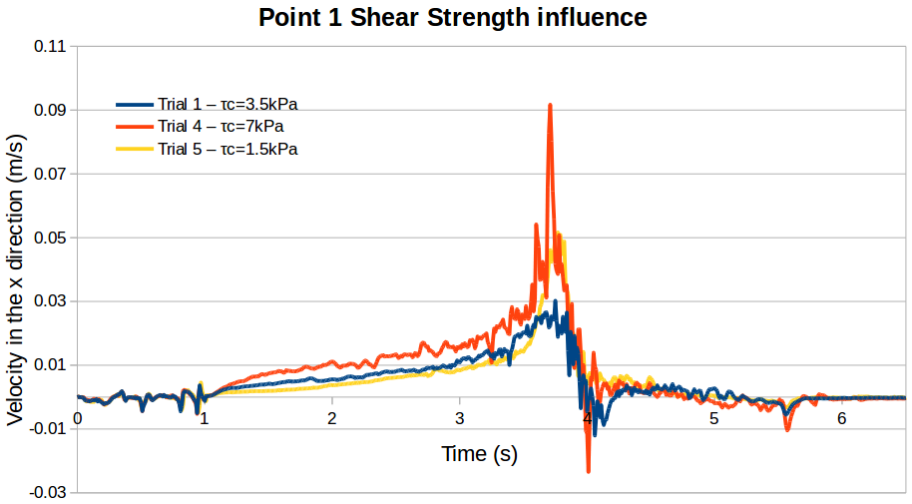

Figure 41: Point 1 Shear strength influence

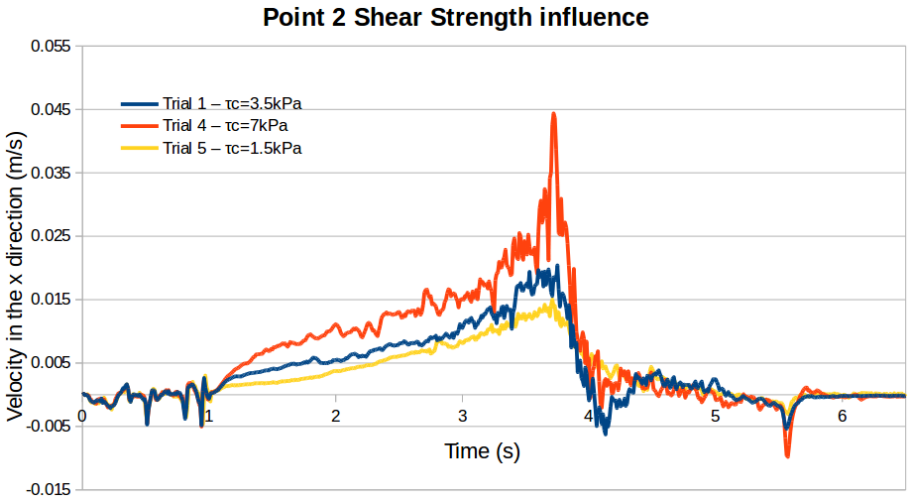

Figure 42: Point 2 Shear strength influence

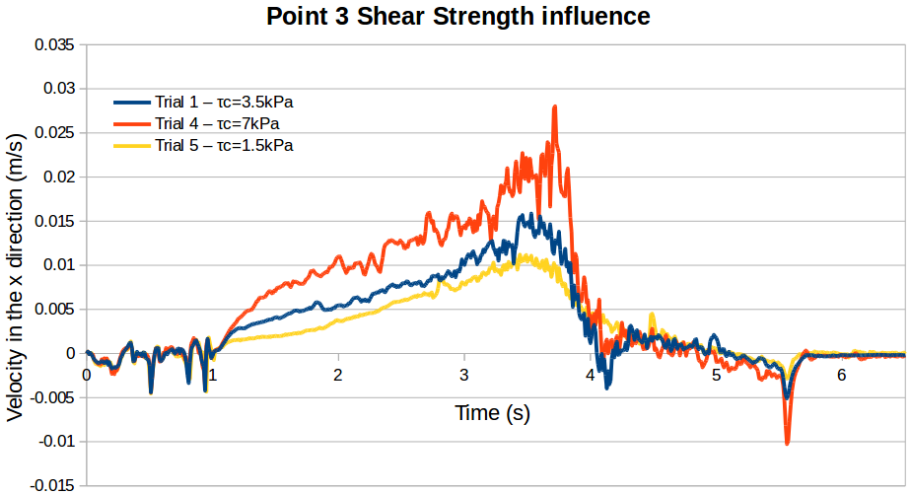

Figure 43: Point 3 Shear strength influence

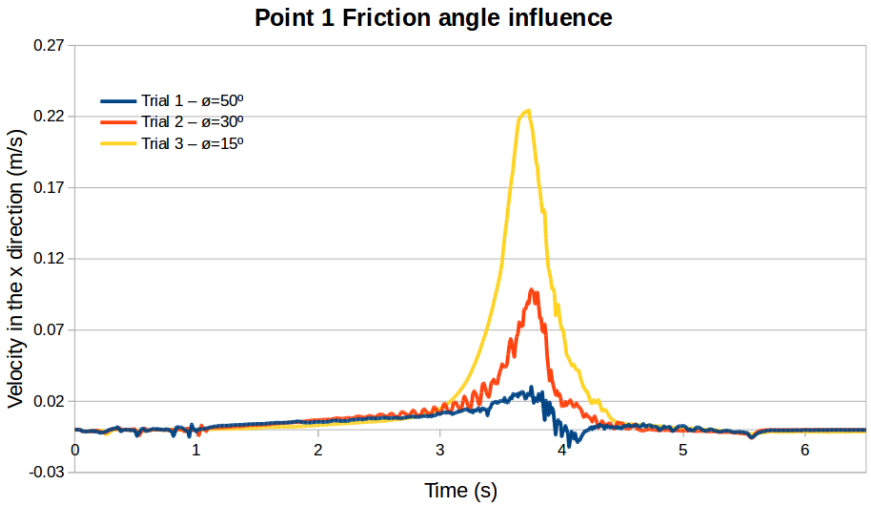

Figure 44: Point 1 Friction angle influence

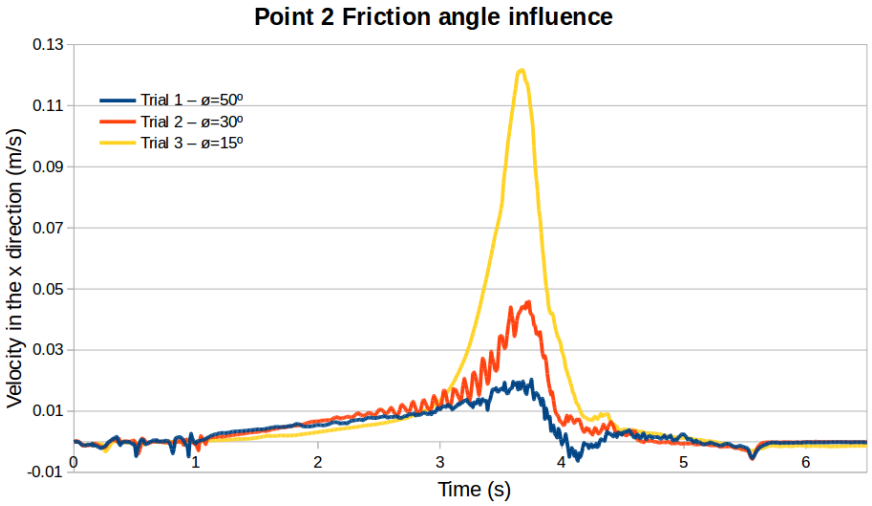

Figure 45: Point 2 Friction angle influence

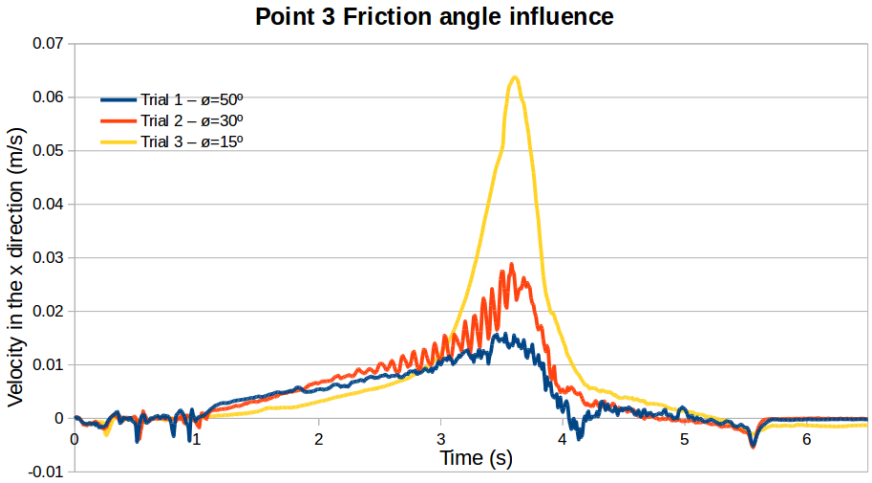

Figure 46: Point 3 Friction angle influence

As it can be observed the lower the frictional angle the greater the velocities of the particles as expected since the friction is lower and takes more pressure to get to the shear strength value. Also the greater the shear strength the greater the velocities, this is also expected since shear forces between particles are allowed to be bigger and thus particles can pull each other with a bigger strength.

A small discrepancy of the previous observation can be seen in the Figure 41 between the trials 1 and 3 (blue and yellow curves), a tentative explanation is that there is a trade between the shear strength and the frictional angle that will control the movement of the particles located very near the perturbation of the cylinder, so for some frictional angles with specific shear strengths different results could be expected near the perturbation.

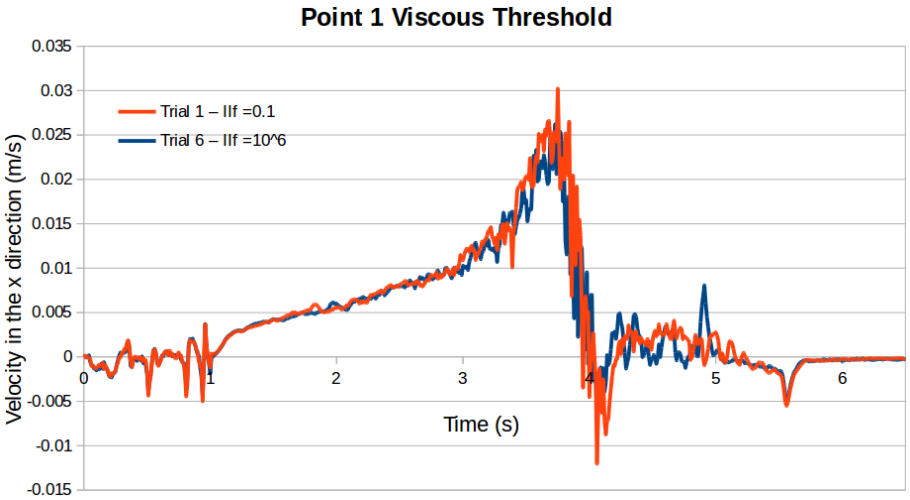

Figure 47: Point 1 No viscous influence

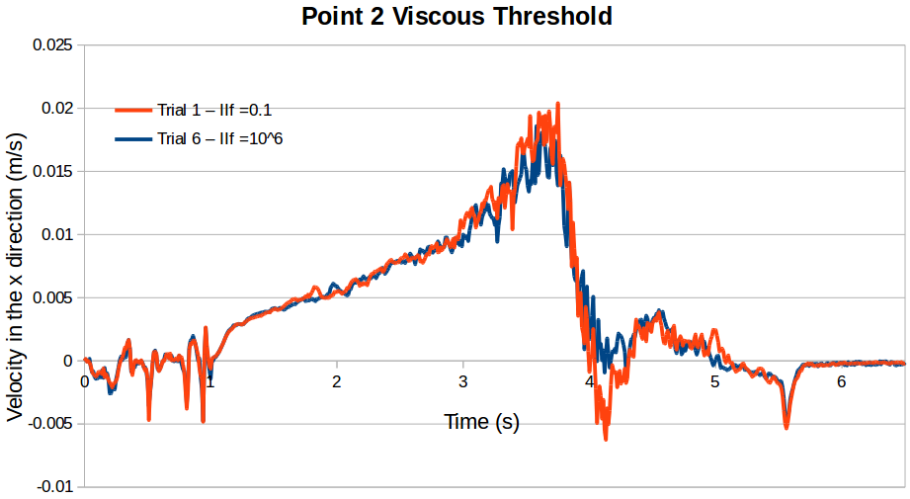

Figure 48: Point 2 No viscous influence

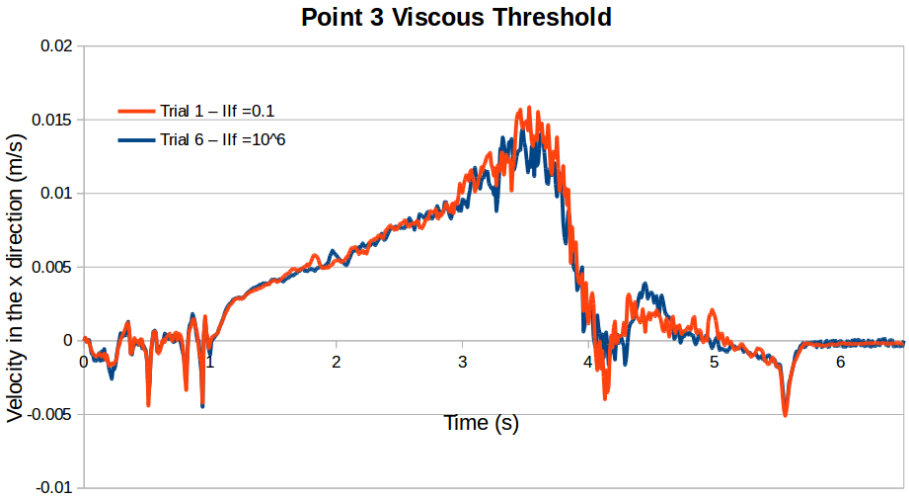

Figure 49: Point 3 No viscous influence

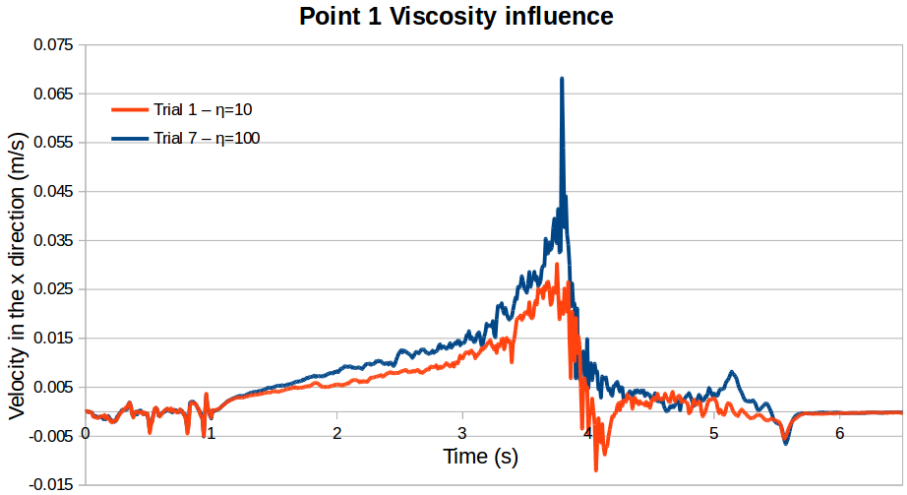

Figure 50: Point 1 Viscosity influence

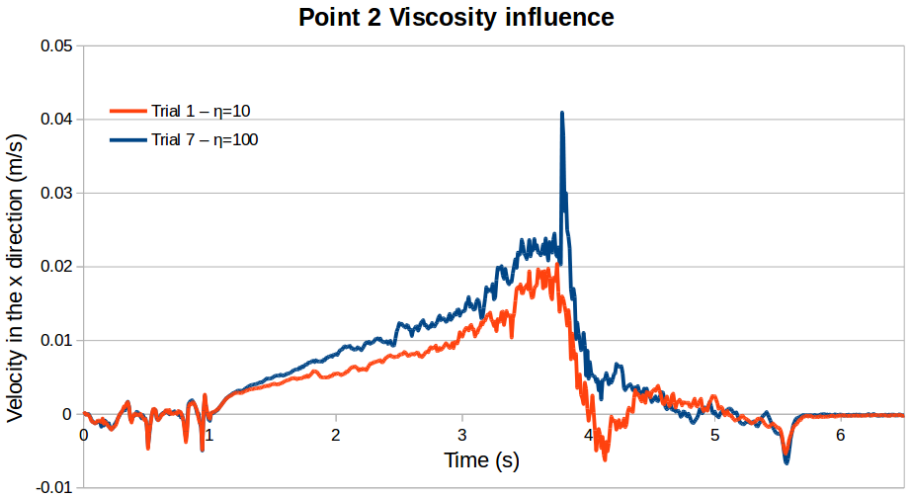

Figure 51: Point 2 Viscosity influence

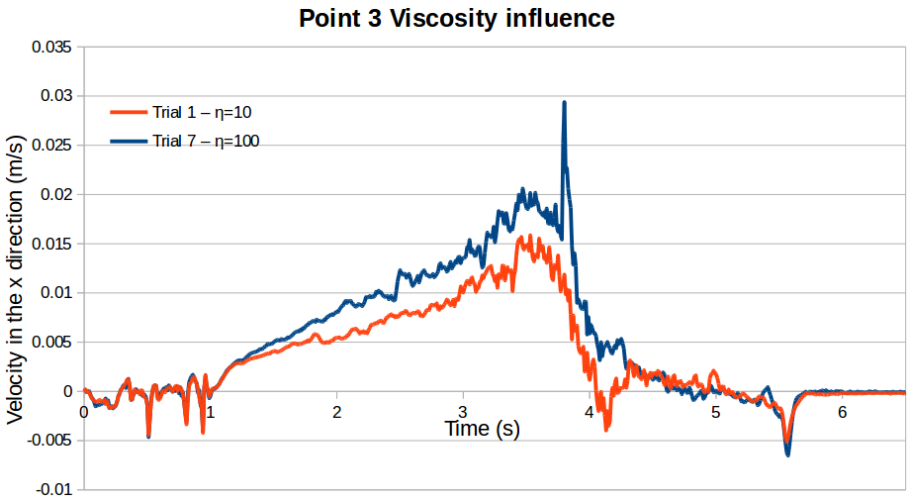

Figure 52: Point 3 Viscosity influence

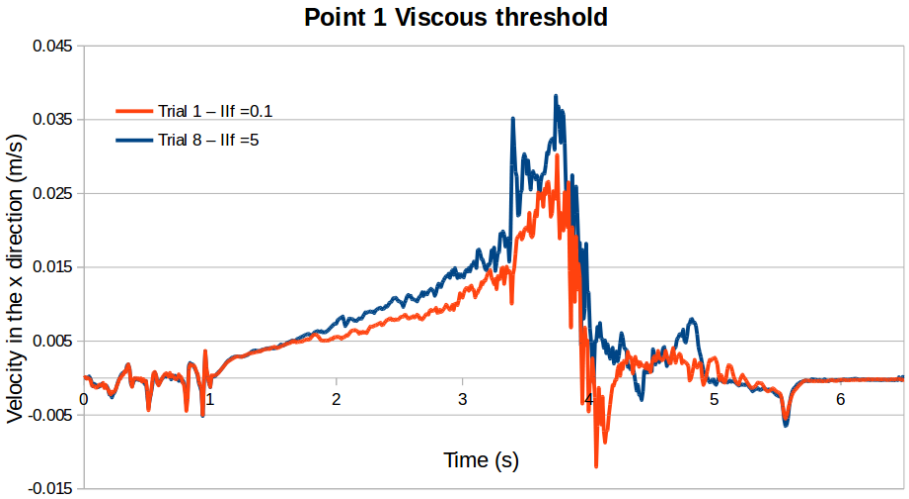

Figure 53: Point 1 Viscous threshold influence

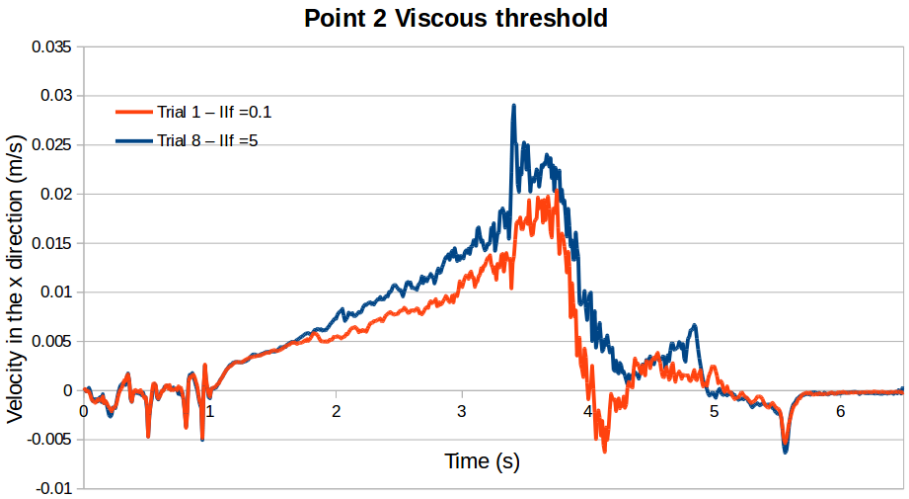

Figure 54: Point 2 Viscous threshold influence

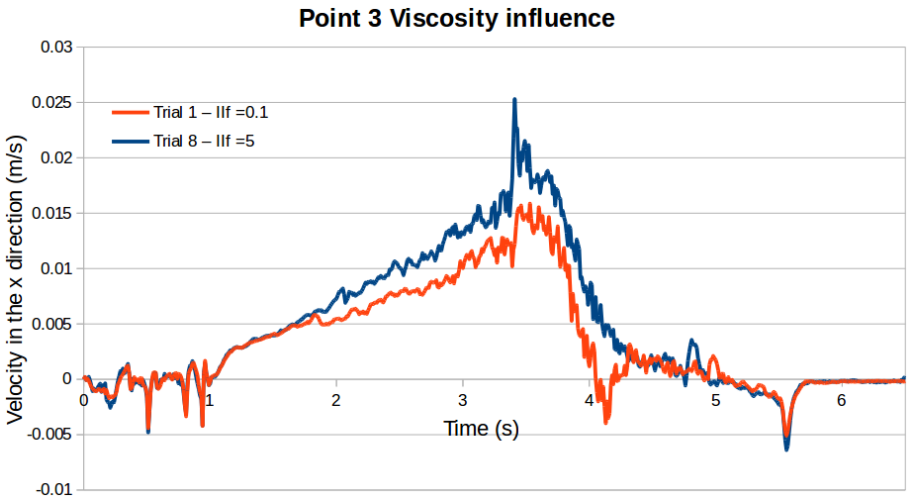

Figure 55: Point 3 Viscous threshold influence

First it can be observed that the viscosity selected for the benchmark trial is too low to actually have some effect in the model for the other given parameters, Figures 47, 48 and 49, clearly show this effect for purely frictional models.

As it can be observed in Figures 50, 51 and 52, for the values selected, the viscosity effect is only appreciable for values greater than 100, then it can be observed an increase in the velocity x component since the viscosity accounts for bigger shear forces between particles. Also as it is expected the strain-rate threshold delays the viscosity effects until they go above the value.

From Figures 53, 54 and 55, the effect of the viscous threshold can be observed, by moving the value the beginning of the viscosity influence can be move to delay or advance its effect. It is important to mention that a previous knowledge of the strain-rate tensor component values is needed to appropriately see the influence of this threshold, this means that values in the threshold too high or too low will provide results were the viscous region is either appearing since the beginning or is not appearing at all respectively.

It is clear that for the simplistic nature of the rheology proposed the results are quite as expected, having shown convergence and a satisfactory response of the model, it is the intention of the next section to explain the experiment that was used to compare results, and the simulations attempts under the best parameter values to try to obtain the same resistance force as in the experiments.

8 THE CYLINDER EXPERIMENT

8.1 Description of the experiment

To test our model in a real scenario a specific experiment conducted inside HSVA ice tank facilities was taken as reference, the experiment consists in a vertical cylinder with a fixed draft pull at a constant velocity through two different regions one with only water and one with a layer of brash ice with a specific thickness. First a layer of level ice[40] is

[40]Undeformed ice layer floating in water.

prepared with a certain thickness, then a channel is opened with a width of 1800 mm as shown in Figures 57 and 58, and the pieces of ice of the channel just broken are gather at one side of the channel to account for the brash ice region, Figure 56 shows a longitudinal view of the set up, Figures 59, 60 and 61 show pictures taken of the cylinder in all the aforementioned regions.

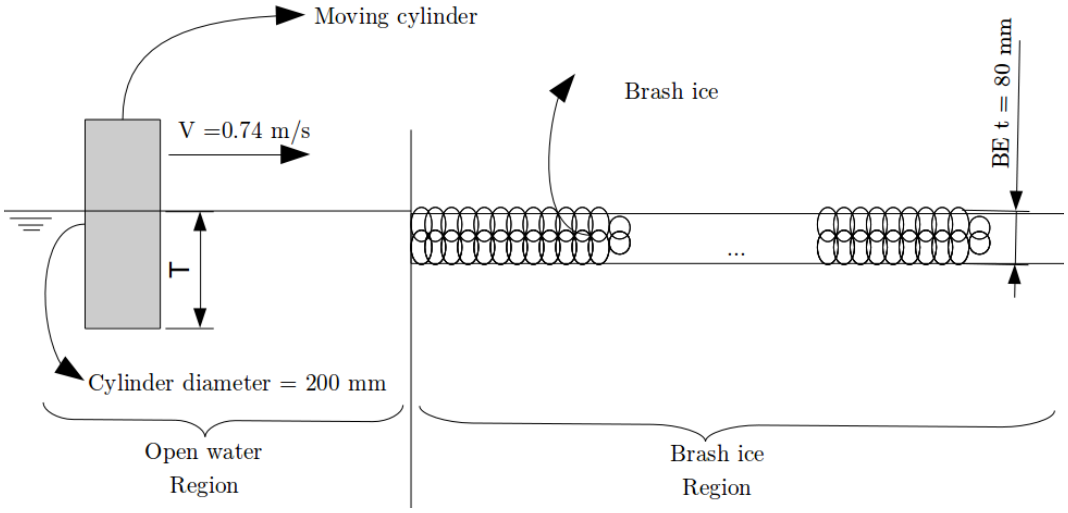

Figure 56: Cylinder experiment brief diagram, longitudinal view

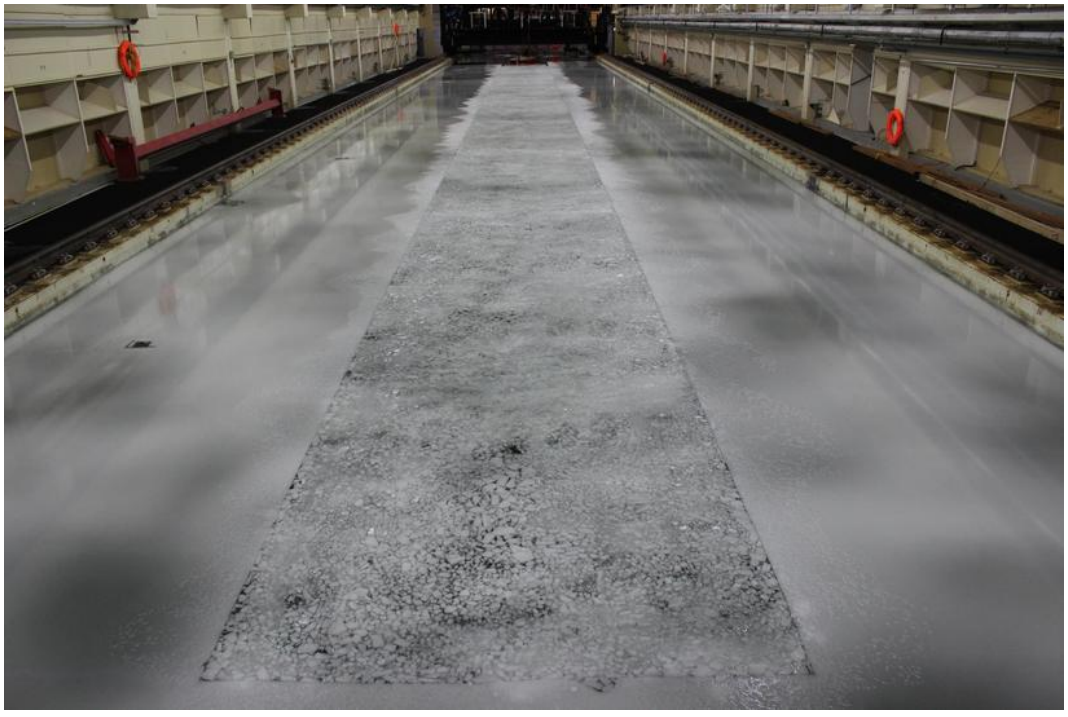

Figure 57: Channel top view

Figure 58: Channel perspective view

The cylinder is fixed and connected to a carriage that moves at a constant speed as indicated in Figure 56, at the same time a device is connected to record the measurements of the resistance in the x direction, at all the moments of the trial.

Figure 59: Water region

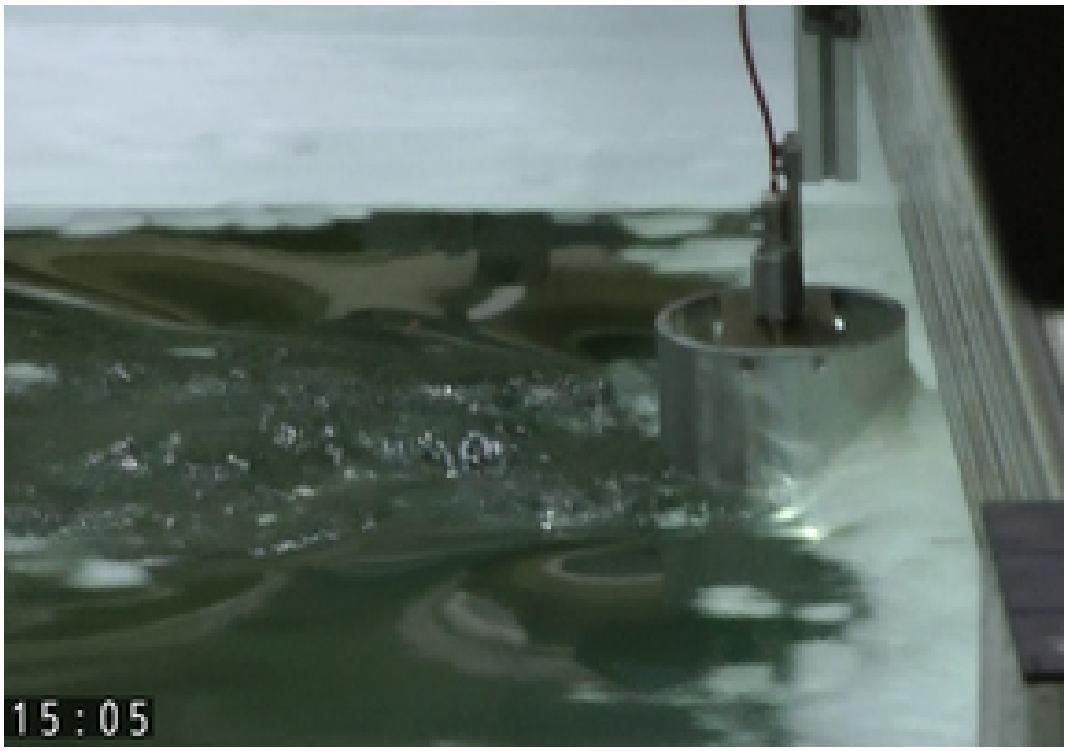

Figure 60: Cylinder arriving to the brash ice region

Figure 61: Brash ice region

Two values of the force measurements were recorded for two different runs, table 4 shows the characteristics of each experiment and Figures 62 and 63 show the results of the force measurement.

Experiment	Draft (mm)	Brash ice thickness (mm)
1	88	52
2	144	84

Table 4: Parameters for cylinder tests

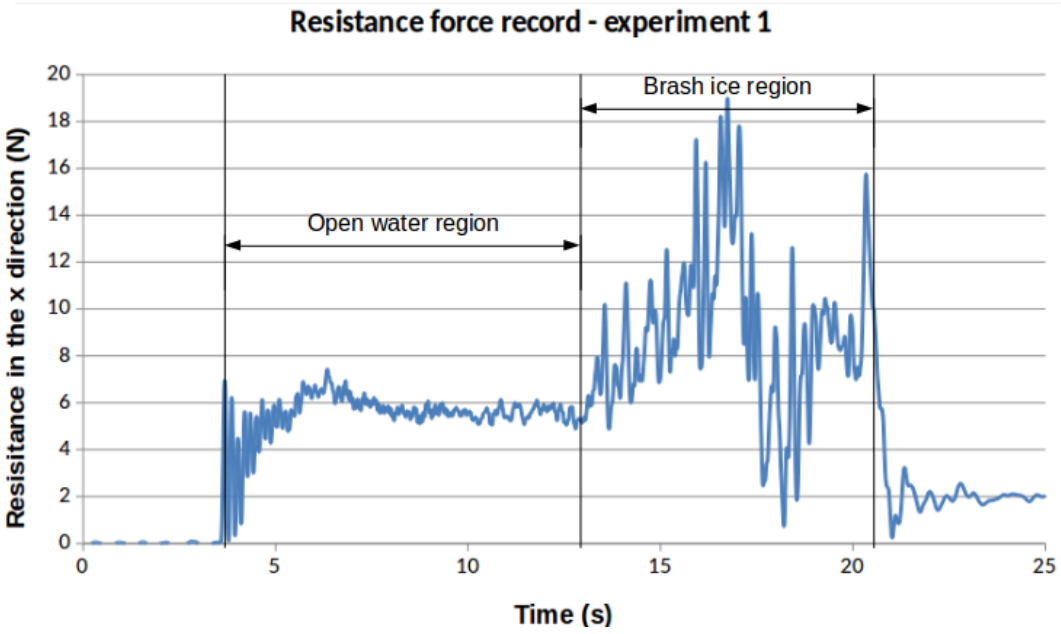

Figure 62: Experiment 1 resistance graph

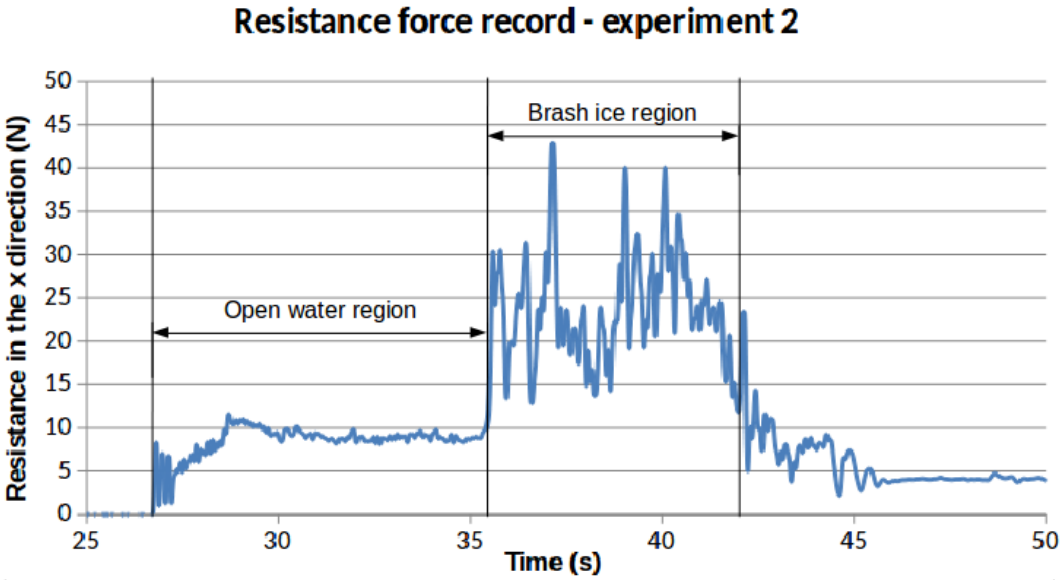

Figure 63: Experiment 2 resistance graph

As it was already explained two basic regions can be clearly observed in the curves, the next two sections compared the results of the simulations attempts and the experimental ones in these two regions separately.

8.2 Open water region software set up and comparison

The main purpose of this part is to compare the simulation results directly for the water region, measuring basically the resistance force in the x direction for the case already described and test the accuracy of the results. It is important to mention that this analysis is made to test the original code in water with the experimental data obtained, but in no case it should be taken as a validation for water which is out of the scope of this work.

The relevant dimensionless numbers of the experiments shown above are:

$F_n = 0,53$ (See Figure 56)

$Re = 1,48 \cdot 10^5$

The Reynolds number shows that the experiment is conducted in the transition regimen, for this reason the laminar + SPS formulation[41] for viscosity is chosen, to try to capture the turbulent effects expected in the model. If the other viscosity formulation is taken, the parameters could be adjusted to obtain similar viscous effects but not to account for the turbulent influence in the field variables.

Several important aspects must be briefly discussed:

1. **Particle distance:** The distance between particles was set to $0.02m$.
2. **Geometry creation:** Since the same particle distance is used throughout the whole model, the exact values of the geometry cannot be exactly replicated, thus a realistic approximation is proposed. This implies that any geometry has to be built inside a grid of particles that are equally spaced, thus rounding edges and also modifying curvatures.
3. **Lateral boundaries:** Two lateral walls were located in the position where the channel edges are, these are $1800mm$ apart from each other. To complete the boundaries and avoid a particle leak a back and front wall are added. The boundary positions were picked in order to affect the least the measurements but also having in mind to keep the simulation times at a reasonable level.
4. **Vertical boundaries:** A bottom wall was placed in a position equivalent to at least 3 times the draft of the cylinder to reduce any effect of the bottom wall.
5. **Boundary conditions:** All boundaries interactions, fixed or moving, are evaluated with a method called dynamic boundary conditions (DBC) [21], basically it calculates the momentum equation for all particles including the boundary particles but it does not update the position or velocities of these, instead it keeps the prescribed velocities and avoids the penetration by regulating the density of the fluid and boundary particles near to each other.
6. **Geometry distortion:** The previous boundary treatment generates a gap between the boundary and fluid particles, this gap affects the boundary dimensions and has to be taken into account when the geometry is modeled.

[41] Explained in section 6.4.

7. **Time step:** The CFL number was set as recommended for water 0.2. Although it is worth to mention that no convergence in time was performed.

The simulation was performed and some images of the results are show in Figures 64-70.

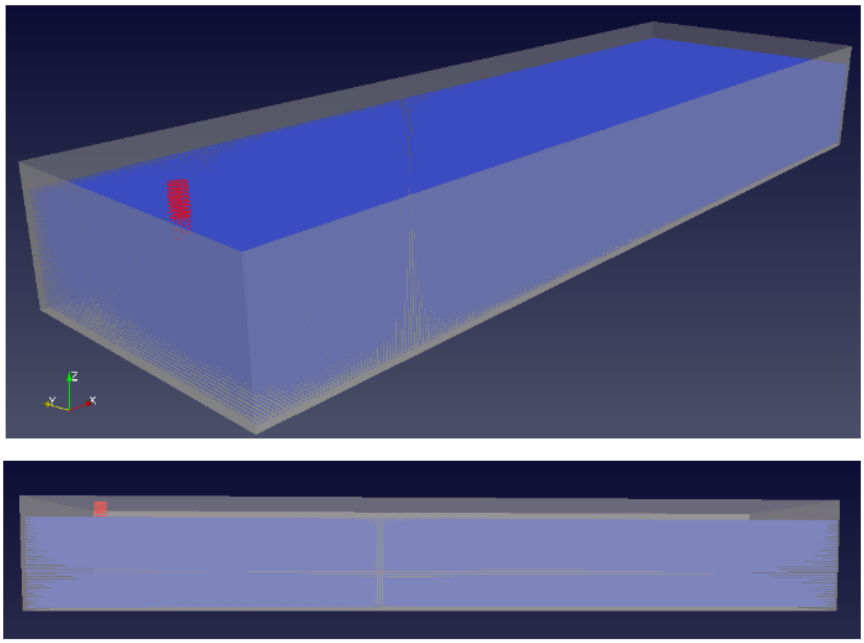

Figure 64: Model perspective and longitudinal view

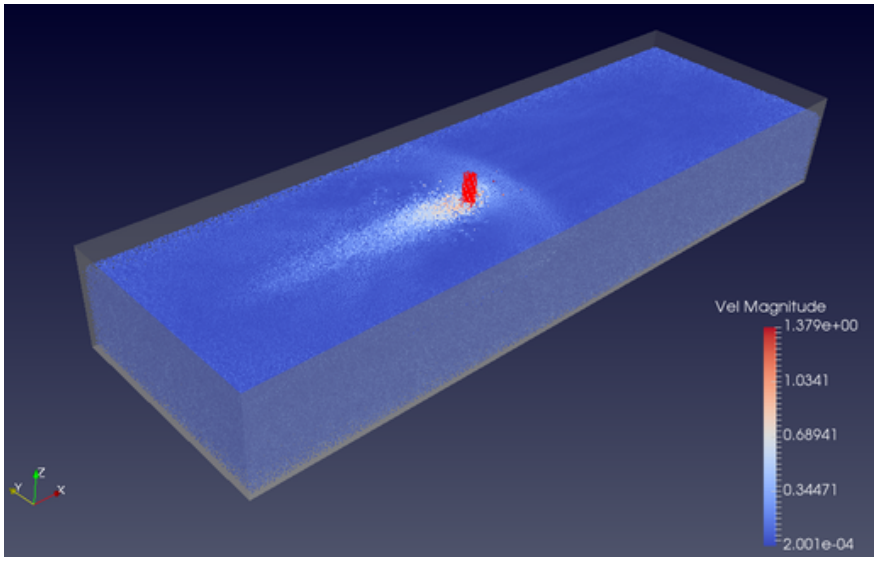

Figure 65: Particle perspective view

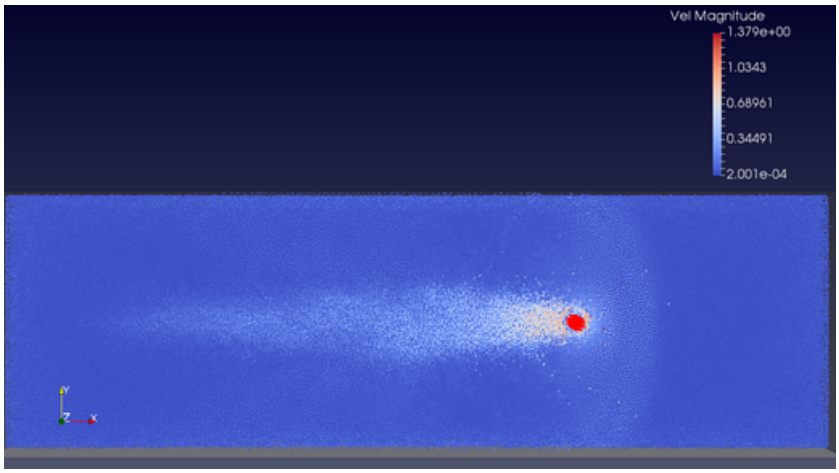

Figure 66: Particle top view

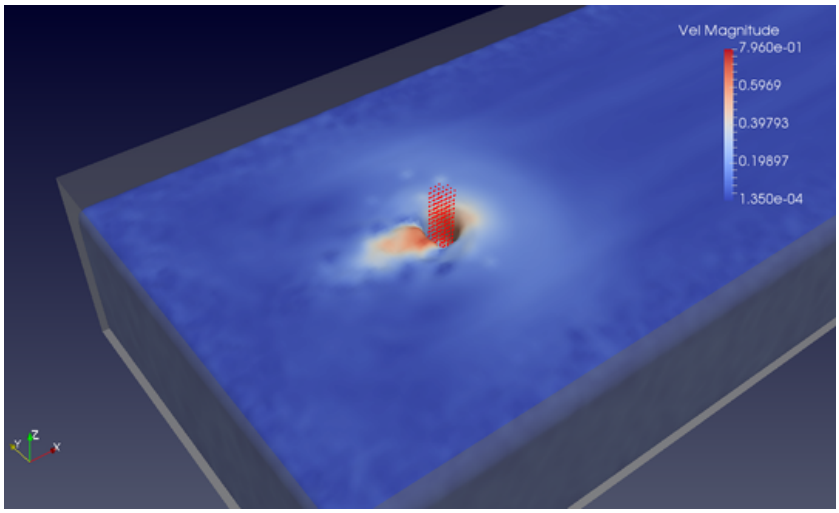

Figure 67: Isosurface view

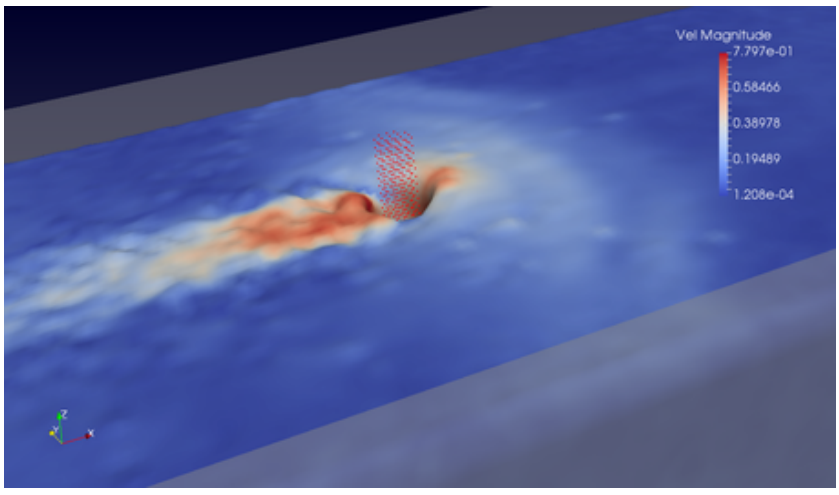

Figure 68: Isosurface view

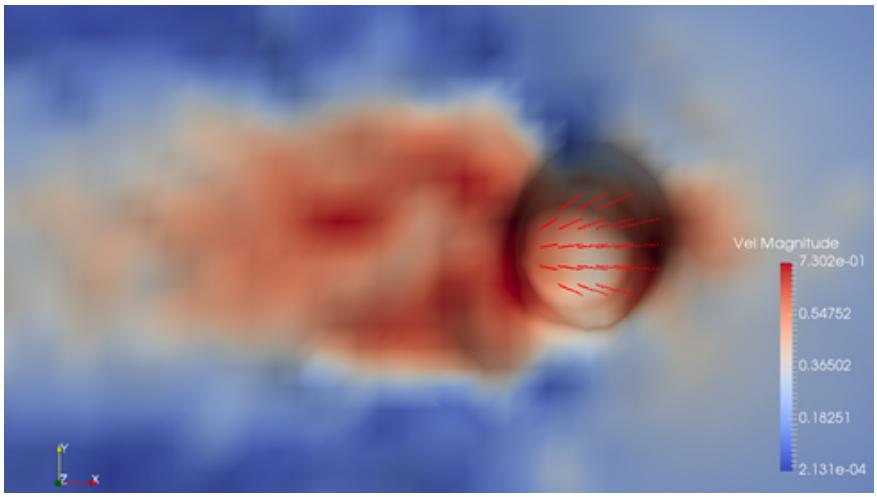

Figure 69: Isosurface top view close-up

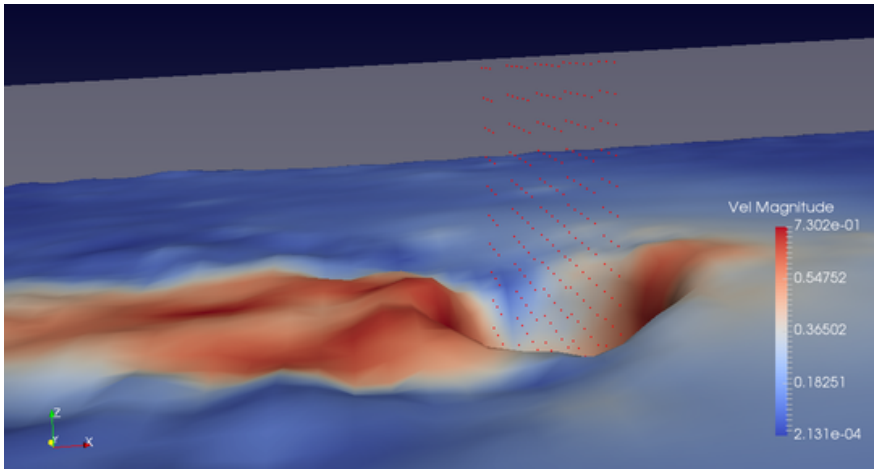

Figure 70: Isosurface view close-up

COMPARISON WITH EXPERIMENTAL DATA:

The force was also measured with the open source post-processing tool to recover the force exerted on any given boundary, which basically consists in calculating the acceleration of the boundary particles with the SPH methodology and then multiplying it by the mass of each boundary particle thus rendering the force, the same method will be used for the brash ice region. Experiment 1 curve was selected from 8.5 to 13.5s. Experiment 2 curve was selected from 30 to 35 seconds.

Below two comparative graphs of experiment 1 and 2 with their respective results in the open source code:

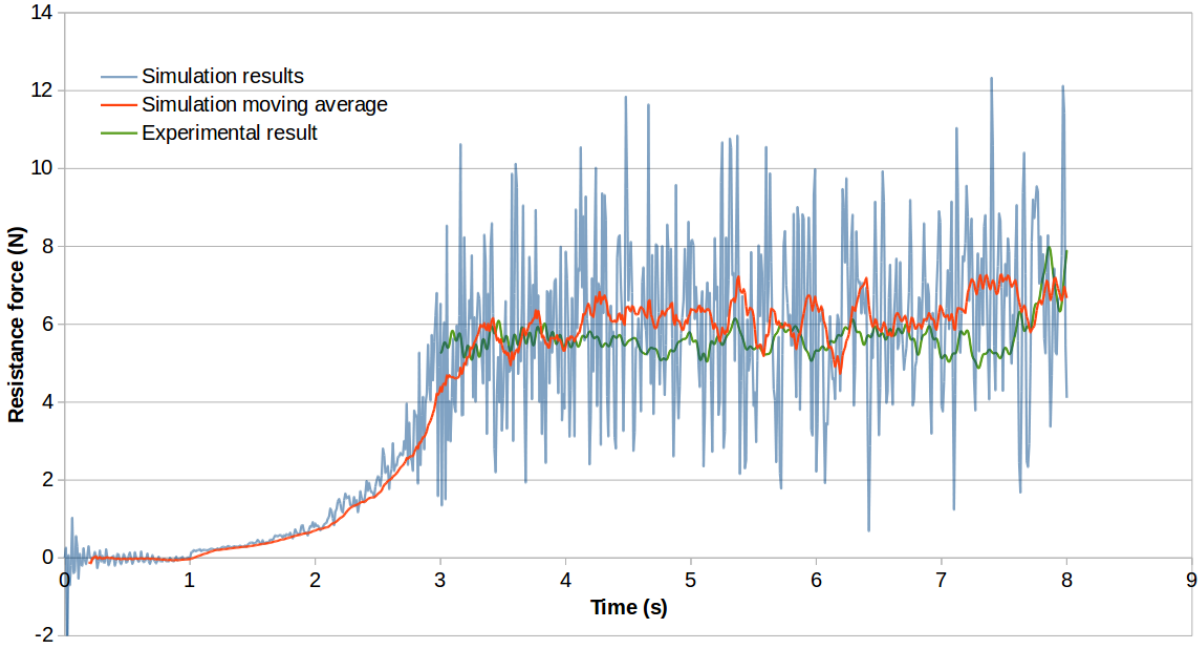

Figure 71: Resistance comparison - experiment 1

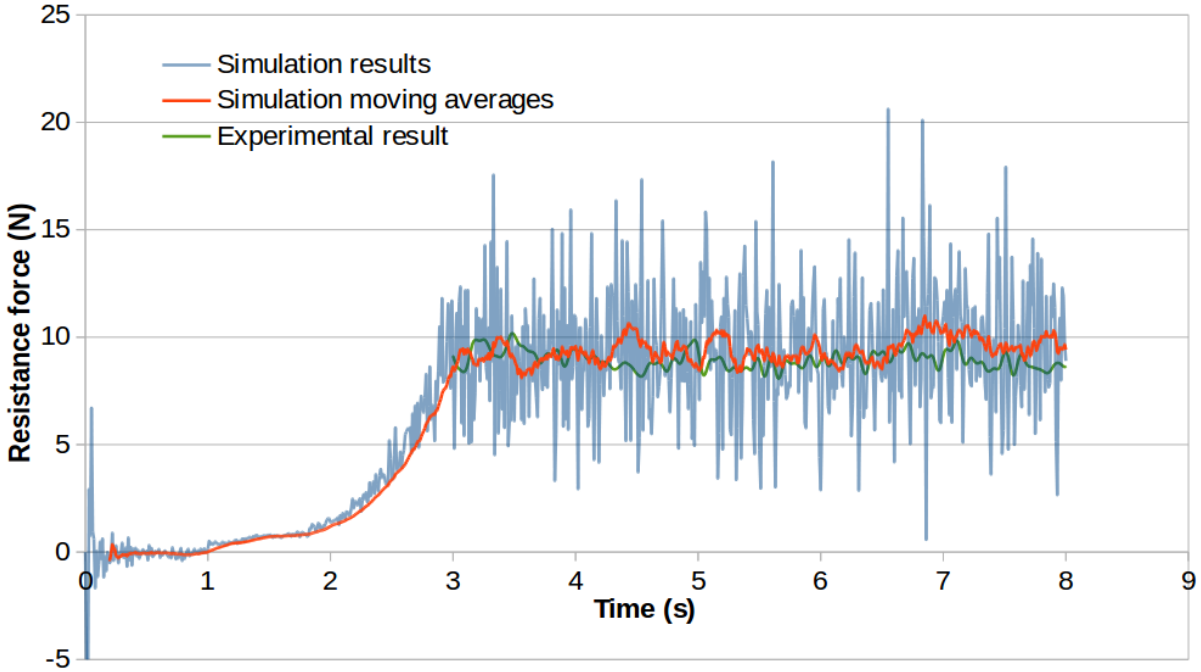

Figure 72: Resistance comparison - experiment 2

As it can be observed the agreement between the simulation and the experiments is pretty good, even though there is a high level of noise in the force captured with the SPH method. It is worth to remark that more runs to test the accuracy particle distance and of the time step for the given formulation are needed to consider this as a validation, but are not part of the scope of this investigation.

This agreement is considered as a verification of the general algorithm and of the force calculation post-processing tool, which is important because it was mimicked to obtain

the force measurements for different rheological models in the next section.

8.3 Brash ice region comparison

In this last section a similar procedure as for the open water region is performed, but the set up is defined for the new medium as in Section 7.4. Here some different set of possibilities for the values of the rheological parameters are tried and the resistance force in the x direction is calculated to compare it with the experimental results.

To capture the force for this modification a similar procedure to the of the post-processor tool mentioned in Section 8.2 was implemented inside the code, this is, calculating the acceleration of the boundary particles with the normal momentum equation in the SPH formulation and then multiplying the results with the mass of the boundary particles.

In the following table three cases are presented with the following characteristics:

Trial	τ_c (kPa)	ϕ $(°)$	$II_{\dot{D}}^{f}$ (s^{-2})	μ $(Pa.s)$	Observation
1	3,5	50°	0,1	10	Benchmark run for comparison
2	1,5	20°	0,1	10	First attempt
3	0,75	10°	0,1	10	Second attempt

Table 5: Parameters for Resistance Force measurement

The parameters for all trials are taken directly from inside the range of possible experimental values. From the maximum known values set for trial 1 to the minimum possible values set for trial 3. Figures 73 to 78 show images of the 3 trials at the same point in time for a better understanding and for visual comparison.

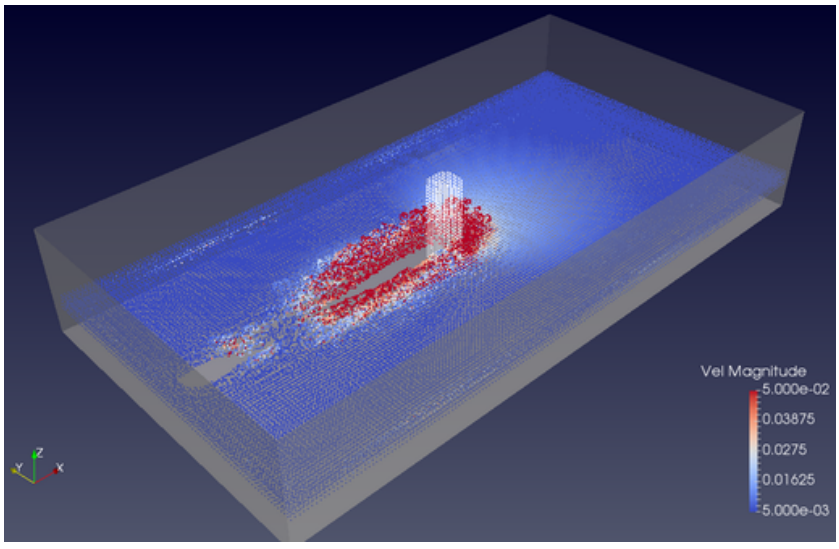

Figure 73: Trial 1 Particle perspective view

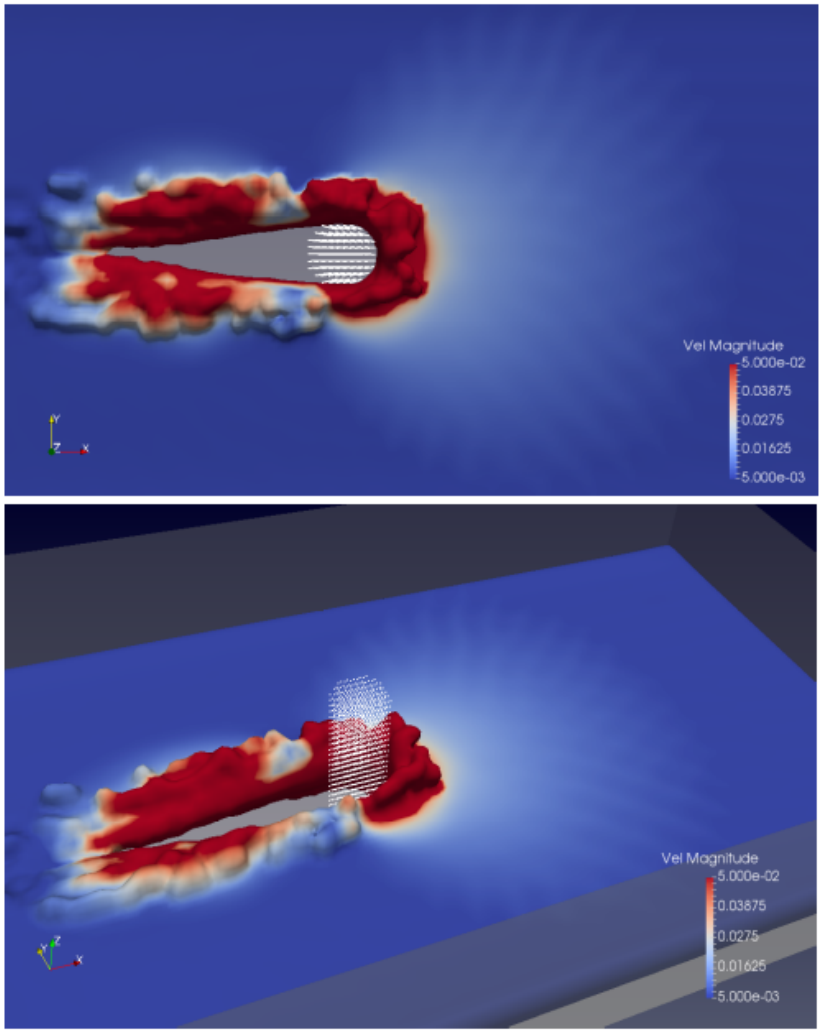

Figure 74: Trial 1 Isosurface top and perspective view

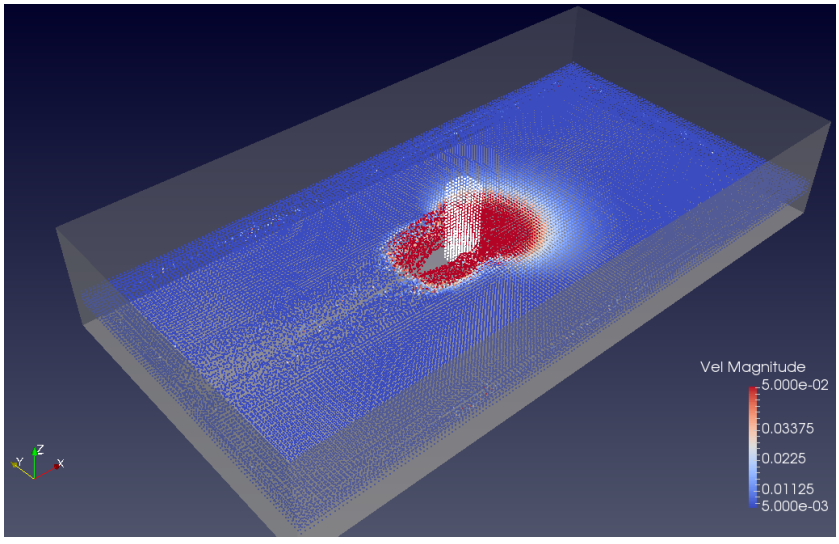

Figure 75: Trial 2 Particle perspective view

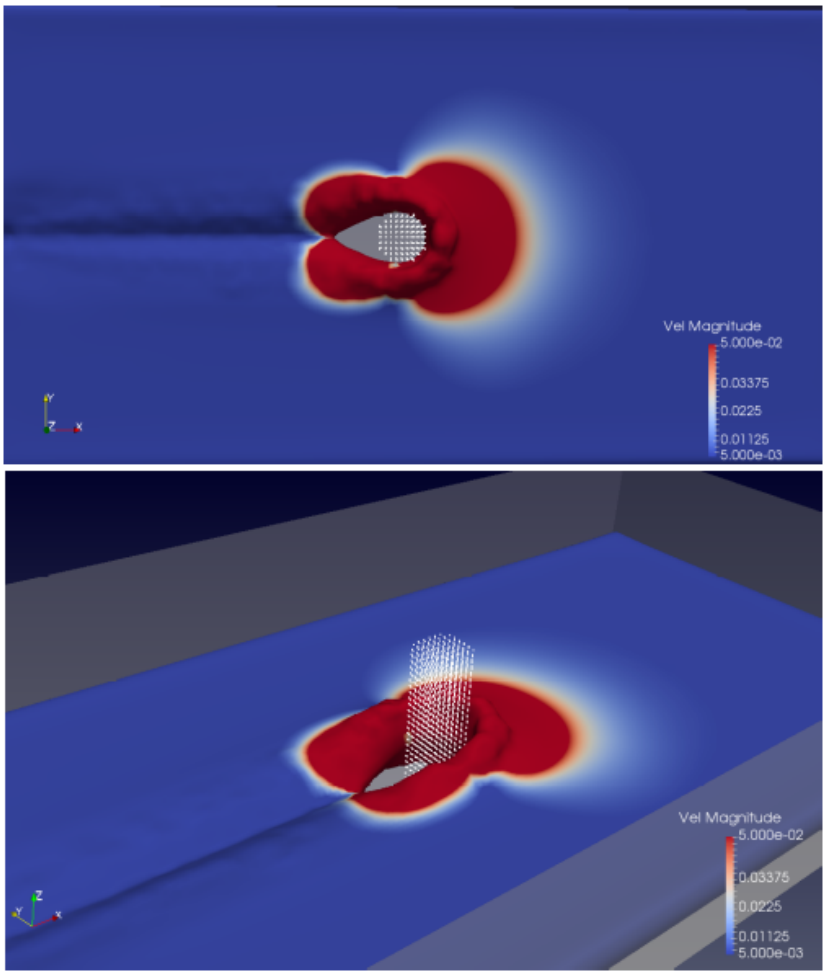

Figure 76: Trial 2 Isosurface top and perspective view

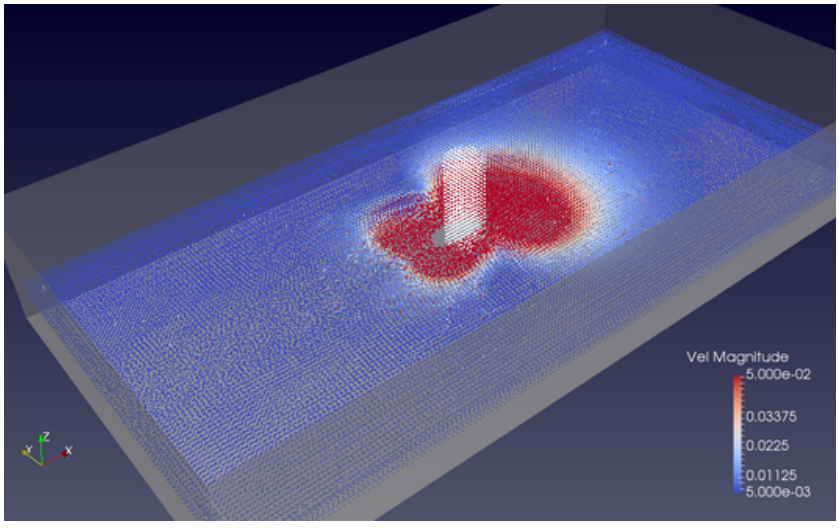

Figure 77: Trial 3 Particle perspective view

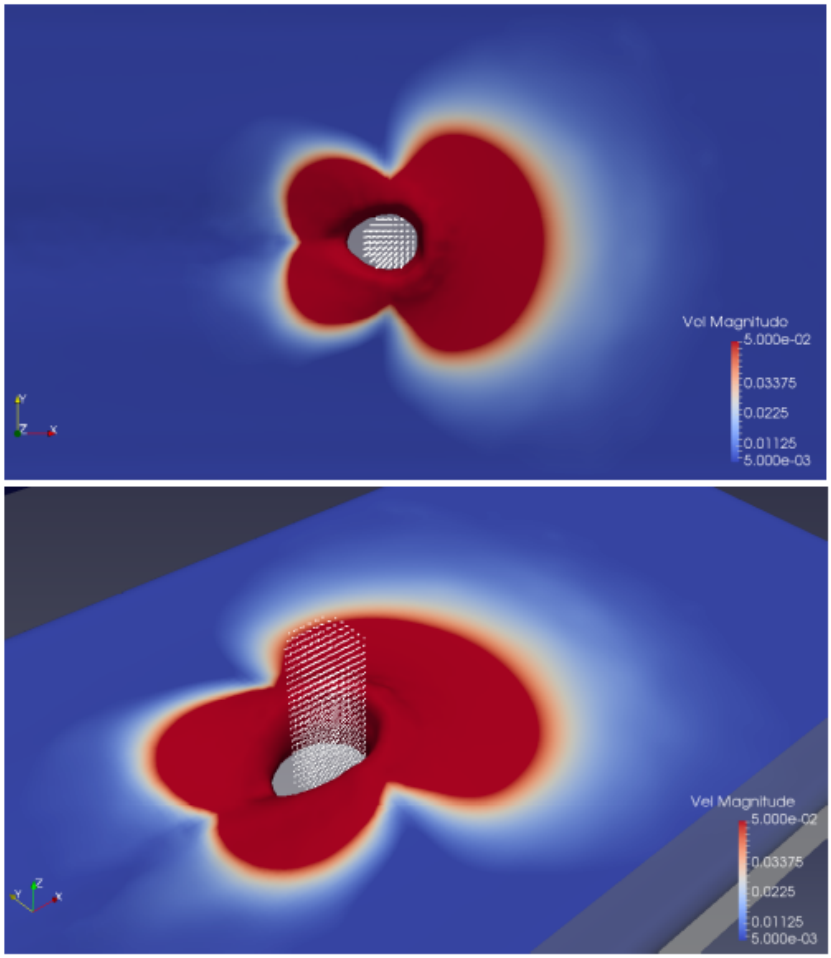

Figure 78: Trial 3 Isosurface top and perspective view

As it can be observed in the previous images, the velocity fields have different behaviors and are disturbed more and more as the fluid gets less stiff, this fact is also reflected in figure 79 where a force measurement is shown for each trial and also compared with the experimental data of the experiment 2 of section 8.2.

As it can be observed, the values obtained have the same order of magnitude of the experimental data, but the first two trials are between 4-6 times and 3-4 times bigger than the experimental data, the third trial has parameters in the lower limit of the possible experimental data gather but the agreement is much accurate.

The comparison above shows that a reasonable agreement between the mean values of the simulation and experiment can be obtained by adjusting some values, although a clear discrepancy between shapes and behavior of the curve is noticed. This discrepancy could be studied in different trials to improve the model towards a more similar behavior.

COMPARISON WITH EXPERIMENTAL DATA:

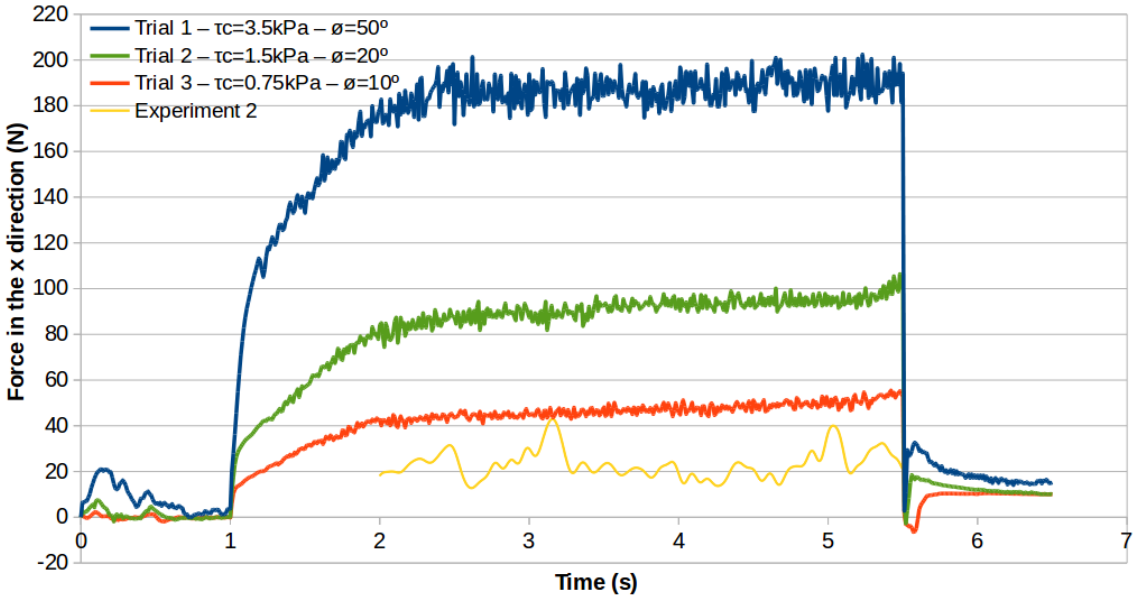

Figure 79: Comparison of simulation trials with experimental data

The experimental results were taken from experiment 2, Figure 63, from 36 to 39.5 s. To make possible the comparison the time axis was shifted appropriately.

But in general the medium created renders a lot of possible values to attempt to reproduce the experimental data obtained, although to correctly address the problem more experiments are needed to correctly predict the viscous behavior parameters.

Following a series of images are presented to comment on the overall behavior of the medium against the one observed during the cylinder tests.

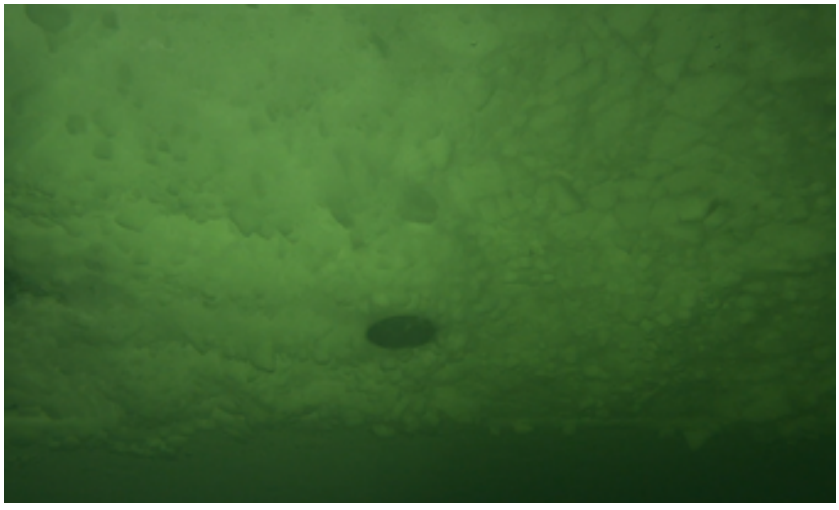

Figure 80: Cylinder experiment side bottom view

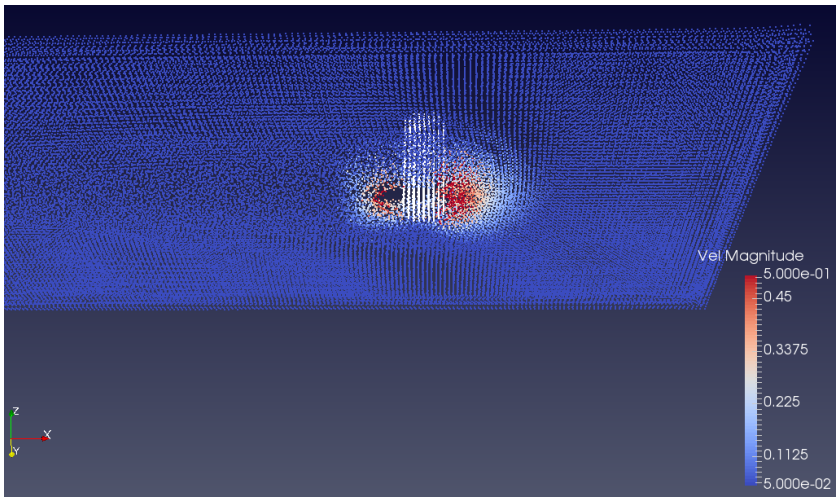

Figure 81: Cylinder simulation side bottom view

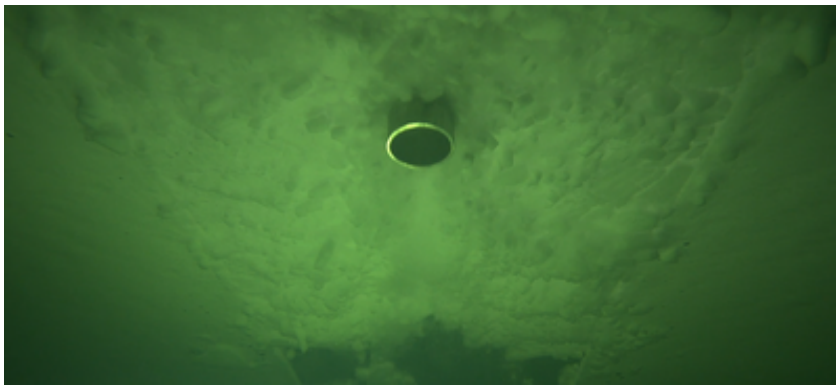

Figure 82: Cylinder experiment front bottom view

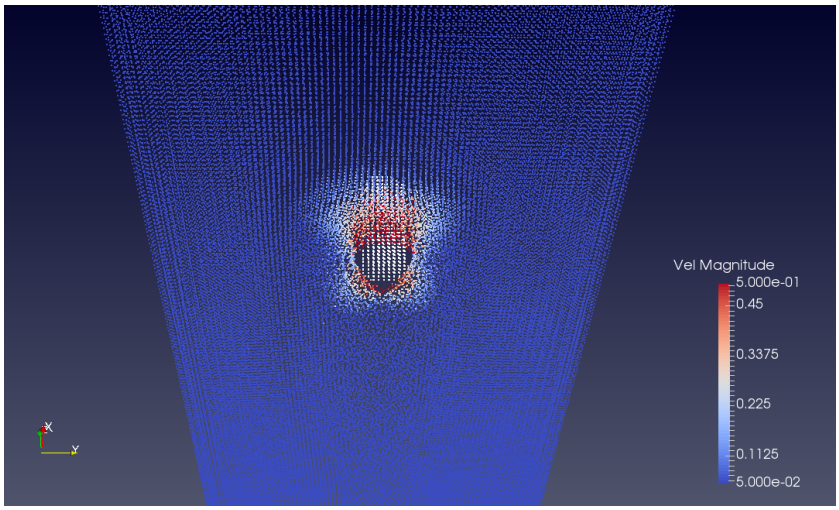

Figure 83: Cylinder simulation front bottom view

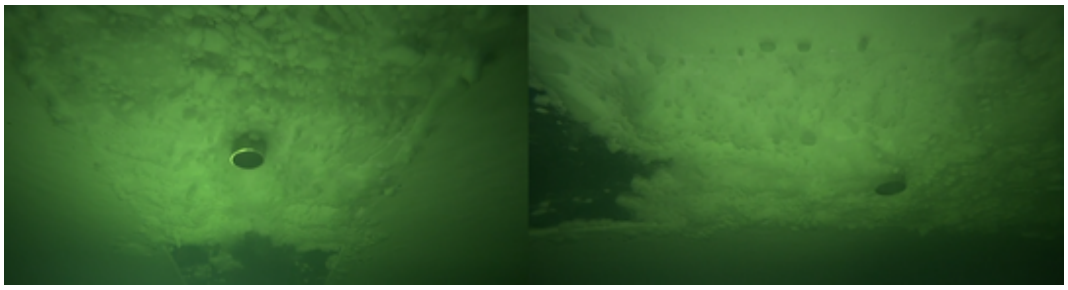

Figure 84: Cylinder experiment two views

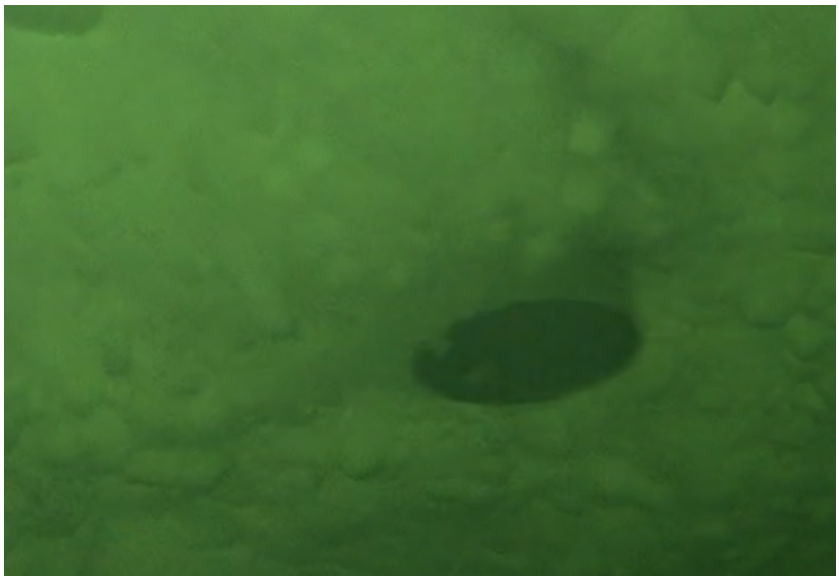

Figure 85: Cylinder experiment bottom close-up

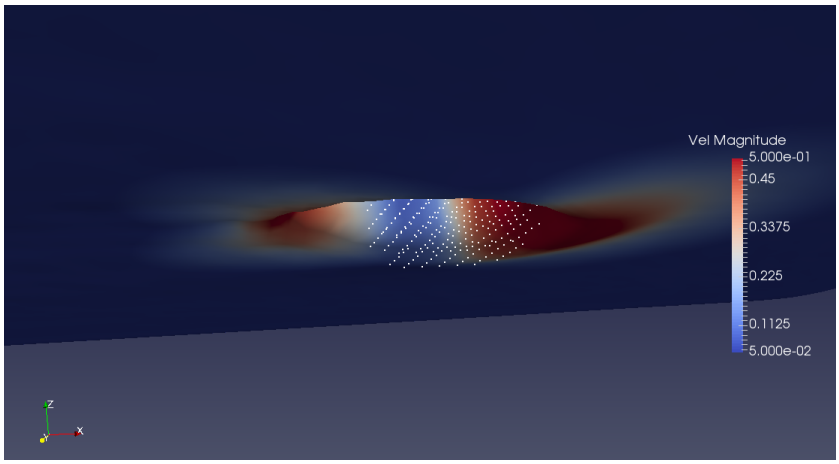

Figure 86: Cylinder experiment simulation bottom close-up

From a visual point of view, although not completely appreciable in the figures 80 to 86, the brash ice layer velocity field is almost not disturbed in the proximity of the cylinder, which agrees up to some extent with the low velocities registered in figures of section 7.4.

CONCLUSIONS AND FUTURE PROSPECTS

ON THE METHODOLOGY AND IMPLEMENTATION

The methodology selected for this work, this is, a single phase granular flow model solved with the SPH method, seems to be a good candidate for a complete numerical model of the full range of the brash ice behavior. Although to fully confirm this other methodologies should be studied implemented and tested, to compare their advantages and disadvantages in a more complete way.

The implementation was proven to be effective, and the results shown here provide good insights on the time steps needed for convergence, and thus the real computational times that the model actually required to give meaningful results. These results although logical due to the amount of non-linearities added to the equations, were not taken into account when doing the decision making tables of part II, and are regarded as a lesson learned in this work for future developments.

In fact this last remark sets a questions on whether the other methodologies, such as the coupling methods between SPH and DEM are actually more competitive or at least as competitive as the one studied here and opens a door to an attractive set of possibilities to model brash in the future.

ON THE ACTUAL MODEL

Despite this remarks, the results obtained in the simulations performed with the viscoplastic rheology implemented, were reasonably close to the behavior observed in experiments. The granular behavior was correctly captured and the velocity field visual comparison can be regarded as a good first approach, although a numerical comparison is indeed needed to make any further conclusion.

The result of the force measurement comparison in the brash ice region, has to be carefully analyzed. Although it appears to suggest that a set of simulation parameters can be determined to provided sounder results in comparison with experimental data, there are some important remarks to consider:

1. The model is not taking into account the water below the brash ice layer thus, an small increase in the resistance has to be included in order to make a full comparison.

2. More experimental data with different set ups, this is, with different velocities or with different brash ice layer thicknesses is needed to completely test the model prediction capabilities and limits, or to even suggest the best set of parameters to run simulations and compare the results with experimental data.

3. The model fails to provide a realistic representation of the stern flow, leaving a clear gap behind the cylinder, not observed in reality. This can overestimate the pressure parameters and thus the resistance.

4. The particle sizes, which is an important parameter was not taken into account in this model, so its influence remains unknown as far as this research goes.

5. Although the open source code gives the possibility to import of complex geometries, the amount of steps necessaries to upgrade the model from a cylinder to a ship, is huge, taking into account the much more larger domains and the bigger importance of the water region for this problem.

Having said all these, a reasonable set of simulation parameters as the ones presented here can be taken as a good first approximation to overestimate the resistance, thus providing results on the safe side.

ON THE FUTURE POSSIBILITIES

If a extension of this method was to be implemented some details have to be pointed out here:

1. The pressure boundary condition devised here, in spite of being very straight forward, seems to have a major impact on the medium behavior so that an improved version could be developed.

2. A revision on the pressure calculated with the equation of state should be done taking into account both fluid and grain particles contribution, calculating the appropriate thermodynamical balance. In this work this was avoided by assuming weakly compressibility taking into account the proximity of the density of both phases involved.

3. A different rheology should be tested to account for the stern flow, perhaps a more complex dependent on the concentration allowing the stern flow to change its behavior once the perturbation of the moving body has passed.

4. The possibility of including a ship inside this kind of model requires some special considerations, perhaps the inclusion of water as a second phase is completely necessary or maybe a special decomposition of the resistance in brash ice has to be develop to make any attempt of comparison with experimental data.

ACKNOWLEDGEMENT

I would like to express my gratitude to the head of the Arctic Technology Department of HSVA Dipl.-Ing Peter Jochmann for providing full support and interesting insights to develop this topic.

Also I specially would like to express my gratitude to M.Sc. Quentin Hisette for his constant supervision, support and unconditional help, to M.Sc. Matthias Lemmerhirt for helpful programming advices, to Mr. J.-H. Hellmann for an insightful discussion about brash ice, and at last to all the HSVA employees from the Arctic Division for their support and patience during experiments.

This thesis was developed in the frame of the European Master Course in Integrated Advanced Ship Design named EMSHIP for European Education in Advanced Ship Design, Ref.: 159652-1-2009-1-BE-ERA MUNDUS-EMMC.

Ivan Montenegro

REFERENCES

[1] M. MELLOR, *Ship Resistance in Thick Brash Ice*. Cold Regions Science and Technology 3, Elsevier, 1980.

[2] P. GREISMAN, *Brash Ice Behavior*. United States Coast Guard Research and Development Center, 1981.

[3] J.H. HELLMANN, *Widerstand Einfacher Geometrischer Körper in Eisbrei*. Budesministerium für Forschung und Technologie MTK 0234 A8 Eistechnik, Hamburg, 1985.

[4] J. SANDKVIST, *Brash Ice Shear Properties - Laboratory Tests*. Division of Structural Engineering, University of Lulea, Sweden, 1985?.

[5] A. CRESPO Et Al.,DualSPHysics v4.0, Manchester University and University of Vigo, 2015.

[6] L.MALVERN, *Introduction to the Mechanics of a Continuos Medium*. Chapter 6 *Constitutive Equations*, Prentice-Hall Inc., 1969.

[7] R. GUTFRAIND & S. SAVAGE, *Smoothed Particle Hydrodynamics for the Simulation of Broken-Ice Fields: Mohr-Coulomb-Type Rheology and Frictional Boundary Conditions*. Journal of Computational Physics 134, 203-215, McGil University, 1997.

[8] E. MITSOULIS, *Flows of Viscoplastic Materials: Models and Computation*. Rheology Reviews 2007, 135-178, National Technical University of Athens, 2007.

[9] G. FOURTAKAS & B.D. ROGERS, *Modelling Multi-Phase Liquid-Sediment Scour and Resuspension Induced by Rapid Flows Using Smoothed Particle Hydrodynamics (SPH) Accelerated with Graphics Processing Unit (GPU)*. Advances in Water Resources, ELSEVIER, 2016.

[10] X. YAN Et Al., *Multiphase SPH Simulation for Interactive Fluids and Solids*. Tsinghua University, Cardiff University and Swansea University, 2016.

[11] A. KONNO, *Resistance Evaluation of Ship Navigation in Brash Ice Channels with Physically Based Models*. Port and Ocean Engineering under Arctic Conditions. Kogakuin University, 2009.

[12] S. DARTEVELLE, *Numerical and Granulometric Approaches to Geophysical Granular Flows*. Doctoral Thesis Dissertation. Michigan Technological University, 2003.

[13] GRANULAR VOLCANO GROUP, *http://www.granular.org*. 2003.

[14] G.R. LIU & M.B LIU, *Smoothed Particle Hydrodynamics a Meshfree Particle Method*. Chapter 3 *Constructing Smoothing Functions*, Word Scientific., 2003.

[15] H.T. SHEN & J. SU & L. LIU, *Numerical Simulations of Granular Free-Surface Flows Using Smoothed Particle Hydrodynamics*. Journal of Computational Physics 165, 752-770, 2000.

[16] G. CHAMBON Et Al., *SPH Simulation of River Ice Dynamics*. Journal of Non-Newtonian Fluid Mechanics,ELSEVIER, 2011.

[17] A. CRESPO Et Al., *User Guide for the SPHysics code*, Manchester University and University of Vigo, 2010.

[18] A. CRESPO Et Al., *User Guide for parallel SPHysics v2.0 using MPI*, Manchester University and University of Vigo, 2011.

[19] A. CRESPO Et Al., *DualSPHysics v4.0 GUIDE*, Manchester University and University of Vigo, 2016.

[20] R.A. DALRYMPLE & B.D. ROGERS, *Numerical Modeling of Water Waves with the SPH Method*, ELSEVIER, Coastal Engineering 53 141-147, 2006.

[21] A. CRESPO Et Al., *Boundary Conditions Generated by Dynamic Particles in SPH Methods*, Tech Science press, 2007.

[22] J. SANDKVIST, *Conditions in Brash Ice Covered Channels with Repeated Passages*. Water resources engineering, 1985?.